

# **UNAVCO Academic Research Infrastructure (ARI) Receiver and Antenna Test Report**

C. Rocken, C. Meertens, B. Stephens, J. Braun, T. VanHove, S. Perry, O.  
Ruud, M. McCallum, J. Richardson

INTRODUCTION .....	iv
1    Zero Baseline Tests.....	iv
2    Short Baseline Tests.....	v
3    QC Results .....	v
4    Power tests .....	v
5    Download Speed .....	v
6    Real Time Kinematic Tests.....	vi
7    Antenna Tests: Chamber Experiments and Mixed Baselines .....	vi
1 Zero Baseline Tests.....	1-1
1.1 Introduction and Experiment Description.....	1-1
1.2 Pseudorange Zero Baseline Solutions.....	1-2
1.3 Phase Zero Baseline Solutions.....	1-2
1.4 High Rate Zerobaseline Tests .....	1-15
1.5 Ambiguity Resolution Summary .....	1-17
1.6 Receiver Mixing - 5 way splitter .....	1-22
2 Short Baseline Solutions .....	2-1
2.1 Introduction and Experiment Description.....	2-1
2.2 Summary of Phase and Pseudorange Solutions .....	2-2
2.3 L1 Phase Solutions.....	2-3
2.4 L2 Phase Solutions.....	2-6
2.5 L3 Phase Solutions.....	2-9
2.6 L1 Pseudorange Solutions.....	2-12
2.7 L2 Pseudorange Solutions.....	2-15
2.8 L3 Pseudorange Solutions.....	2-18
3 Summary of quality check results.....	3-1
4 Power Tests.....	4-1
4.1 Power Consumption.....	4-1
4.2 Mid-Survey Power Failure Tests .....	4-2
5 GPS Receiver Download Speed Comparison:.....	5-1
5.1 Purpose:.....	5-1
5.2 Description:.....	5-1
5.3 Summary of Measurements: .....	5-2
5.4 Related Issues/Discussion:.....	5-5
5.5 Conclusions:.....	5-7
5.6 Receiver Options Related to Downloading: .....	5-8
5.7 Remote Operation Capabilities:.....	5-10
6 Real Time Surveying Systems Demonstration .....	6-1
6.1 Purpose of Work: .....	6-1
6.2 Dates and Location: .....	6-1
6.3 Procedures:.....	6-1
6.4 Comments: .....	6-3
6.5 Comparison of Results:.....	6-3
6.6 Persons Contacted:.....	6-7
6.7 Summary of Features and specifications for Real-time Surveying Systems based on Manufacturers Brochures.....	6-8
7 UNAVCO ARI Antenna Tests.....	7-1

7.1	Abstract .....	7-1
7.2	Introduction.....	7-1
7.3	Application of Antenna Chamber Results in GPS Software .....	7-2
7.4	Horizontal Phase Centers - Rotation Tests and Antenna Chamber results.....	7-3
7.5	Test of the UNAVCO/Ball Antenna Chamber Results.....	7-6
7.6	Results.....	7-8
7.7	Ashtech CR Antenna Dome Tests .....	7-9
7.8	Results of the Dome Tests .....	7-10
7.9	Conclusions and Future Work .....	7-11
A	.....	A-1
B	SUMMARY OF OBSERVATIONS AT TABLE MOUNTAIN TEST SITE .....	B-1
C	Details of Download Timing Tests .....	C-1
D	Real-time GPS Vectors .....	D-1
E	Vendor Responses.....	E-1

## INTRODUCTION

The UNAVCO GPS research community has been funded under National Science Foundation's Academic Research Infrastructure (ARI) program to purchase GPS equipment for scientific applications. There is a large variety of commercial GPS receivers available and the UNAVCO facility tested several of these instruments to aid ARI participants in selecting the appropriate receiver for their research.

The tested equipment had to satisfy several minimal requirements: (1) Full wavelength L1 and L2 carrier phase has to be tracked under A/S and non-A/S conditions, and (2) Pseudorange data are required at both GPS frequencies. The manufacturers and instruments which fulfilled the requirements and participated in these tests are given in Table 1 and include Allen Osborne Associates, Inc., Ashtech, Leica, Inc. and Trimble Navigation, Ltd. Antennas tested are given in Table 2 and Table 3 and general receiver specifications are listed in Table 4.

These tests are in many ways different from earlier tests conducted by the UNAVCO facility. The purpose of earlier tests was to find the receiver which was best suited for UNAVCO supported geodetic research. This "best" receiver was then recommended to the UNAVCO Steering Committee for purchase. The tests presented here do not intend to identify the best receiver. Different aspects may be of different importance to various investigators in the UNAVCO community. Some investigators may consider download speed or compatibility with other equipment more important than zero baseline or real time kinematic performance. Receiver costs obviously will play a major role in equipment selection.

In order to ensure optimal receiver performance using the most recent equipment and software, the vendors were invited to participate in any or all aspects of these tests. Vendors have also reviewed drafts of this report and were invited to submit their comments, contained in Appendix E.

Tests conducted were intended to provide a wide range of information to be used by the individual investigators for selecting the appropriate receiver according to their own priorities and needs. Data for short, zero, and mixed antenna baselines were processed using the Bernese GPS software with typical processing parameters such as indicated in the ARI Vendor Ordering Agreements Exhibit A. Unless noted, the epoch interval was 30 seconds with 15 degree elevation cutoff. These tests were designed to show optimal receiver performance. Not all receiver data could, however, be processed with the same degree of automation. In particular, the AOA Turborogue and Rascal data at times required extra manual data editing and/or special tuning of default processing parameters. These problems typically, but not exclusively, occurred between 15 and 20 degrees. AOA recommends using a 20 degree cutoff when A/S is activated on the satellites. Problems encountered may differ with other processing packages.

### 1. Zero Baseline Tests

In zero baseline tests two receivers are connected to the same antenna and low-noise amplifier (LNA). These tests are conducted to examine receiver performance. All common errors due to multipath, LNA noise, propagation effects, etc. cancel in the GPS processing. Since receivers use

different tracking algorithms and apply different data averaging times which can affect noise levels, some of the major differences are summarized in Table 5.

We operated all tested receivers for 5 days on zero baselines for 20 hours each day. The data were processed with the Bernese GPS software. Statistics on baseline results for L1, L2 and LC (ionosphere free combination) phase and pseudorange solutions are summarized. All receivers obtained zero baseline phase results of better than 1 mm. Pseudorange zerobaselines were better than 190 mm in all cases.

High rate (one second) epoch interval zerobaseline test results and ambiguity resolution summary are also contained in this section.

## **2. Short Baseline Tests**

In short baseline tests the receivers are operated like in a typical high accuracy GPS survey application. These tests address the performance of the full system, antenna, LNAs, cables and receiver.

Each tested receiver pair was operated on several short (~5- 10 meters), known baselines. Results of the short baseline processing agreed with ground truth to 2.0 mm in the vertical and to within 1.0 mm in the horizontal for all receivers.

## **3. QC Results**

Short and zero-baseline data processing were done above 15 degree elevation angles. We had operated all the receivers in the field to track to zero degree elevation angles. In this section we look at the data quality for the various receivers at very low, as well as “normal”, elevation ranges. We compare the cycle slip counts, as provided by the receivers through the RINEX files. We also plot pseudorange + multipath noise and phase noise for different elevation angle ranges.

## **4. Power tests**

Power consumption of the receivers is an important parameter, especially for operation at remote sites without AC power. The power needs for the tested receivers were measured and are summarized in tabular form. We also examined what happens in the case of a power failure. What happens if the power fails suddenly, what happens if it fails slowly due to draining of the battery? These are again very important considerations for remote operation of GPS sites and this section describes how the receivers respond to these conditions.

## **5. Download Speed**

Exhaustive tests were run to test how fast the data from the various receivers can be downloaded for three different modes: (1) Direct connection between the receiver and computer, (2) Modem connection; (3) Radio Modem connection.

Download speed has always been an important consideration because it significantly affects field operations. With emerging permanent networks where data are downloaded from remote sites through phone lines, download speed also affects operating expenses. This section summarizes in

tabular form the download performance of the tested receivers in all three modes.

## **6. Real Time Kinematic Tests**

A test network had been established by UNAVCO outside Boulder, Colorado and surveyed with GPS. Three GPS manufacturers that offer real time kinematic (RTK) operation as an optional enhancement of their equipment surveyed the test network with RTK. Our report describes the demonstration and compares the RTK results with the results from our static survey. The results show that RTK accuracies are now at the cm-level, making it a very attractive technology for many scientific applications.

## **7. Antenna Tests: Chamber Experiments and Mixed Baselines**

As GPS receiver performance appears to be converging, GPS antenna performance is increasingly important for the highest accuracy GPS applications. Therefore, the UNAVCO facility tested several geodetic antennas. First, we operated different antennas in the field on short baselines and compared the obtained GPS results with ground truth. Next we placed all the tested antenna types (Ashtech choke ring, AOA choke ring, Trimble SSE, Trimble SST, Leica SR399 External, AOA Rascal) in the anechoic chamber operated by BALL Aerospace, Inc. In the anechoic chamber we measured antenna phase center variations and antenna amplitude (gain) patterns as a function of direction. The resulting phase patterns from our chamber tests were applied to field data from mixed antenna (and receiver) baselines and results were compared to ground truth. We find that, using our anechoic chamber values, data from the different tested antennas can be mixed with an accuracy of about 5 mm in the vertical and 1 mm in the horizontal components when the ionospheric free linear combination LC of the GPS carriers is processed. L1 and L2 solutions are even better. If we process the same LC data but also estimate a tropospheric delay parameter every hour the vertical accuracy is still about 10 mm or better for almost all antenna pairs. The horizontal accuracy is not significantly affected by the tropospheric estimation.

## **GPSHIP WWW Bulletin Board**

The purpose of the GPSHIP World Wide Web bulletin board and interactive email archive is to provide an information exchange forum about high-precision GPS receivers and antennas. The GPS user community and vendors are invited to submit/respond to items such as announcing new receiver firmware, new receiver hardware, antennas, data translators, bug reports, user experiences, etc. Mail messages will automatically be logged and are publicly accessible. GPSHIP is fashioned after the current UNAVCO Working Groups bulletin board. The WWW URL will be:

<http://unavco.ucar.edu/gpschip>

## **Acknowledgments**

These tests were funded by the National Science Foundation through a grant to UNAVCO. We appreciate the additional assistance by Jim Normandeau, Eric Nienhouse, Kurt Conquest, Gretchen Wallhaus, and Raphael L'Hoste-Morton. We are very grateful to all the vendors for their contributions to these tests.

**Table 1: TESTED RECEIVERS**

UNAVCO Name.	IGS Name	Manufacturer Model Name	P/N	Firmware
Ashtech Z-XII3	ASHTECH Z-XII3	Ashtech Z-12	700845-6 (B)	1E76
AOA Turborogue SNR-8000	ROGUE SNR-8000 (TurboRogue (field unit))	Allen Osborne Associates Turborogue SNR-8000	7490540	3.2.32.1
AOA Rascal	None Assigned yet	Allen Osborne Associates Rascal	8490330	3.0.32.0X
Trimble 4000 SSI	Trimble 4000 SSI	Trimble 4000 SSi	24840-21	7.01
Leica SR399 (see footnote) <sup>a</sup>	SR399E	Leica SR399E/CR344		3.4

a. The Leica datalogger unit is separate and mistakenly contained SR299E software. This resulted in less than optimal pseudorange noise values. This is discussed by Leica in Appendix E.

**Table 2: TESTED ANTENNAS**

UNAVCO Name.	IGS Name	Manufacturer Model	Part No.	Serial #
Ashtech Chokering	DORNE MARGOLIN ASH	Ashtech Antenna L1-L2	700936(B)	11757
AOA Chokering	DORNE MARGOLIN T	Allen Osborne Associates Choke Ring	7490582-1	200
AOA Rascal	(not decided yet)	Allen Osborne Associates SR-2000	8490300	none provided by manufacturer

**Table 2: TESTED ANTENNAS (Continued)**

UNAVCO Name.	IGS Name	Manufacturer Model	Part No.	Serial #
Trimble 4000 SST	4000ST L1/L2 GEOD (Trimble 4000ST L1/L2 GEOD used with SST and SSE receivers)	Trimble Geodetic L1/L2	14532-00	3022A0019 7
Trimble GEOD W/ GP	TR GEOD L1/L2 GP (Trimble Geodetic L1/L2 compact with removable ground plane included used with SSE and SSi receivers)	Trimble Compact L1/L2 with removable- Groundplane	23033-00	0080050642
Leica SR399 Exter- nal W/GP	EXTERNAL	Leica	AT202	none pro- vided by manufac- turer

**Table 3: Other ANTENNAS used in real-time tests**

UNAVCO Name.	IGS Name	Manufacturer Model	Part No.
Ashtech Z12	GEODETIC L1/L2 L (Ashtech patch antenna with compass, handles, built in aluminum ground- plane)	Ashtech Antenna L1-L2	700718(B)
Ashtech RTK		Ashtech Antenna L1-L2	700700(A)

**Table 3: Other ANTENNAS used in real-time tests**

UNAVCO Name.	IGS Name	Manufacturer Model	Part No.
Trimble GEOD	TR GEOD L1/L2 W/O GP (Trimble Geodetic L1/L2 compact without removable ground plane included used with SSE and SSi receivers)	Trimble Compact L1/L2 without removable-Groundplane attached	22020-00

**Table 4: General Receiver Specifications**

	AOA Rascal	AOA Rogue SNR-8000	Trimble 4000 SSi	Ashtech Z-12	Leica SR399E
Dimensions (inches) (W x D x H)	4.1 x 8.6 x 1.9	9.5 x 12 x 2.5	9.8 x 11 x 4	8.5 x 10 x 4	9 x 9 x 4.5 (8 x 10.5 x 2.5; Controller)
Weight receiver (lbs)	2.2	9.5	6.8	8.0	4.0 (2.3; Controller)
Weight antenna (lbs)	1.5	9.5	5.8	10.0 (includes choke ring+cover)	2.1
Operating Voltage Receiver	6 VDC	9-36 VDC	10.5-35 VDC	10-32 VDC	12 VDC
Operating Voltage Antenna	5-7 VDC	12 VDC	9 VDC	12 VDC	6 VDC
Operating Temperature	-20 C to +55 C	-20 C to +55 C	-20 C to +55 C	-20 C to +55 C	-20 C to +55 C
Humidity	100%	100%	100%	100%	100%

**Table 4: General Receiver Specifications (Continued)**

	AOA Rascal	AOA Rogue SNR-8000	Trimble 4000 SSi	Ashtech Z-12	Leica SR399E
Antenna connector (at antenna end)	N-type	N-type	N-type	N-type	TNC
Antenna connector (at receiver end)	Fisher	N-type	Lemo	N-type	TNC

**Table 5: Receiver Tracking Characteristics**

Receiver	version	mode	phase averaging [seconds]		code averaging [seconds]	
			L <sub>1</sub>	L <sub>2</sub>	L <sub>1</sub>	L <sub>2</sub>
AOA SNR-8000	3.2	No A/S	10	10	30	30
AOA SNR-8000	3.2	A/S	10	30	30	30
AOA Rascal	3.2	No A/S	10	10	30	30
AOA Rascal	3.2	A/S	10	30	30	30
Ashtech Z-XII3	1E76-1D01	No A/S	1	1	1	1
Ashtech Z-XII3 (see footnote) <sup>a</sup>	1E76-1D01	A/S	1 (300)	1 (300)	1 (300)	1 (300)
Ashtech Z-12/RTZ	1J00-1D01	No A/S	1	1	1	1
Ashtech Z-12/RTZ	1J00-1D01	A/S	1 (300)	1 (300)	1 (300)	1 (300)
Leica SR399E	3.4	No A/S	1	1	300	300
Leica SR399E	3.4	A/S	1	1	300	300
Trimble 400SSi	7.04	No A/S	1	1	1	1
Trimble 400SSi	7.04	A/S	1	10	1	8

- a. The Ashtech Z-XII3 receiver, like the other receivers, uses the carrier phase and averaging to smooth the pseudorange observations, but with the Ashtech translator the smoothing rate can be selected at the data translation step by the user. The receiver stores the raw data with an smoothing rate of 1 second but also internally computes a smoothing correction using approximately 300 seconds of phase observations. These corrections are stored in the raw observation file (the BEN file). The RINEX translator supplied by Ashtech, ASHTORIN, applied these corrections to the pseudorange observations when it created the RINEX file. The Bernese translator does not apply these corrections and writes the one second smoothed pseudoranges into the RINEX file.

# 1. Zero Baseline Tests

## 1.1 Introduction and Experiment Description

Zero baseline tests primarily compare receiver performance. Errors associated with antennas, LNAs, and the local environment (multipath, troposphere delay, etc.) are the same for both receivers and these errors difference out.

Five days of data were taken for the zero baseline tests using five of the ESG marks on Table Mountain. Every daily session had an epoch rate of 30 seconds and tracked for 20 hours. Each of the receiver types was operated once on every mark to insure that all receivers had approximately the same data to sample. In addition, the cable and signal splitters (manufactured by WR Incorporated) were kept at the mark so every receiver and antenna type used each of the cable/splitter pairs. Details of the data files collected and observation schedule are presented in Appendix A and Appendix B.

Data were processed in an automated shell script. On a single station level, the pseudorange observations were checked for gross outliers. Observations with residuals of greater than 100 m or more than 5 times the RMS of all the pseudorange measurements were deleted. Pseudorange observations above 15 degrees were used to compute receiver clock corrections. Pseudorange baseline lengths were calculated using observations above 20 degrees. L1 and L2 phase observations were checked separately for outliers and cycle slips using triple difference observations. Fixing of cycle slips was only attempted for data gaps shorter than 181 seconds. Phase ambiguities were introduced for any larger data gaps. Phase baseline lengths were calculated using observations above 15 degrees.

Various translators were used to convert the raw data files into RINEX format. Table 1 lists the source of the translators used for each receiver type. It also defines abbreviations that will be used to describe results throughout this document. The data from the Ashtech receiver was processed using two different translators. The translator supplied by Ashtech applies smoothing corrections computed by the receiver to the pseudorange observations. The Bernese translator does not apply these smoothing corrections. Please refer to the introduction for more details.

**Table 1.1: Receiver Abbreviations**

Receiver Type	Abbreviation	Translator Used	Comments
Ashtech Z-XII3	AZ12B	Bernese Translator	No Pseudorange Smoothing
Ashtech Z-XII3	AZ12A	Ashtech Translator	Phase Smoothed Pseudorange
AOA Rogue SNR-8000	AOAT	JPL Translator (DC and SRX)	No Pseudorange Smoothing
AOA Rascal	AOAR	JPL Translator (DC and SRX)	No Pseudorange Smoothing

**Table 1.1: Receiver Abbreviations (Continued)**

Receiver Type	Abbreviation	Translator Used	Comments
Leica 399E	L399	Leica Translator (With SKI)	No Pseudorange Smoothing
Trimble 4000 SSI	TSSI	Bernese Translator	No Pseudorange Smoothing

## 1.2 Pseudorange Zero Baseline Solutions

- Baseline length biases for all receivers were less than 190 mm for all receivers, with RMS scatters of less than 70 mm, using the L3 linear combination of L1 and L2 pseudorange observations.
- The Ashtech phase smoothing translator appears to improve the quality of the pseudorange solutions over non-smoothed solutions. This can be seen in L1, L2, and L3 baseline length and height.
- The noise level as computed from the zero baseline single difference rms of the L1 pseudorange solutions is approximately the same for all receiver types. All receivers have biases of less than 20 mm and scatters of less than 10 mm except the L399 (which has a bias of 49.1 mm).
- The major difference between the pseudorange solutions appears to be in the L2. The AZ12A and the TSSI solutions have the lowest L2 noise levels (the AZ12A is slightly lower than the TSSI). The difference in the bias and RMS scatter for the L3 solutions between receivers is primarily caused by the different L2 noise levels.

## 1.3 Phase Zero Baseline Solutions

- All receivers exceeded UNAVCO ARI specifications. All have sub-millimeter RMS scatter of baseline lengths in both frequencies and the ionosphere free, L3, linear combination.
- Bernese translated Ashtech data have slightly better scatter for the L2 and L3 solutions than the Ashtech translated data.
- Both ASH and TSSI data appear to have slightly lower L2 noise than the three other receivers. This lower L2 noise is seen in the lower solution scatter for both the ASH and TSSI receivers compared to the other three for both the L2 and L3 length and height solutions.

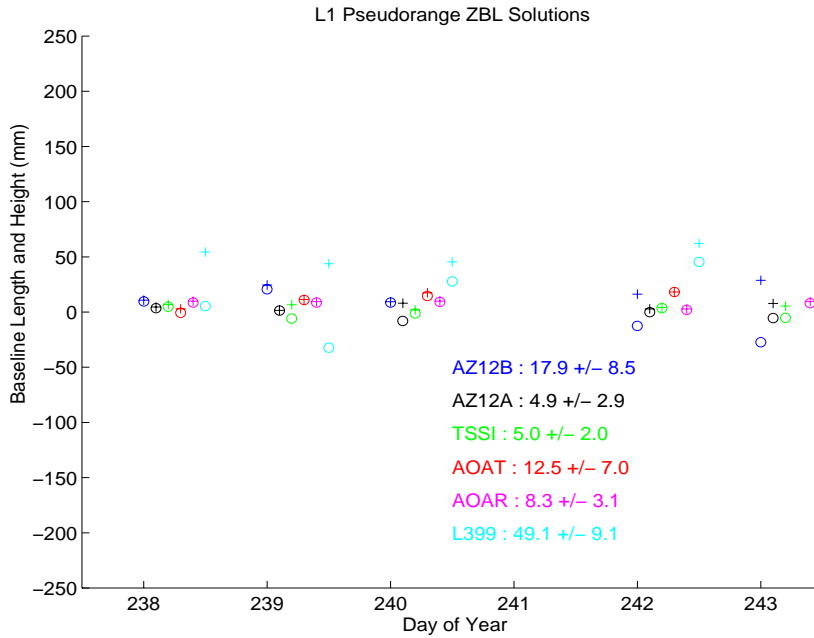


Figure 1.1: Color coded zero baseline solutions using L1 pseudorange observations. The daily solutions are plotted in pairs (baseline length and height) in the following order: AZ12B, AZ12A, TSSI, AOAT, AOAR, and L399. Each color represents solutions from a particular receiver type. Baseline length solutions are plus marks (+). Baseline height solutions are circles (o).

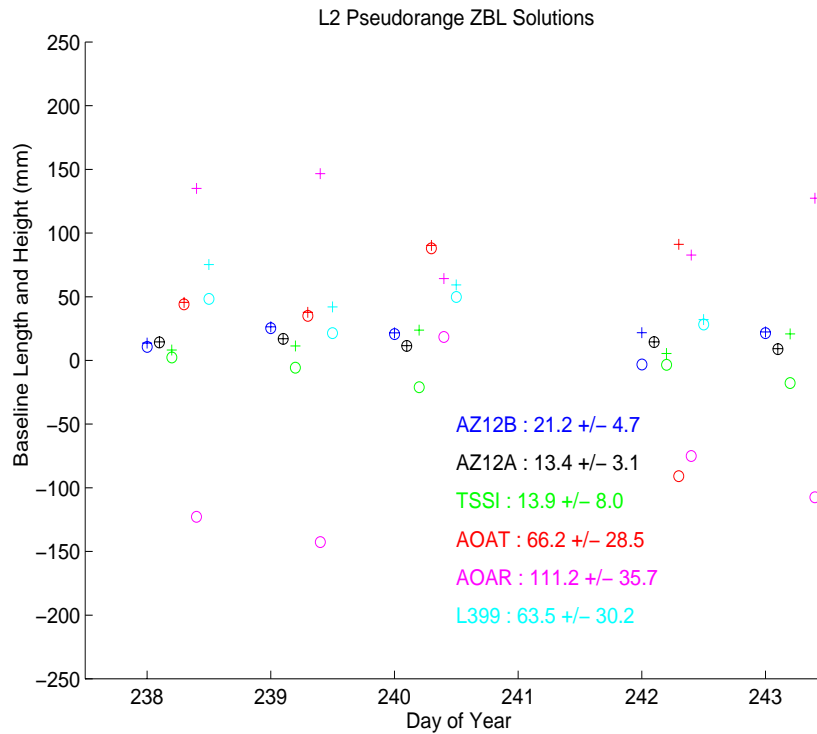


Figure 1.2: Color coded baseline and height solutions using L2 pseudorange observations. The order and color scheme are the same as the L1 pseudorange solutions.

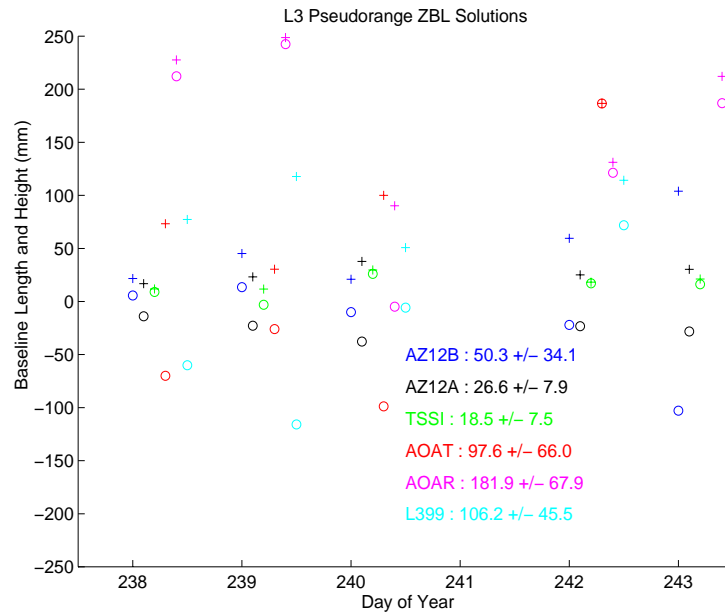


Figure 1.3: Color coded baseline and height solutions using L3 pseudorange observations. The order and color scheme are the same for the L1 and L2 pseudorange solutions.

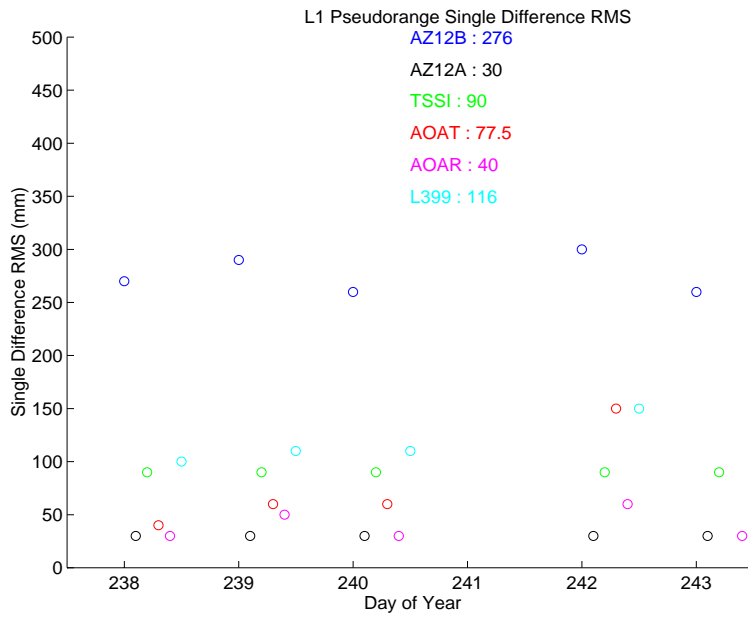


Figure 1.4: Single difference RMS values for L1 pseudorange observations. The daily receiver solutions are plotted in the following order: AZ12B, AZ12A, TSSI, AOAT, AOAR, and L399.

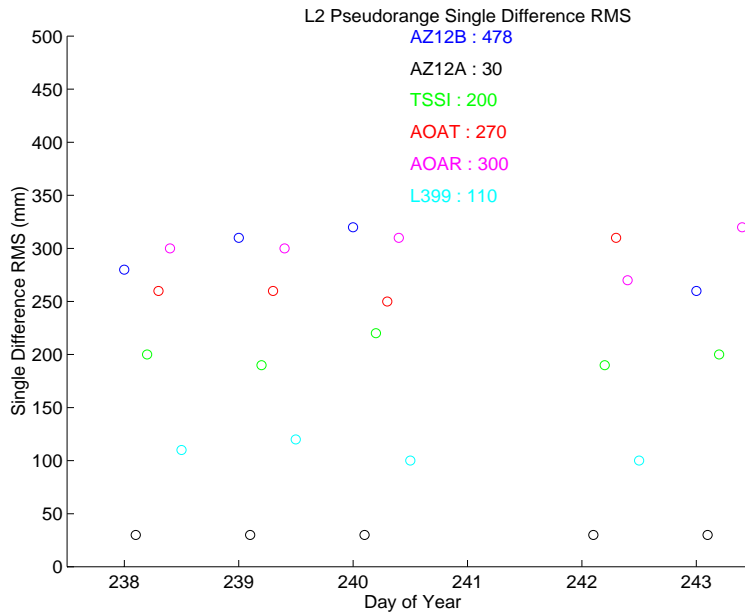


Figure 1.5: Single difference RMS values for L2 pseudorange observations. The color scheme and order are the same as the L1 single difference RMS plot.

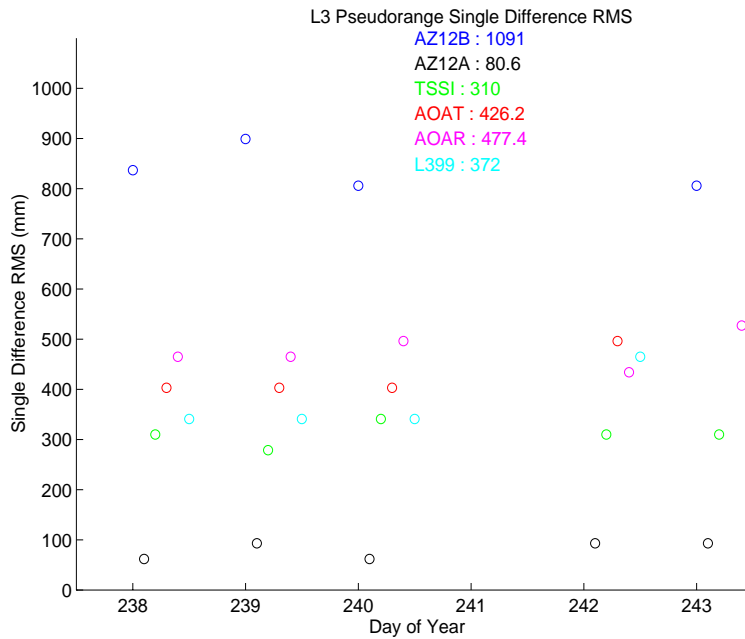


Figure 1.6: Single difference RMS values for L3 pseudorange observations. The color scheme and plotting order are the same as the L1 and L2 pseudorange single difference observations.

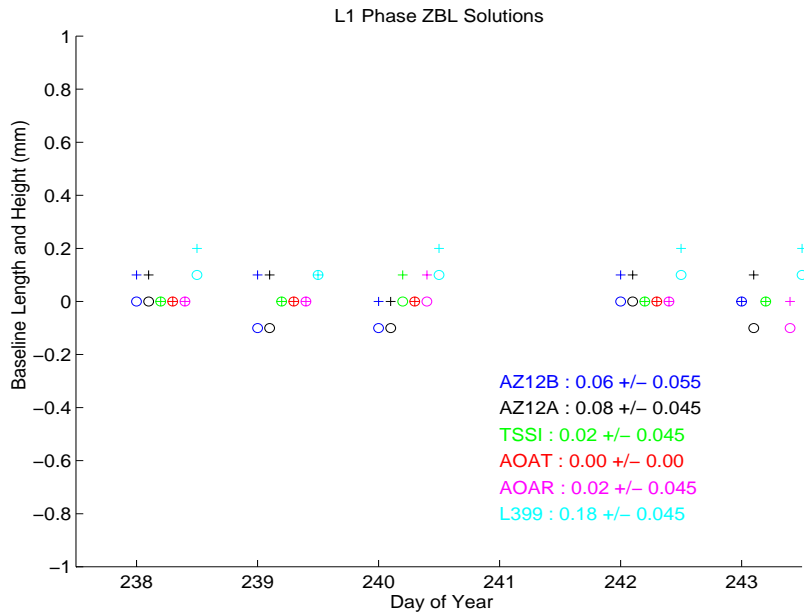


Figure 1.7: Color coded baseline and height solutions using L1 phase observations. The daily receiver type solutions are plotted in the following order: AZ12B, AZ12A, TSSI, AOAT, AOAR, and L399. Each color represents a different receiver type. The length solutions are plus marks (+). Height solutions are circles (o).

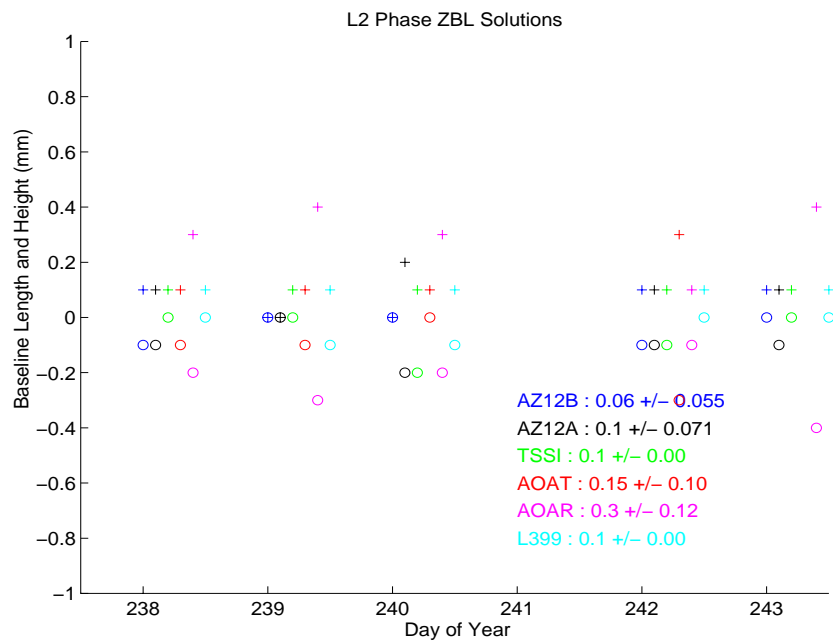


Figure 1.8: Color coded baseline and height solutions using L2 phase observations. The order and color scheme is the same as the L1 phase plot. The AZ12B, AZ12A and TSSI solutions have slightly smaller biases and RMS scatters than the other three receivers.

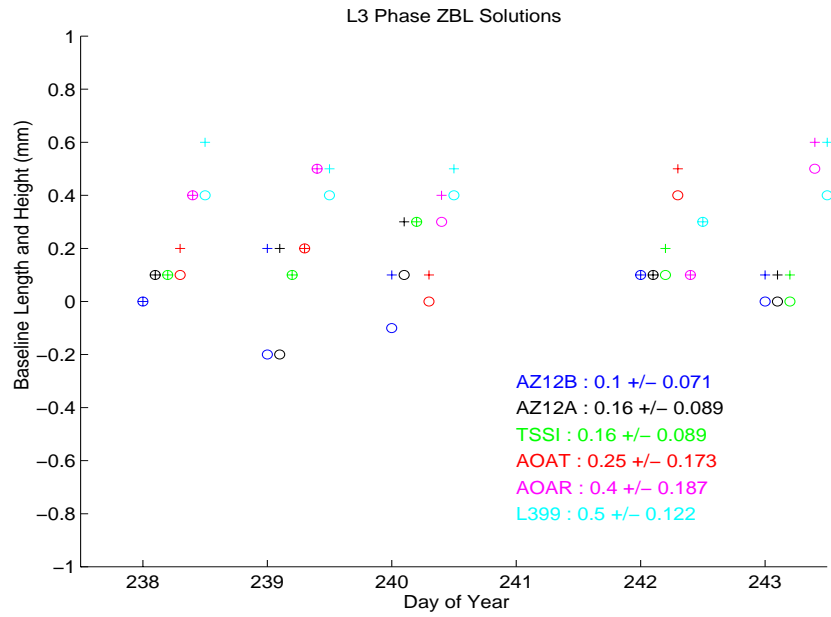


Figure 1.9: Color coded baseline and height solutions using L3 phase observations. The order and color scheme is the same for the L1 and L2 phase baseline solutions.

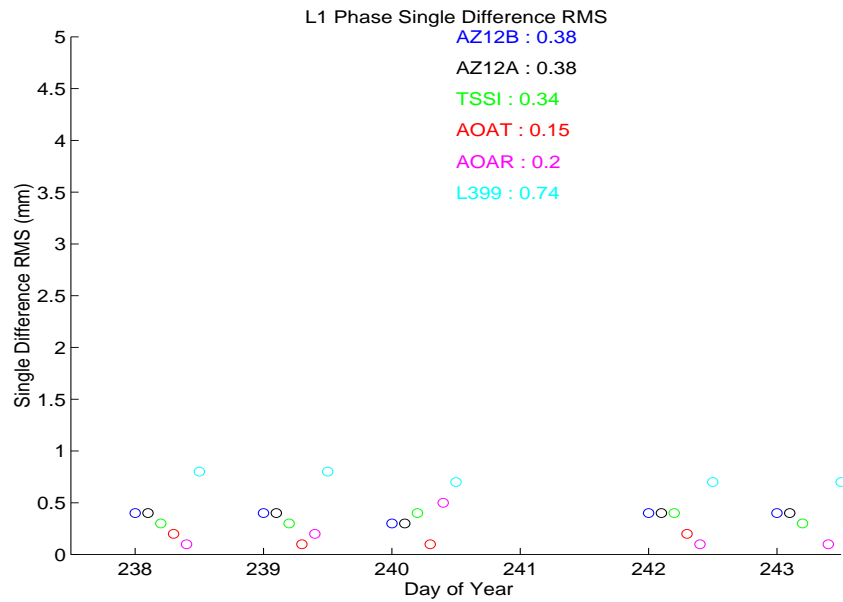


Figure 1.10: Single difference RMS values for L1 phase observations.

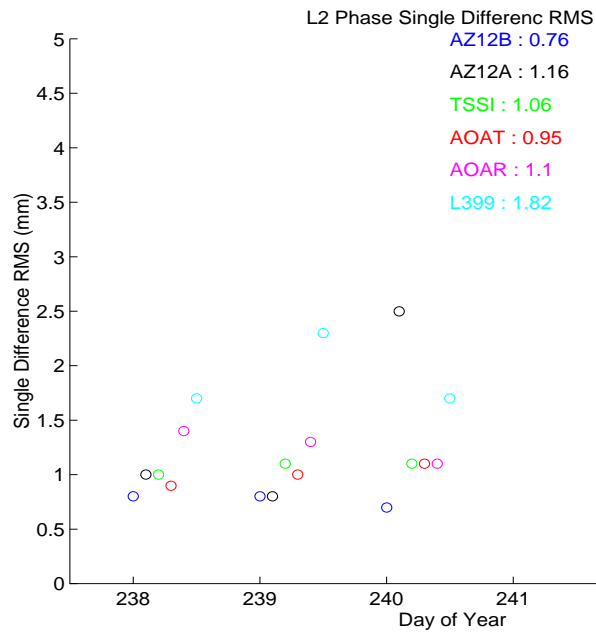


Figure 1.11: Single difference RMS values for L2 phase observations.

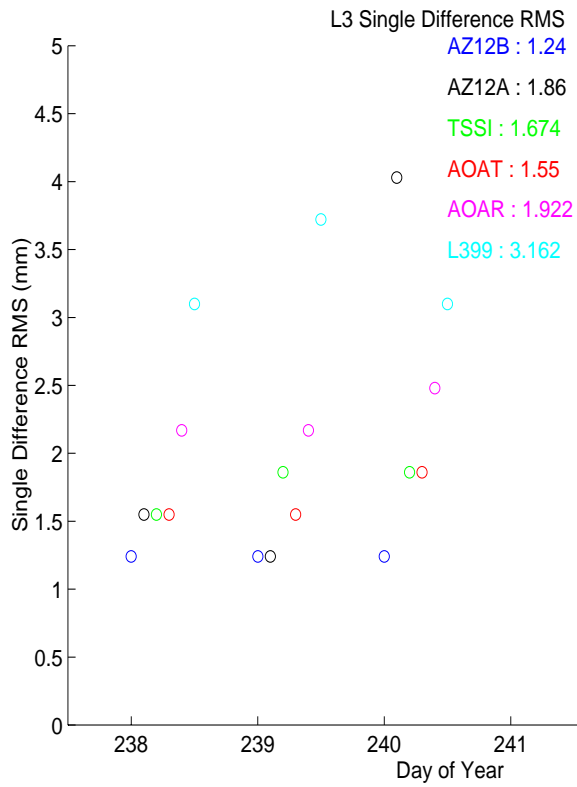


Figure 1.12: Single difference RMS values for L3 phase observations.

# Pseudorange Double Difference Residuals

## L1 Pseudorange Double Difference Residuals

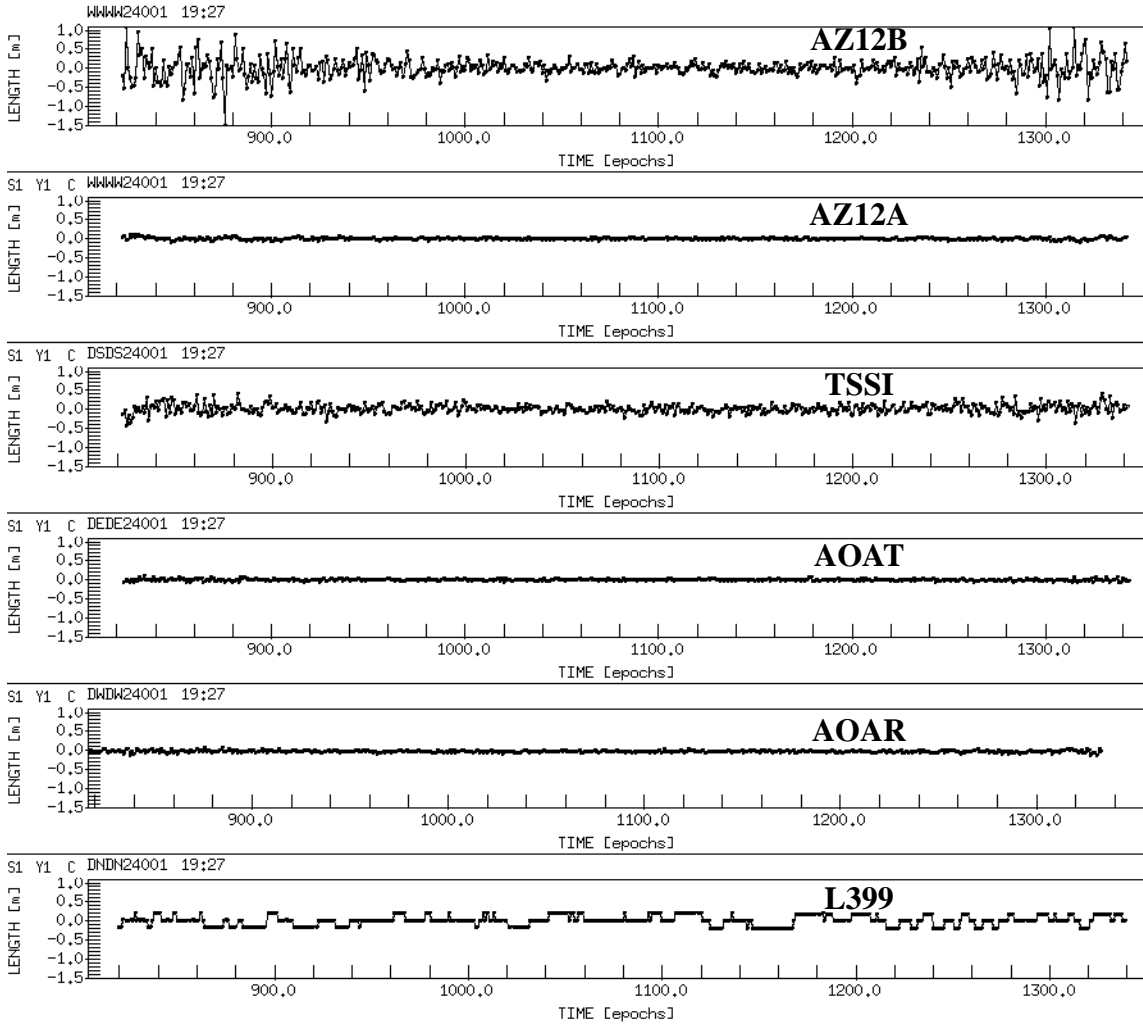


Figure 1.13: L1 pseudorange double difference residuals for all receiver types. The double difference pair is of SVS 19 and 27 on day 240. Each trace is labeled by its receiver type.

## L2 Pseudorange Double Difference Residuals

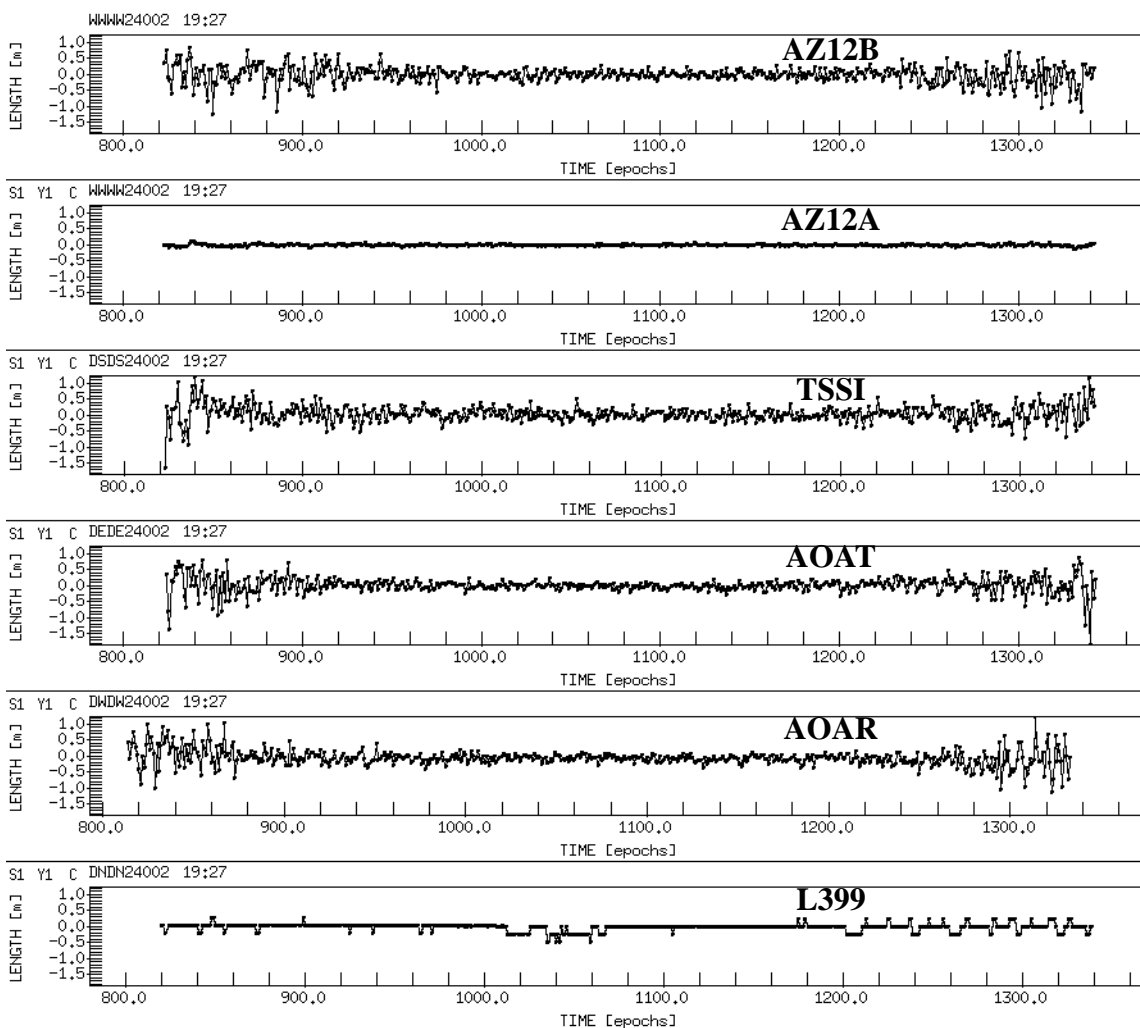


Figure 1.14: L2 pseudorange double difference residuals for all receiver types. The double difference pair is of SVS 19 and 27 on day 240. Each trace is labeled by its receiver type.

### L3 Pseudorange Double Difference Residuals

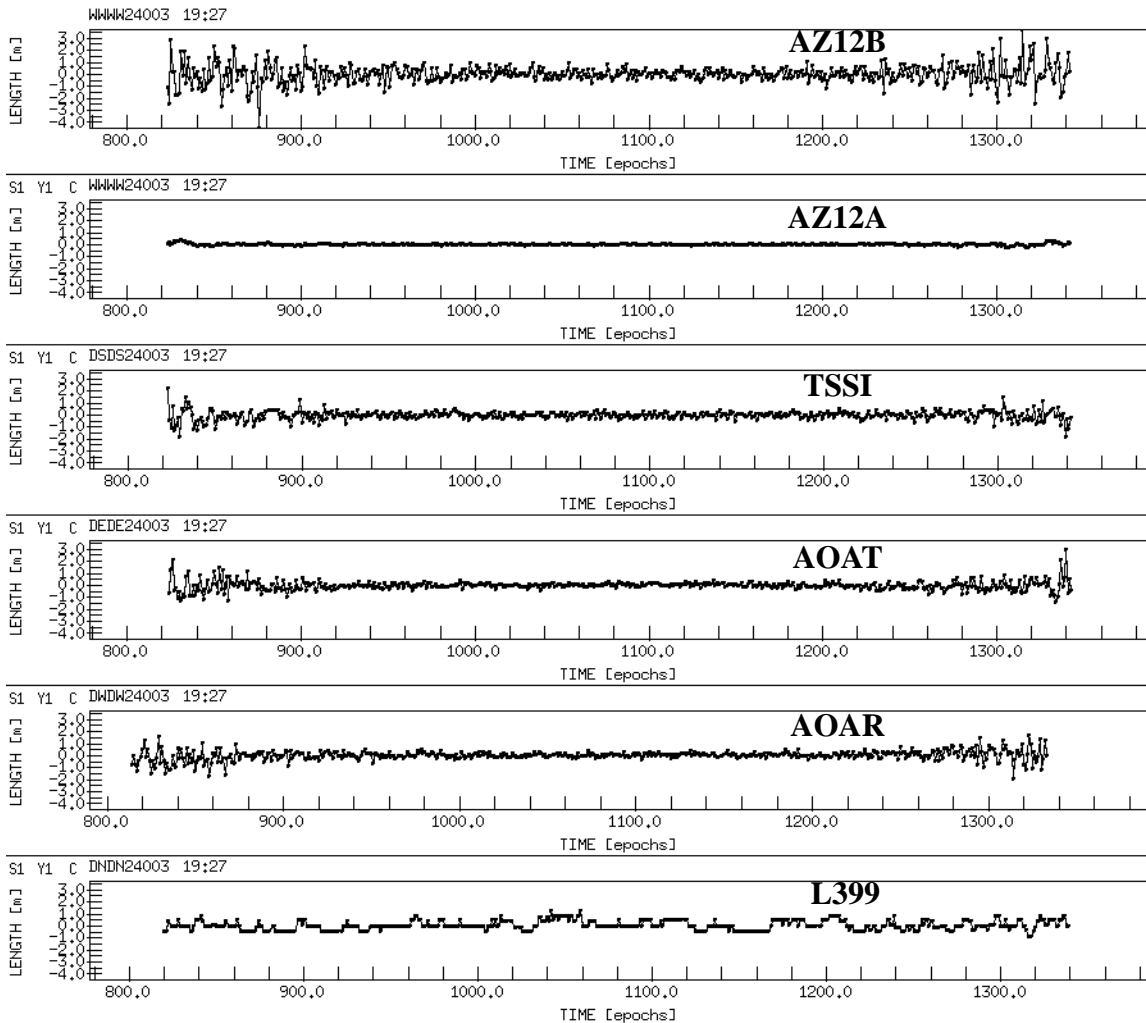


Figure 1.15: Ionosphere free, L3, pseudorange double difference residuals for all receiver types. The double difference pair is of SVS 19 and 27 on day 240. Each trace is labeled by its receiver type.

# Phase Double Difference Residuals

## L1 Phase Double Difference Residuals

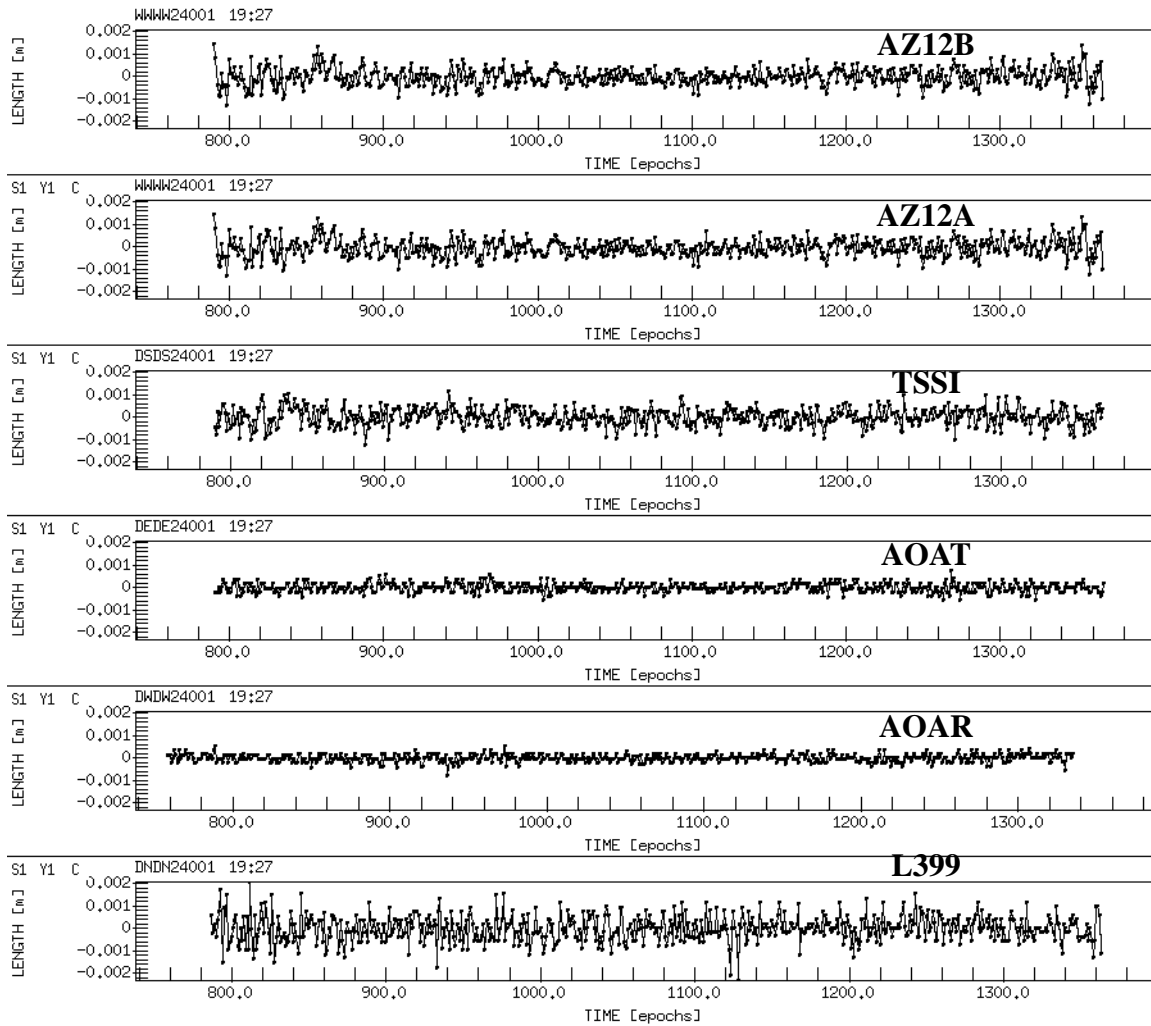


Figure 1.16: L1 phase double difference residuals for all receiver types. The double difference pair is for SVS 19 and 27 on day 240. Each trace is labeled by its receiver type.

## L2 Phase Double Difference Residuals

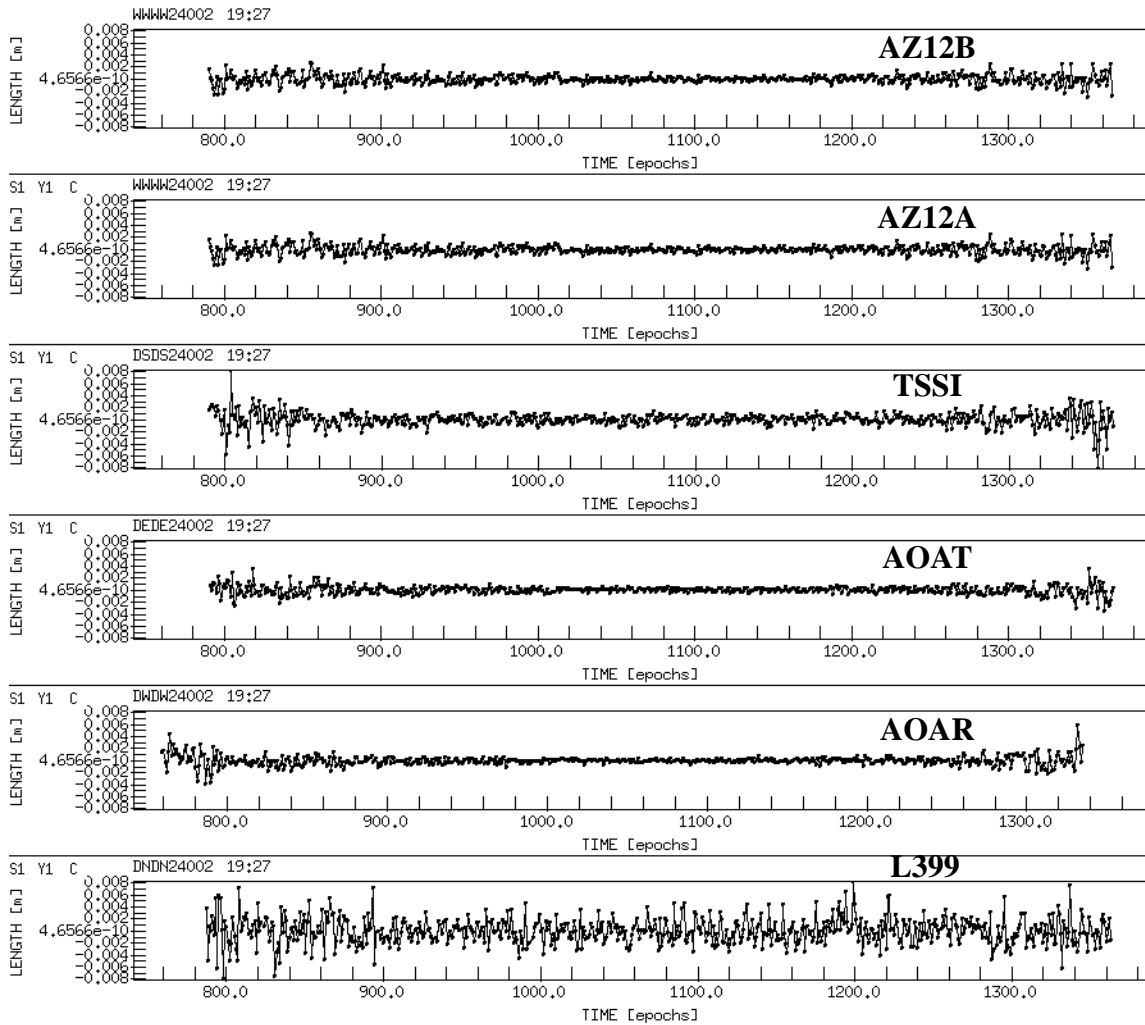


Figure 1.17: L2 phase double difference residuals for all receiver types. The double difference pair is for SVS 19 and 27 on day 240. Each trace is labeled by its receiver type.

### L3 Phase Double Difference Residuals

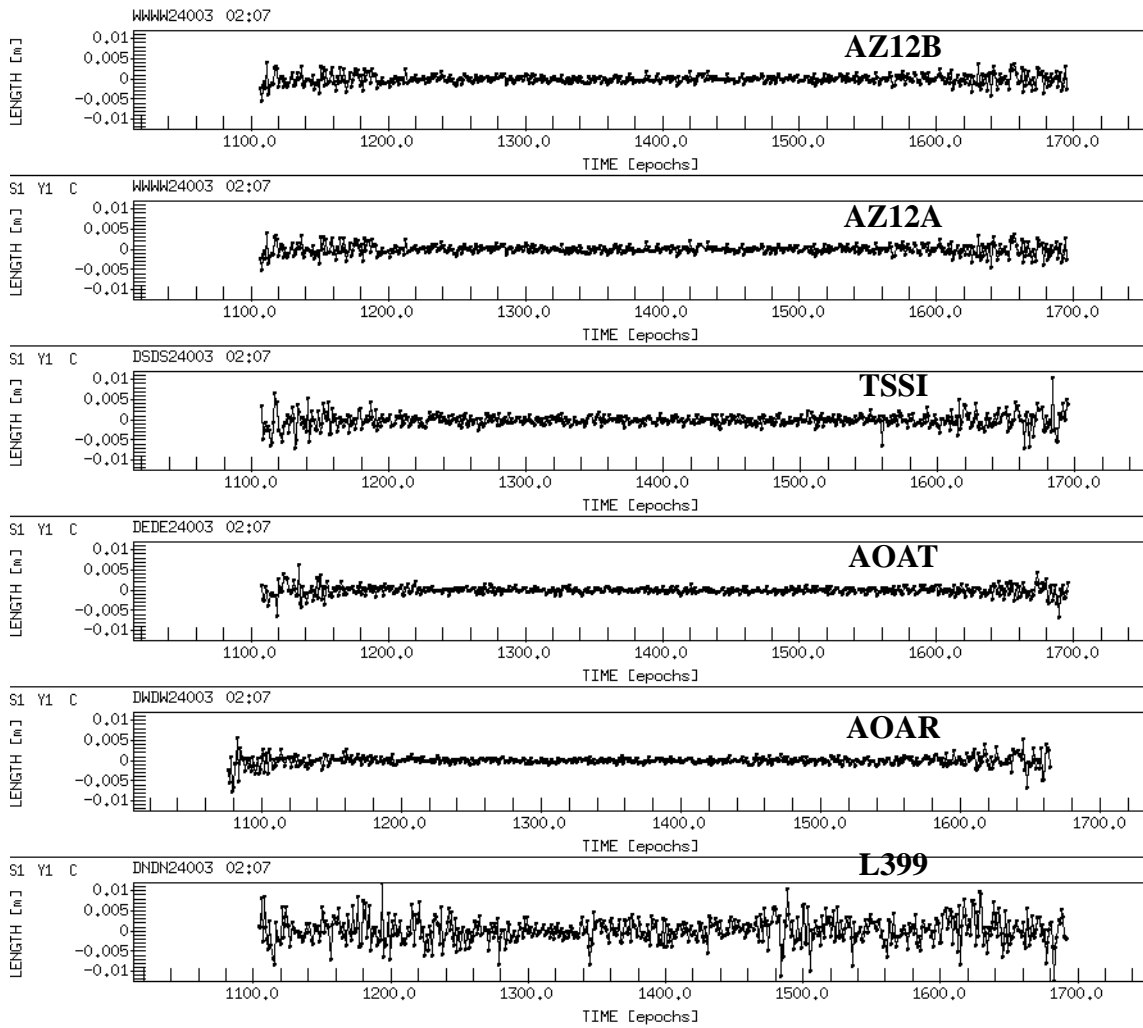


Figure 1.18: Ionosphere free, L3, phase double difference residuals for all receiver types. The double difference pair is for SVS 19 and 27 on day 240. Each trace is labeled by its receiver type.

## 1.4 High Rate Zerobaseline Tests

Each receiver type was tested on a zerobaseline with their respective antenna. Data were sampled at a 1 second interval. The resulting observations reflect receiver noise, with minimum phase or code averaging. The maximum receiver averaging times were shown in Table 5. At one second sampling, the averaging time is minimized for each receiver, and observations are minimally correlated from epoch to epoch. Data were processed with 15 deg elevation cutoff and results are without tropospheric estimates. The RMS of the one-second zerobaseline single difference residuals is given in Table 1.2 and compared with 30 second results given in Table 1.3. The L3 (ionosphere free) double difference residuals are plotted in Figure 1.19.

The most significant differences in RMS between the one second and 30 second sampling rates are with the AOAT and AOAR receivers. Both have L3 phase RMS increased by a factor of 2.5 and the L3 pseudorange RMS increased by a factor of 1.6 and 2.5 respectively.

**Table 1.2: RMS of Single Difference in millimeters (1 second sampling)**

Receiver	L1 Phase	L2 Phase	<b>L3 Phase</b>	L1 Code	L2 Code	L3 Code
AZ12B	0.3	0.8	<b>1.2</b>	330	330	990
AZ12A	0.3	0.8	<b>1.2</b>	40	40	90
SR399	0.4	1.5	<b>2.2</b>	80	90	270
AOAR	0.2	2.9	<b>4.7</b>	150	490	750
TSSI	0.3	1.0	<b>1.6</b>	100	290	420
AOAT	0.7	2.5	<b>4.0</b>	160	700	1050

**Table 1.3: RMS of Single Difference in millimeters (30 second sampling) from Figures 1.4-16 and 1.10-1.12.**

Receiver	L1 Phase	L2 Phase	<b>L3 Phase</b>	L1 Code	L2 Code	L3 Code
AZ12B	0.4	0.8	<b>1.2</b>	276	478	1091
AZ12A	0.4	1.2	<b>1.9</b>	30	30	81
SR399	0.7	1.8	<b>3.3</b>	116	110	372
AOAR	0.2	1.1	<b>1.9</b>	40	300	477
TSSI	0.3	1.1	<b>1.7</b>	90	200	310
AOAT	0.2	1.0	<b>1.6</b>	77	270	426

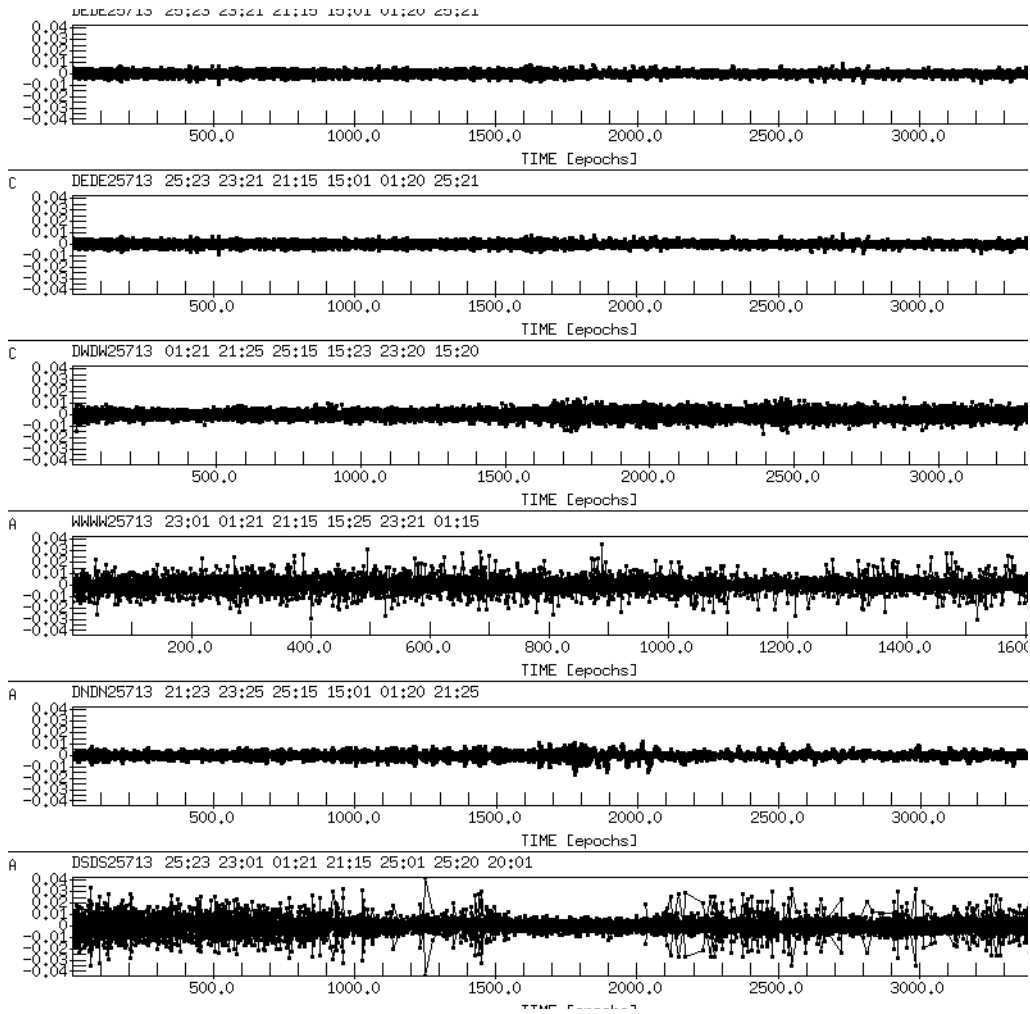


Figure 1.19: L3 phase residuals for 1 second, zerobaseline data. Note that only the first half of the AOAR data could be processed so the trace has half the number of epochs as the rest.

## 1.5 Ambiguity Resolution Summary

All of the zero and short baseline results in this report were computed with resolved double difference carrier phase ambiguities. L1 and L2 ambiguities were resolved when the L1 and L2 phase results were computed. These resolved ambiguities were then introduced for the L3 solutions. We also resolved the widelane (L5) ambiguities using the Melbourne/Wuebbena method. This method is independent of geometric parameters, station coordinates, and satellite position, but depends on the phase and pseudorange measurement noise. Resolution of L5 ambiguities using this method is especially important for ambiguity resolution on long baselines of several hundred to thousand km.

It has been shown that ambiguity resolution is important for achieving highest accuracy geodetic results. In the following we show the non-integer parts of the carrier phase ambiguities for zero (Figures 1.20 and 1.21) and for short (Figures 1.22 and 1.23) baselines.

The smaller the non integer component of the ambiguity, the easier it is to resolve this ambiguity. Zero baseline ambiguities are affected by receiver measurement noise only, while the short baseline ambiguities are also affected by antenna performance and multipath.

Each of the panels in Figures 1.20 - 1.23 summarizes between 60-120 ambiguities from different short and zero baseline solutions and can be used for comparisons.

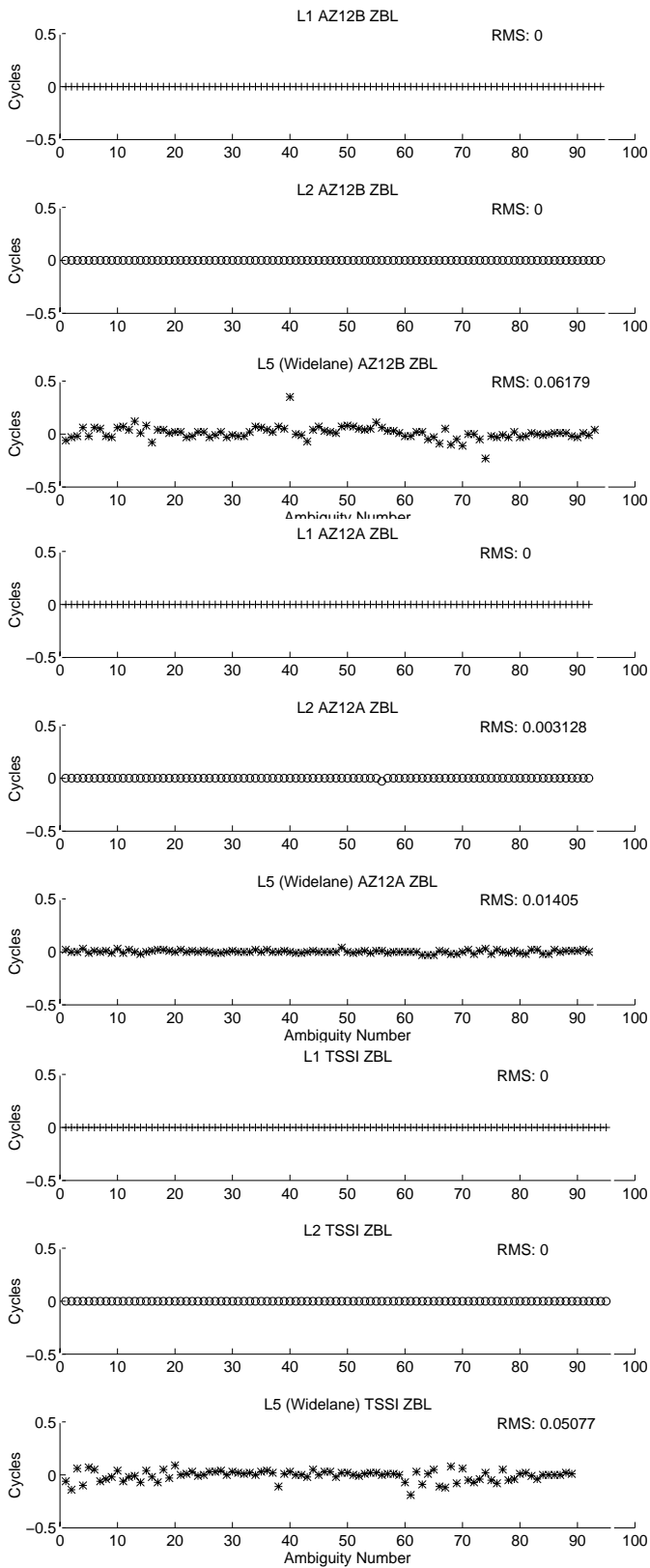


Figure 1.20: Zero-baseline ambiguity non-integer components of the L1, L2 and L5 ambiguities. From top to bottom results for the AZ12B, AZ12A, and TSSI are shown. RMS scatter of all the ambiguities about zero is also shown.

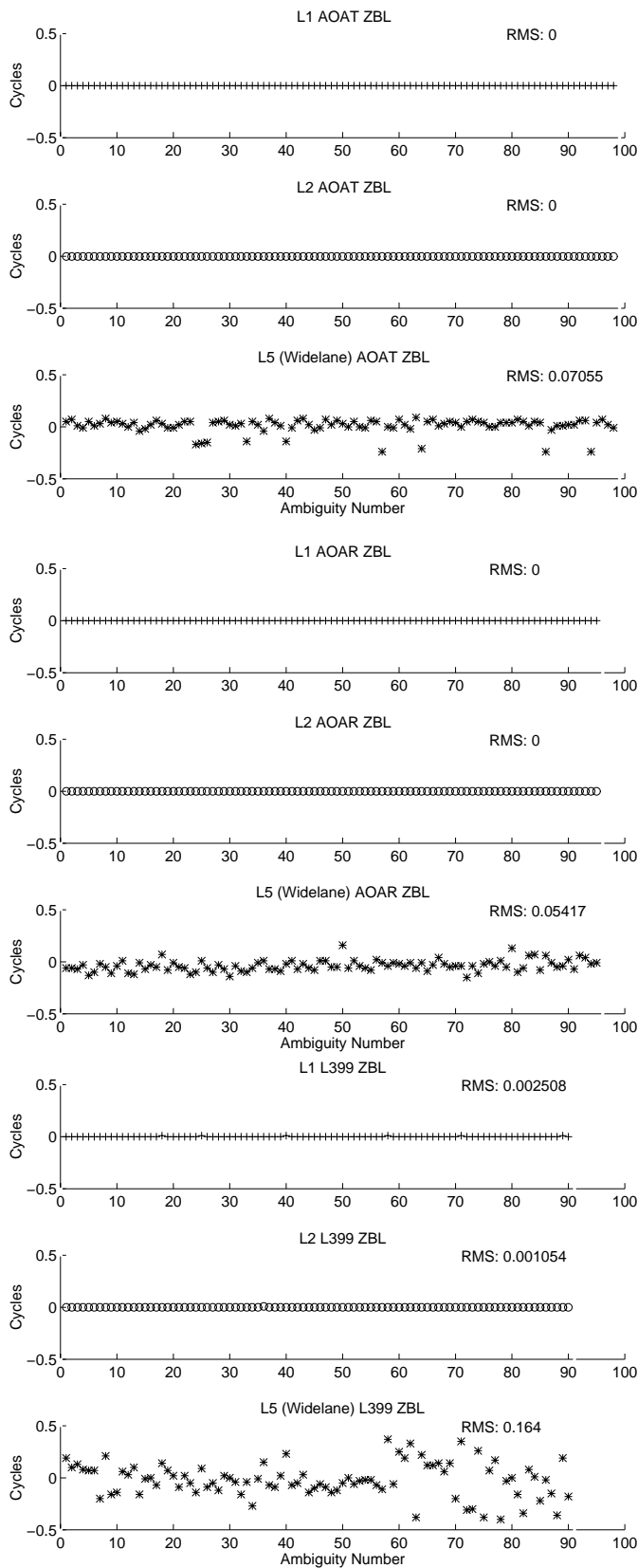


Figure 1.21: Figure 2. Zero-base-line ambiguity non-integer components of the L1, L2 and L5 ambiguities. From top to bottom results for the AOAT, AOAR, and L399 are shown. RMS scatter of all the ambiguities about zero is also shown.

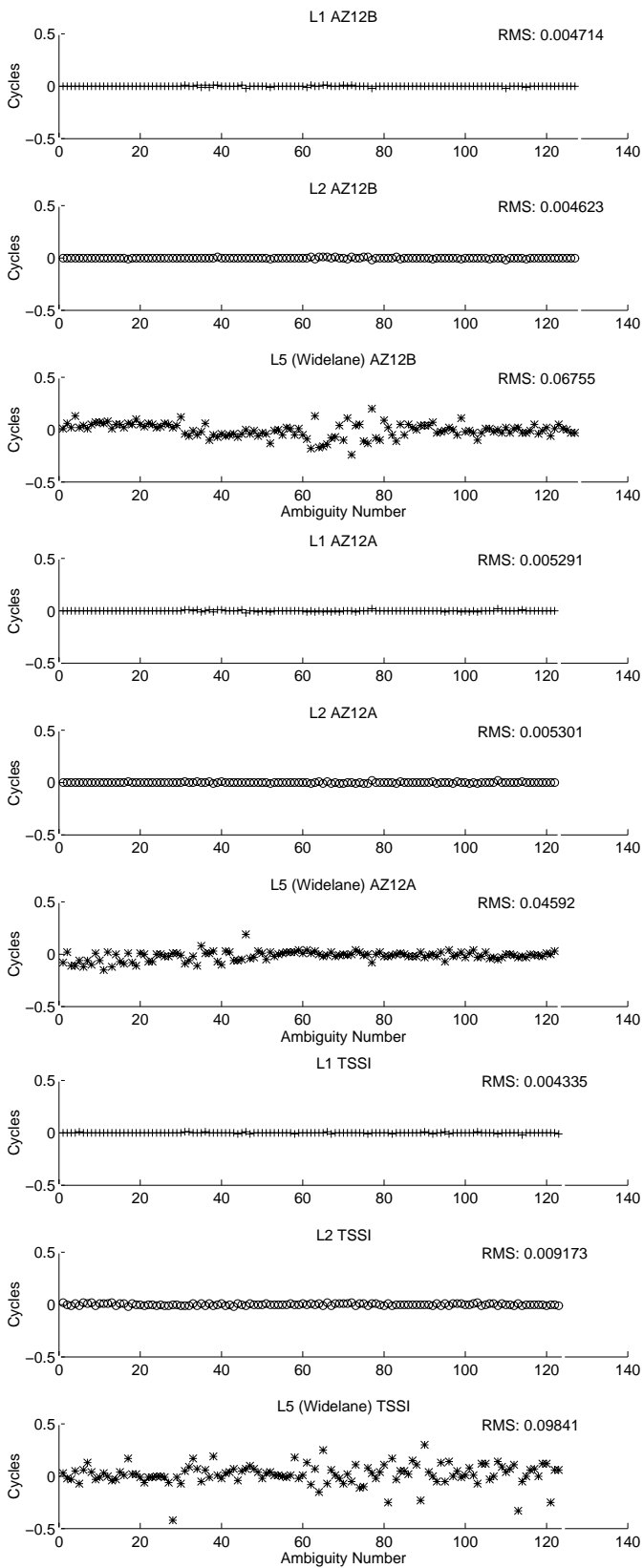


Figure 1.22: Figure 3. Short-baseline ambiguity non-integer components of the L1, L2 and L5 ambiguities. From top to bottom results for the AZ12B, AZ12A, and TSSI are shown. RMS scatter of all the ambiguities about zero is also shown.

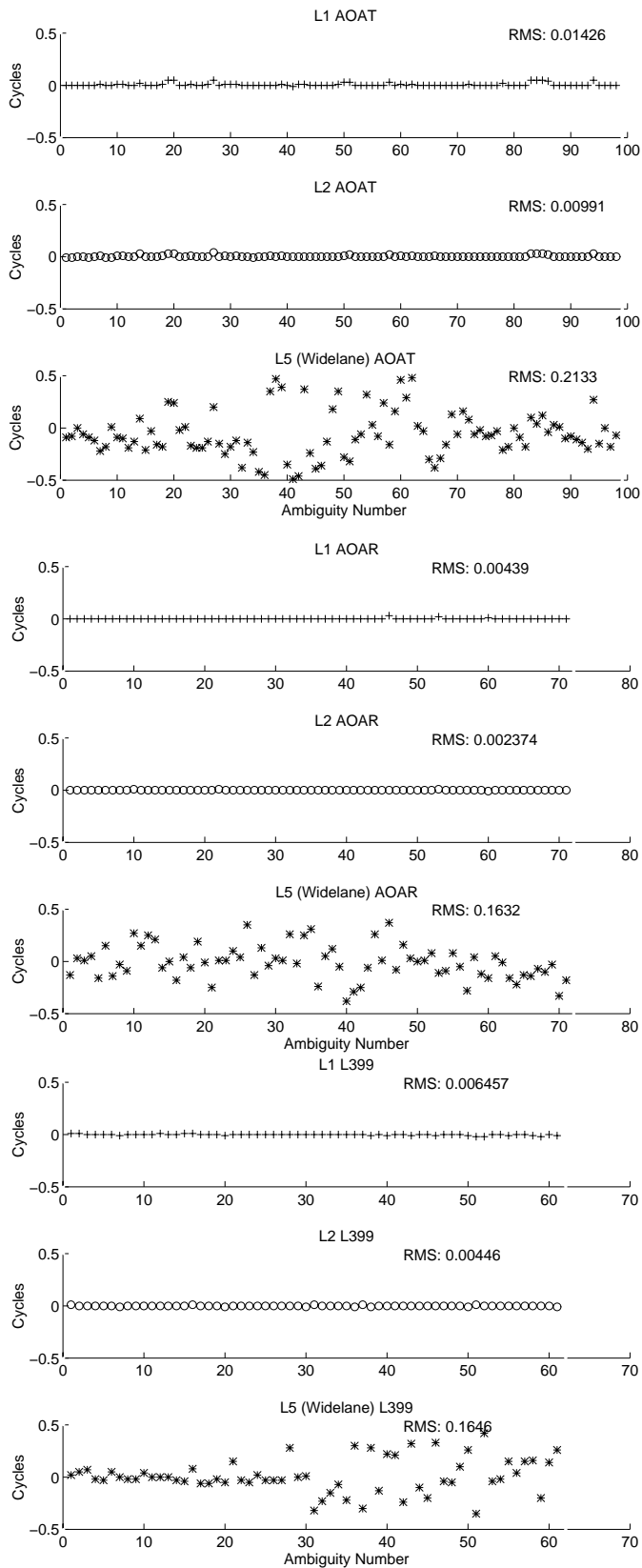


Figure 1.23: Figure 4. Short-baseline ambiguity non-integer components of the L1, L2 and L5 ambiguities. From top to bottom results for the AOAT, AOAR, and L399 are shown. RMS scatter of all the ambiguities about zero is also shown.

## **1.6 Receiver Mixing - 5 way splitter**

A zerobaseline test was made combining all receivers with a 5-way WR, Inc. splitter to a AOA Choking antenna. Data were collected with a 30 second sampling rate and all possible mixed receiver combinations were processed. The mixed zerobaseline phase solutions differed between 1 and 3 mm in the L1 and L2, and from less than 1 mm to 6 mm in the L3 without tropospheric estimation. When the troposphere is estimated, the differences increase to 1 to 4 mm in the L1 and L2 and from 1 to 7 mm in the L3 and are several times larger than obtained with unmixed receivers. These results are preliminary and further tests will be conducted.

## 2. Short Baseline Solutions

### 2.1 Introduction and Experiment Description

The six marks on Table Mountain were used to measure three short baselines (<6 meters). Figure 2.1 contains a small map showing the three baselines used in the tests. These measurements test the receiver and antenna system. Most environmental errors (atmosphere and orbit errors) will difference out.

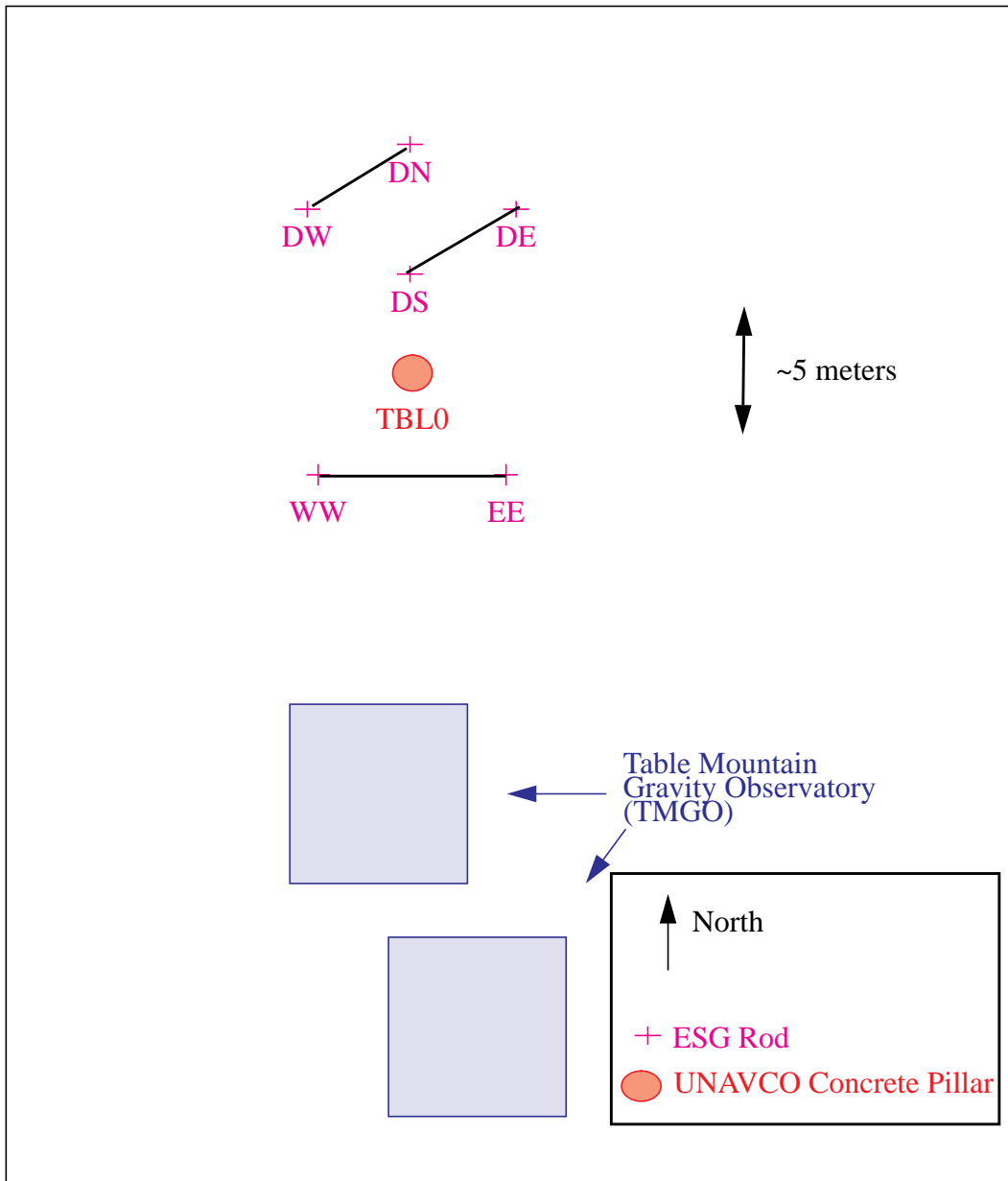


Figure 2.1: Relative location of monuments used for short baseline tests during UNAVCO ARI receiver tests.

For the short baseline tests, each receiver type occupied each of the three baselines. The AOAR and AOAT receivers only had two antennas for the four receivers. This lengthened the number of days needed to complete this part of the testing. While the AOAR and AOAT receivers were completing this section, the AZ12 and the TSSI receivers were used to resurvey one or two of the short baselines. Therefore these two receiver types have more than one measurement for some of the baselines. Every daily session had an epoch rate of 30 seconds and tracked for 20 hours. All data above 15 degrees elevation were processed.

Data were processed in an automated shell script. On a single station level, the pseudorange observations were checked for gross outliers. Observations with residuals of greater than 100 m or more than 5 times the RMS of all the pseudorange measurements were deleted. Pseudorange observations above 15 degrees were used to compute receiver clock corrections. Phase and pseudorange baseline lengths were calculated using observations above 15 degrees. L1 and L2 phase observations were checked separately for outliers and cycle slips using triple difference observations. Fixing of cycle slips was only attempted for data gaps shorter than 181 seconds. Phase ambiguities were introduced for any larger data gaps.

The solutions for this section are plotted relative to a “ground truth”. This “ground truth” was computed using GPS observations from six Trimble 4000 SSE receivers and antennas from the UNAVCO pool. All antennas were mounted approximately 1.5 meters high. Two days of observations were taken, and the L1 phase network solutions were used. The differences between the two daily network solutions were less than or equal to 0.1 mm for all baselines, in all components. As a check on the quality of these solutions, the vertical components of the baselines were compared to vertical differences in station coordinates obtained using conventional surveying equipment. The differences between the conventional heights and the heights used as “ground truth” differ by less than 2 mm for all baselines.

## **2.2 Summary of Phase and Pseudorange Solutions**

In general, all receivers performed well. All packages exceeded the specifications outlined in the ARI purchase agreement. The results may be summarized with the following comments.

- L1 and L2 phase solutions compared to ground truth have a bias and RMS of less than 1.0 millimeters for all receivers
- L3 phase length solutions compared to ground truth have a bias and RMS of less than 1.0 millimeters for all receivers except the AOAR which has an rms of 1.8 millimeters.
- L1 and L2 pseudorange length solutions compared to ground truth have a bias and RMS of less than 50 millimeters for all receivers.
- L3 pseudorange length solutions compared to ground truth have a bias and RMS of less than 100 millimeters for all receivers.

## 2.3 L1 Phase Solutions

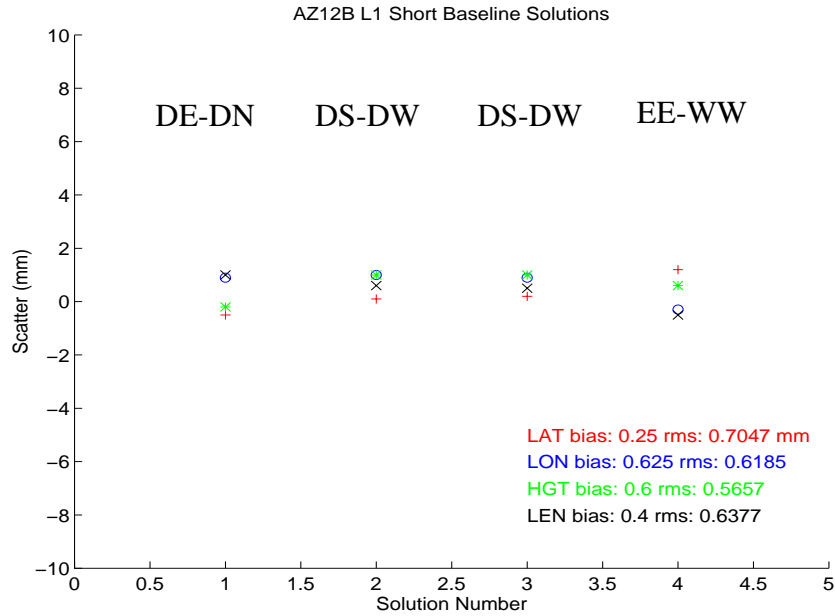


Figure 2.2: L1 short baseline solutions for the AZ12B receiver. The red plus signs (+) represent latitude, the circles (o) represent longitude, the asterisk (\*) represent height, and the crosses (x) represent length. The average and rms of each component has been computed for all the solutions.

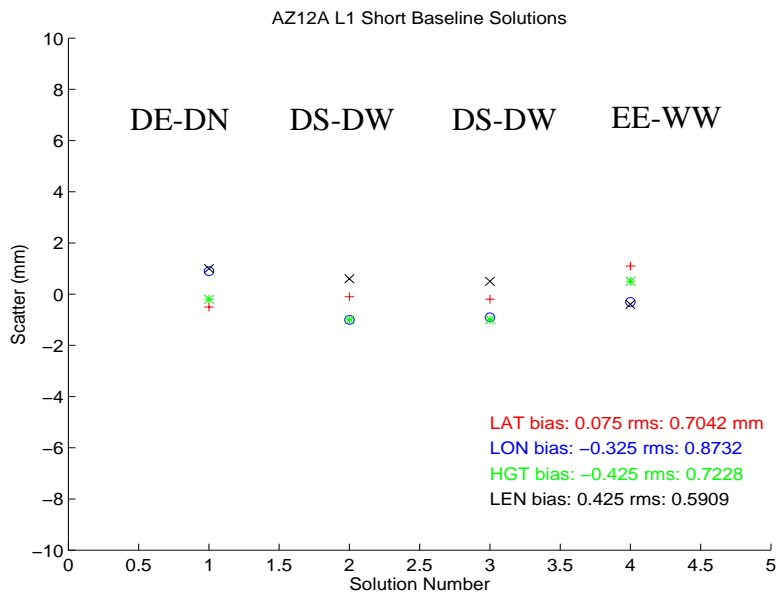


Figure 2.3: L1 short baseline solutions for the AZ12A receiver. The symbols are the same as in Figure 2.2

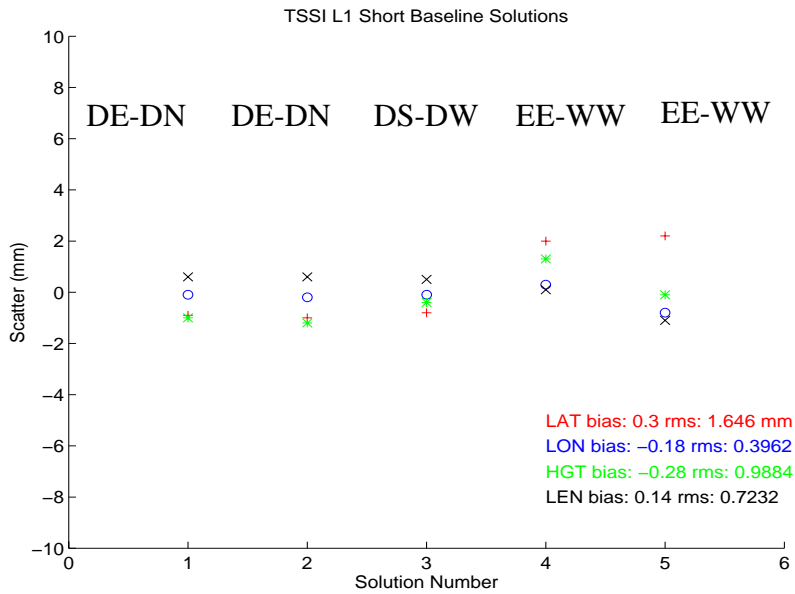


Figure 2.4: L1 short baseline solutions for the TSSI receiver. The symbols are the same as in Figure 2.2.

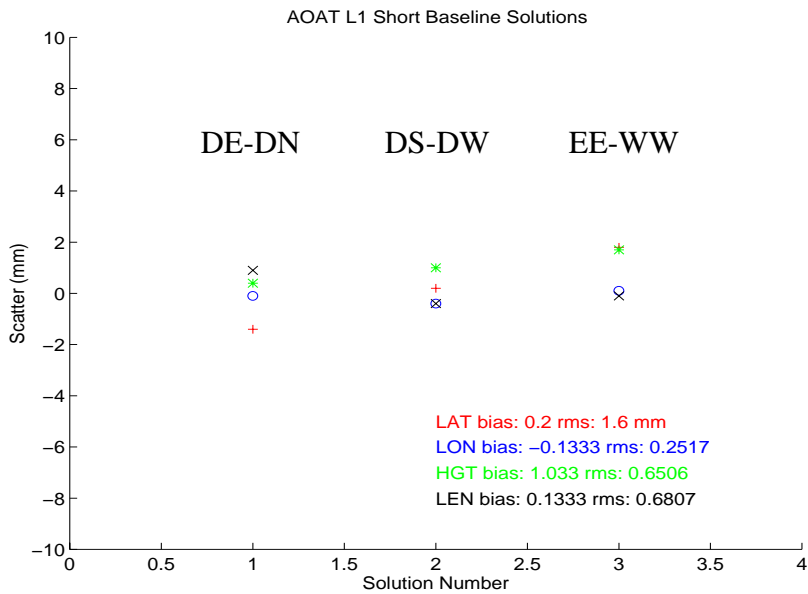


Figure 2.5: L1 short baseline solutions for the AOAT receiver. The symbols are the same as in Figure 2.2.

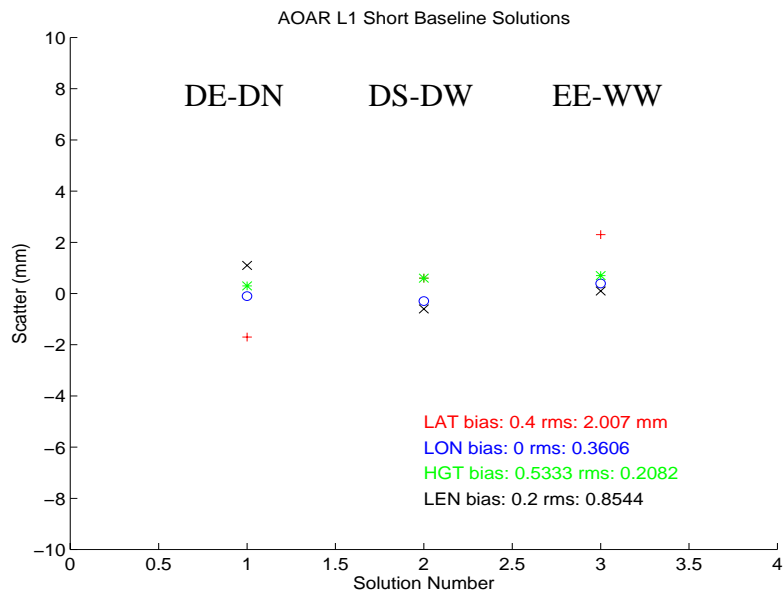


Figure 2.6: L1 short baseline solutions for the AOAR receiver. The symbols are the same as in Figure 2.2.

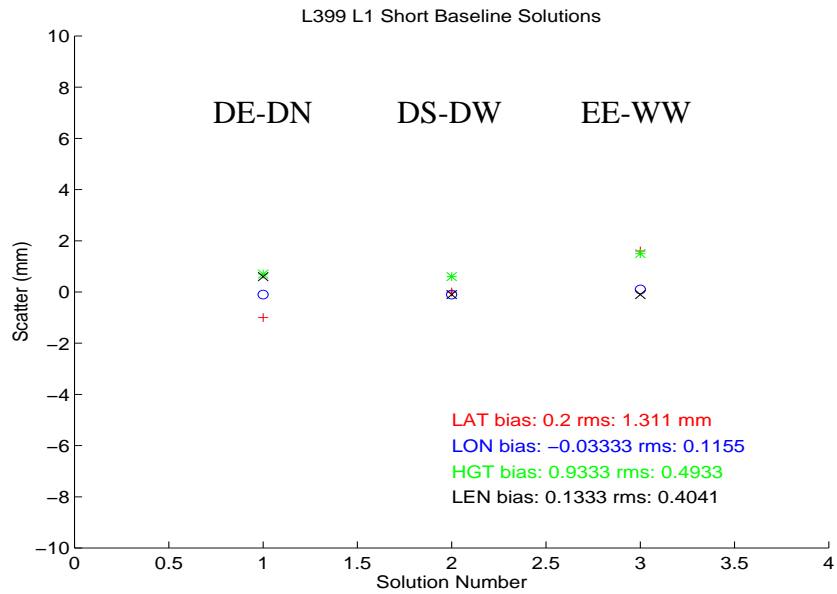


Figure 2.7: L1 short baseline solutions for the L399 receiver. The symbols are the same as in Figure 2.2.

## 2.4 L2 Phase Solutions

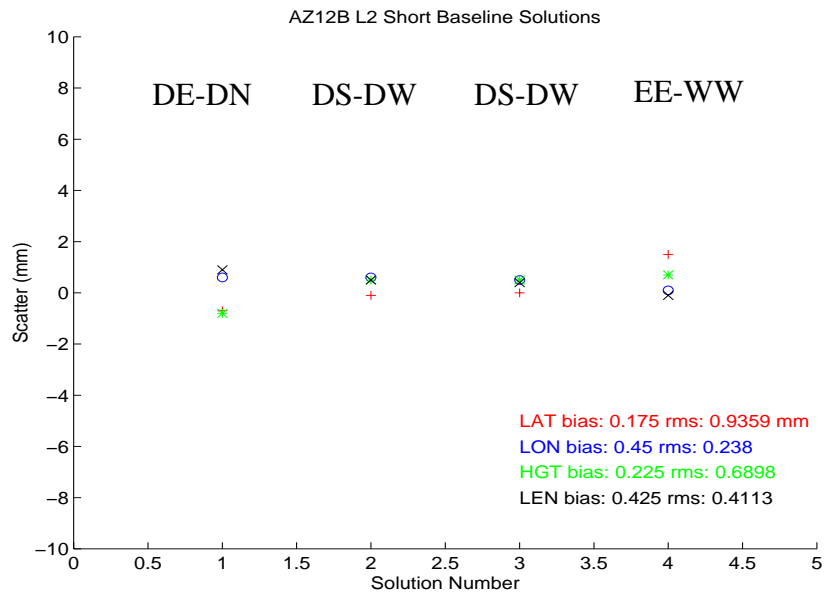


Figure 2.8: L2 short baseline solutions for the AZ12B receiver. The red plus signs (+) represent latitude, the circles (o) represent longitude, the asterisk (\*) represent height, and the crosses (x) represent length. The average and rms of each component has been computed for all the solutions.

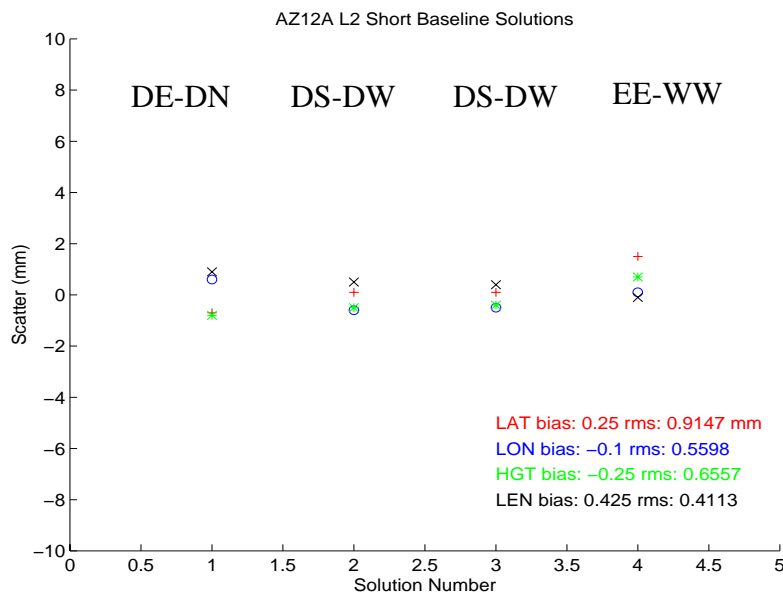


Figure 2.9: L2 short baseline solutions for the AZ12A receiver. The symbols are the same as in Figure 2.8.

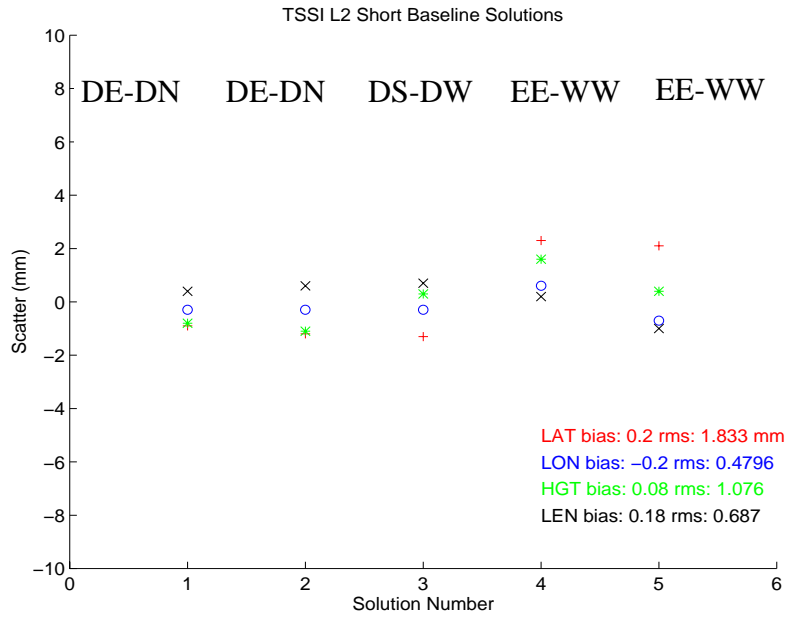


Figure 2.10: L2 short baseline solutions for the TSSI receiver. The symbols are the same as in Figure 2.8.

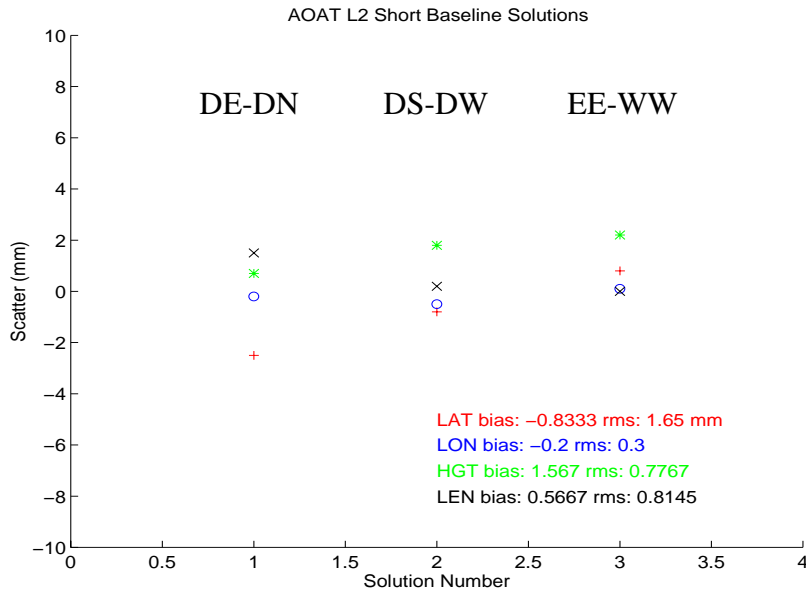


Figure 2.11: L2 short baseline solutions for the AOAT receiver. The symbols are the same as in Figure 2.8.

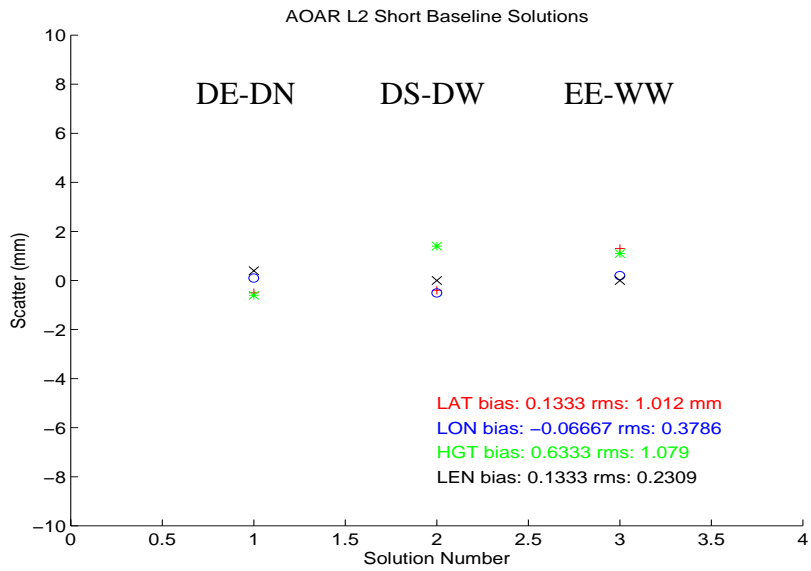


Figure 2.12: L2 short baseline solutions for the AOAR receiver. The symbols are the same as in Figure 2.8.

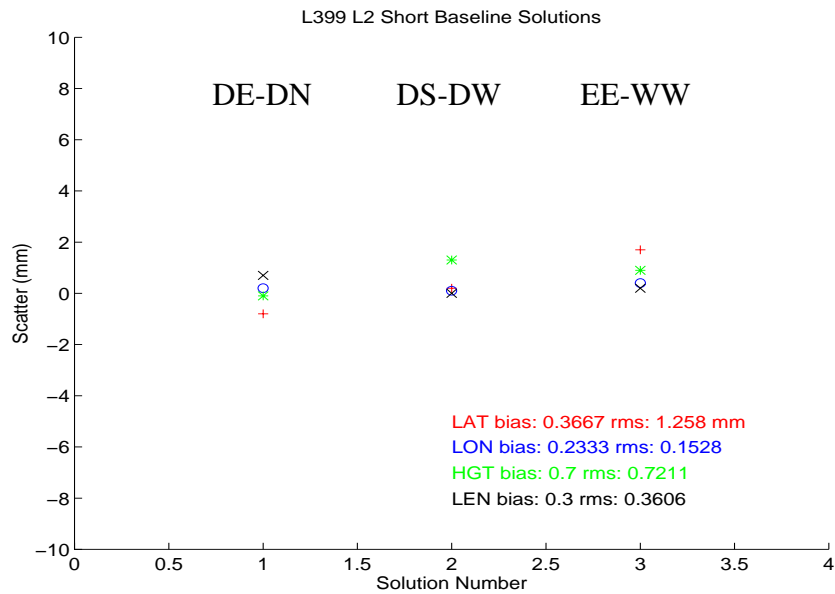


Figure 2.13: L2 short baseline solutions for the L399 receiver. The symbols are the same as in Figure 2.8.

## 2.5 L3 Phase Solutions

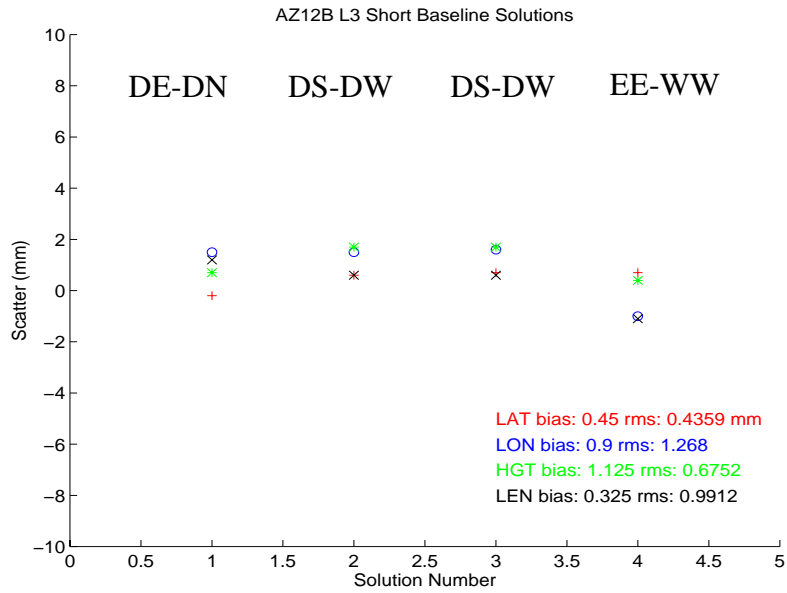


Figure 2.14: L3 short baseline solutions for the AZ12B receiver. The red plus signs (+) represent latitude, the circles (o) represent longitude, the asterisk (\*) represent height, and the crosses (x) represent length. The average and rms of each component has been computed for all the solutions.

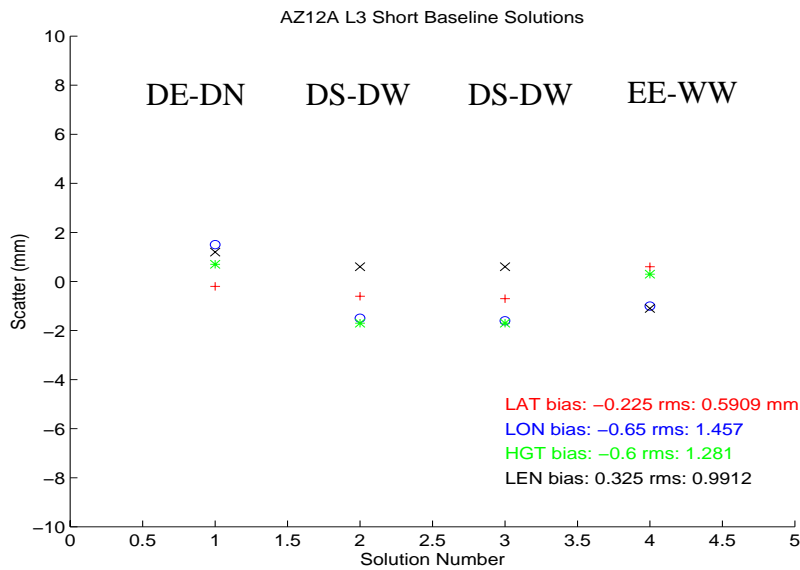


Figure 2.15: L3 short baseline solutions for the AZ12A receiver. The symbols are the same as in Figure 2.14.

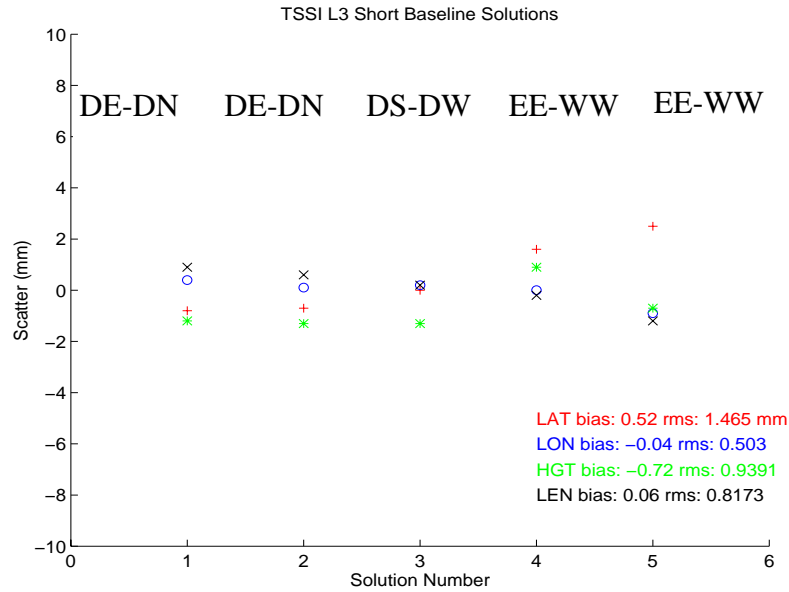


Figure 2.16: L3 short baseline solutions for the TSSI receiver. The symbols are the same as in Figure 2.14.

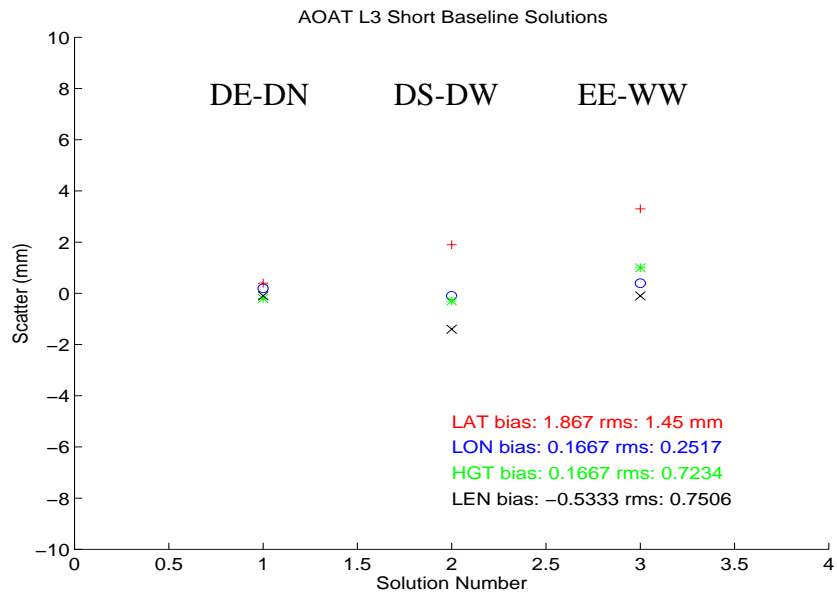


Figure 2.17: L3 short baseline solutions for the AOAT receiver. The symbols are the same as in Figure 2.14.

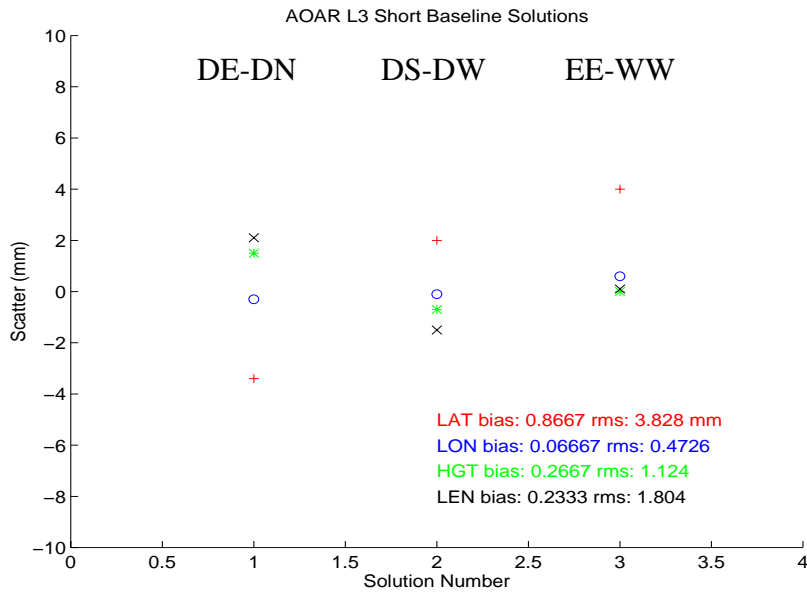


Figure 2.18: L3 short baseline solutions for the AOAR receiver. The symbols are the same as in Figure 2.14.

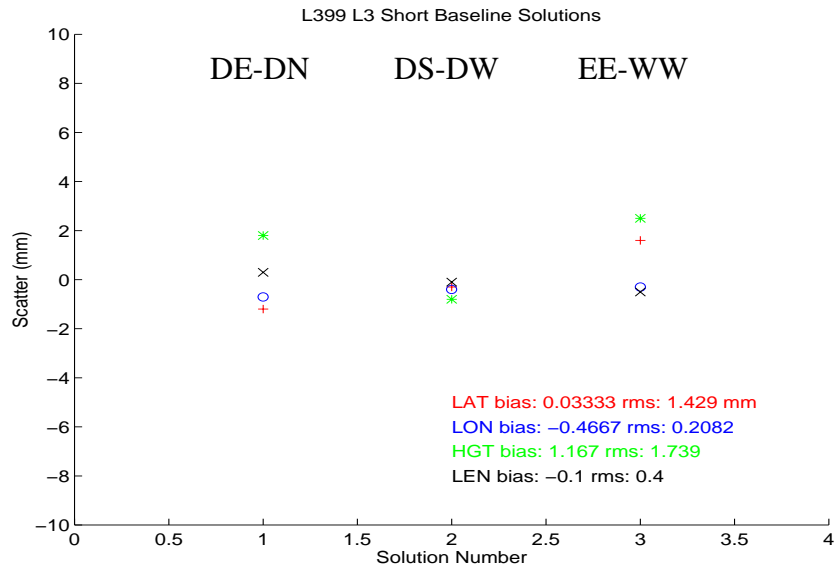


Figure 2.19: L3 short baseline solutions for the L399 receiver. The symbols are the same as in Figure 2.14.

## 2.6 L1 Pseudorange Solutions

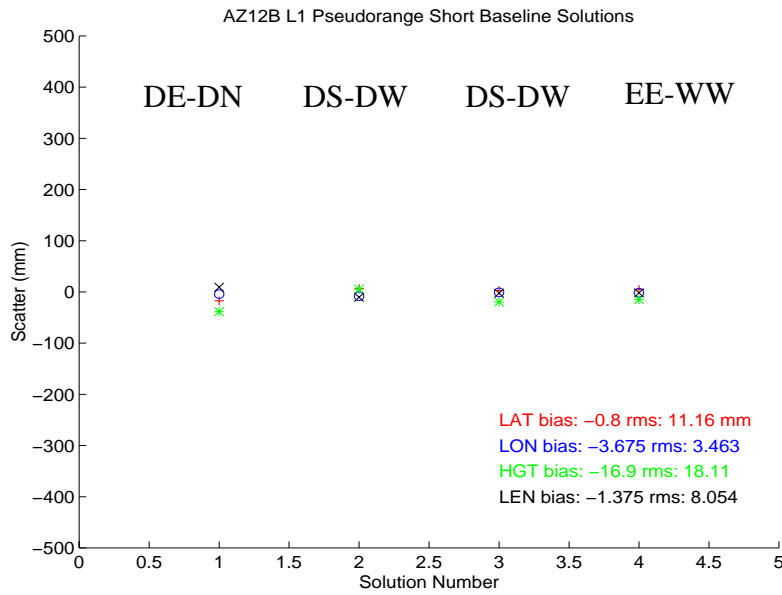


Figure 2.20: L1 pseudorange short baseline solutions for the AZ12B receiver. The red plus signs (+) represent latitude, the circles (o) represent longitude, the asterisk (\*) represent height, and the crosses (x) represent length. The average and rms of each component has been computed for all the solutions.

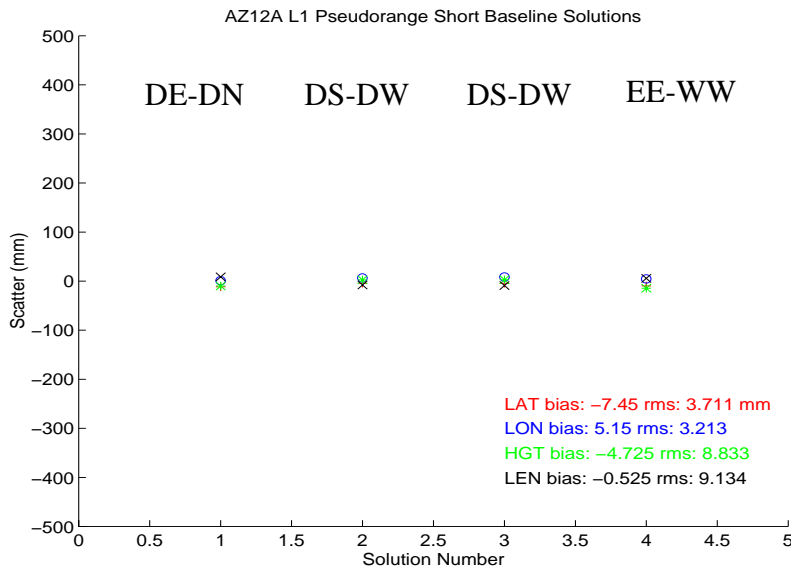


Figure 2.21: L1 pseudorange short baseline solutions for the AZ12A receiver. The symbols are the same as in Figure 2.20.

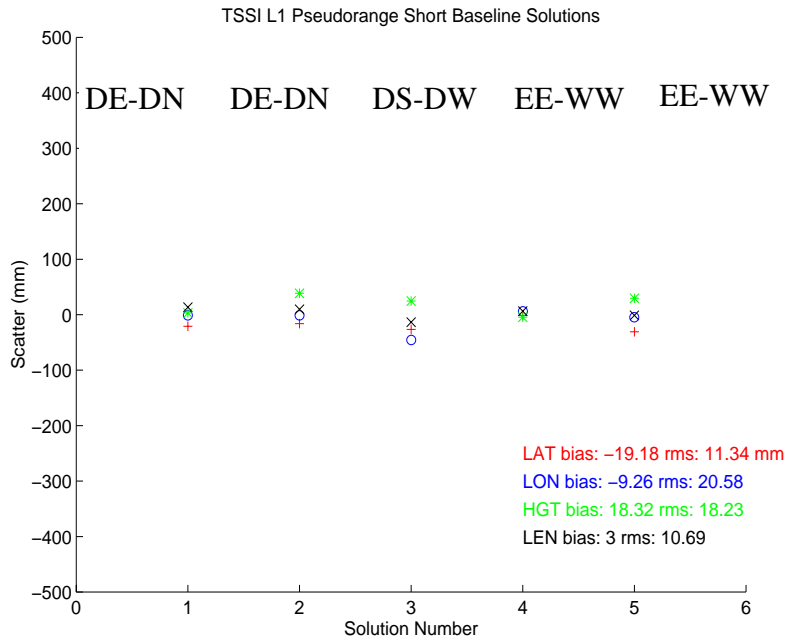


Figure 2.22: L1 pseudorange short baseline solutions for the TSSI receiver. The symbols are the same as in Figure 2.20.

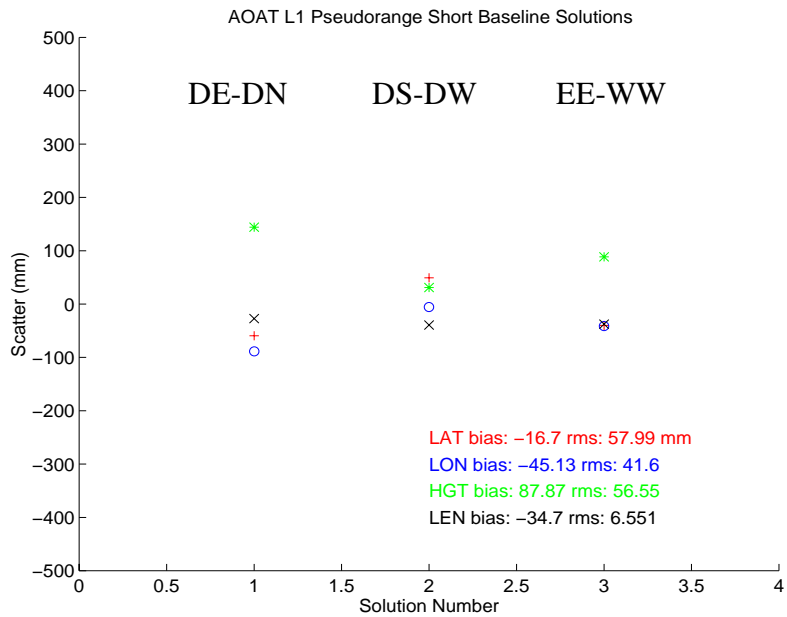


Figure 2.23: L1 pseudorange short baseline solutions for the AOAT receiver. The symbols are the same as in Figure 2.20.

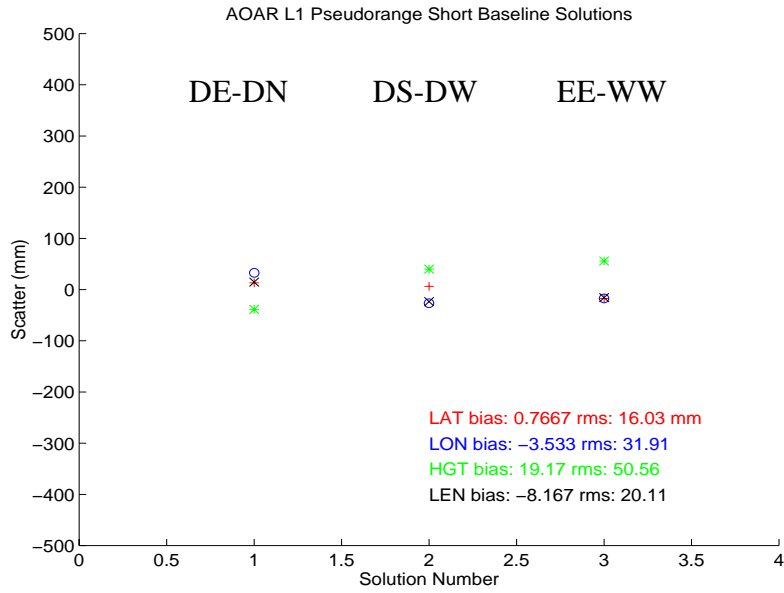


Figure 2.24: L1 pseudorange short baseline solutions for the AOAR receiver. The symbols are the same as in Figure 2.20.

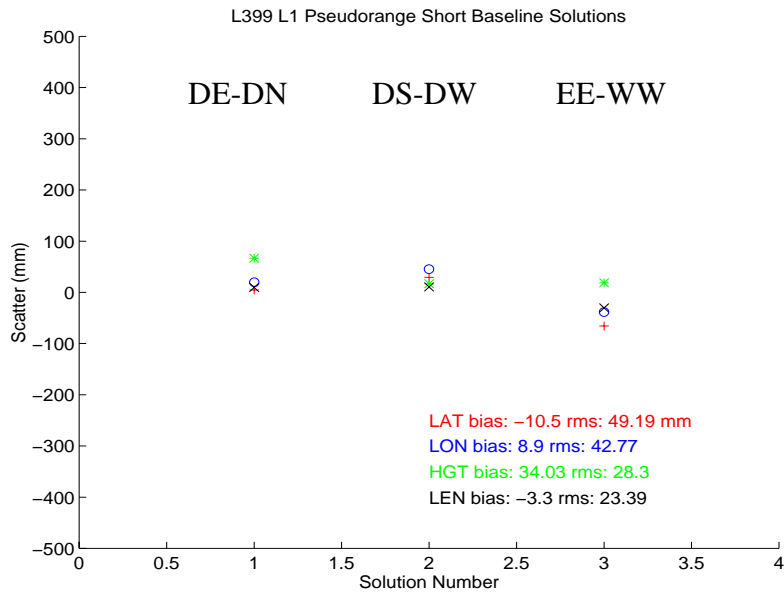


Figure 2.25: L1 pseudorange short baseline solutions for the L399 receiver. The symbols are the same as in Figure 2.20.

## 2.7 L2 Pseudorange Solutions

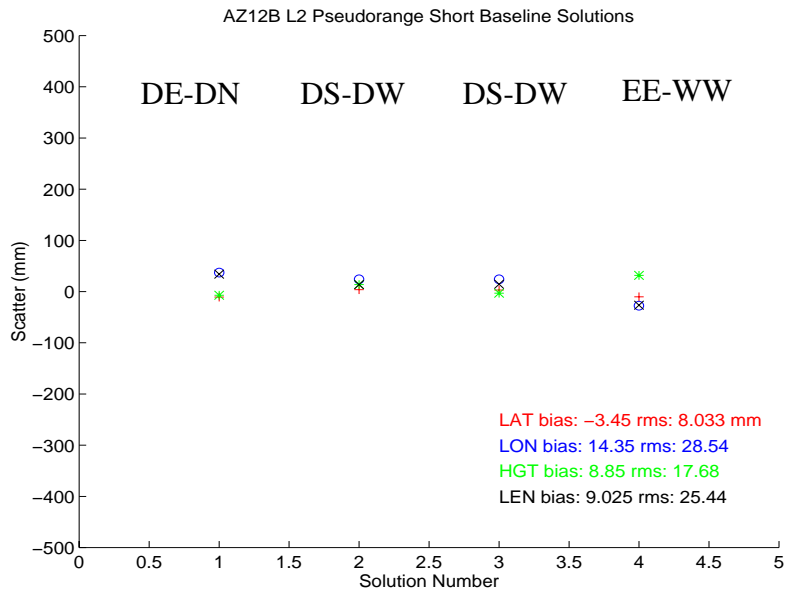


Figure 2.26: L2 pseudorange short baseline solutions for the AZ12B receiver. The red plus signs (+) represent latitude, the circles (o) represent longitude, the asterisk (\*) represent height, and the crosses (x) represent length. The average and rms of each component has been computed for all the solutions.

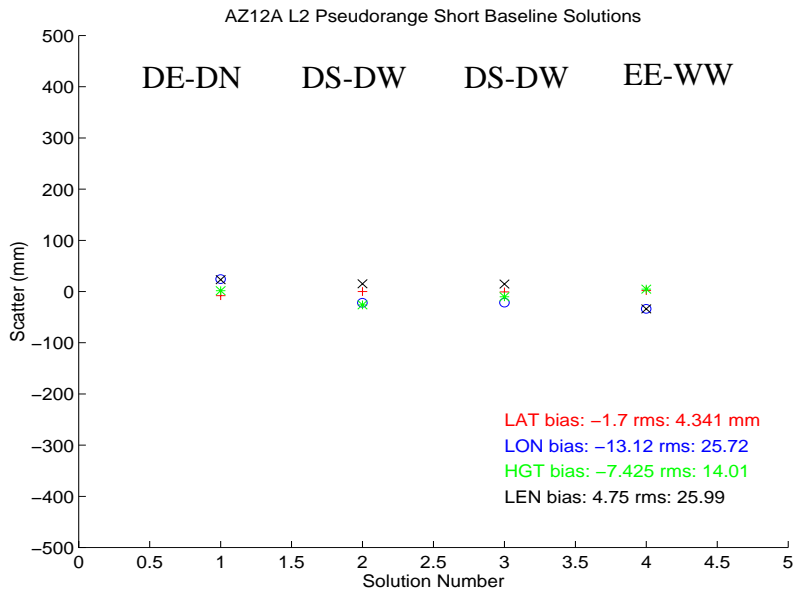


Figure 2.27: L2 pseudorange short baseline solutions for the AZ12A receiver. The symbols are the same as in Figure 2.26.

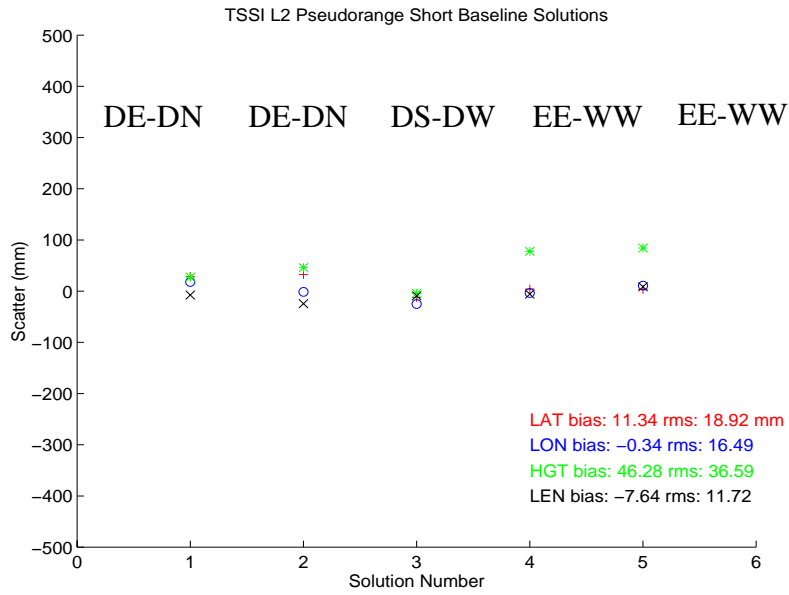


Figure 2.28: L2 pseudorange short baseline solutions for the TSSI receiver. The symbols are the same as in Figure 2.26.

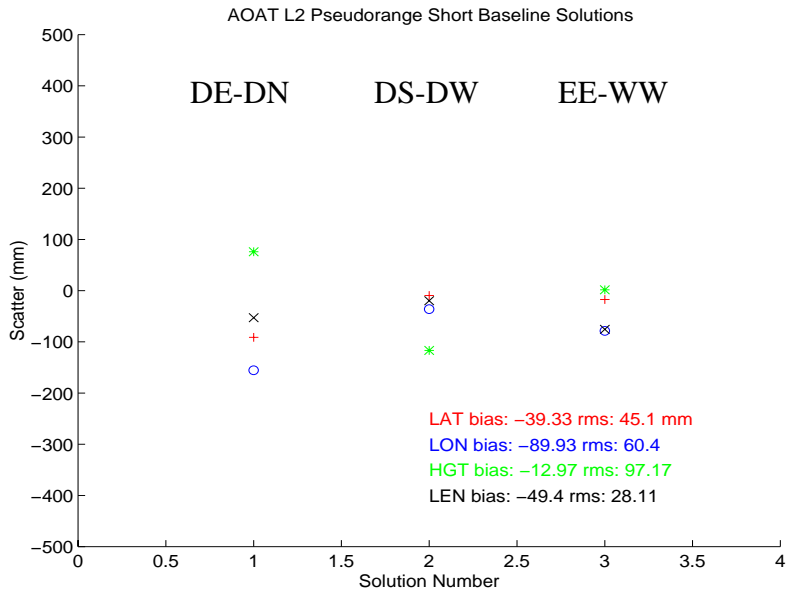


Figure 2.29: L2 pseudorange short baseline solutions for the AOAT receiver. The symbols are the same as in Figure 2.26.

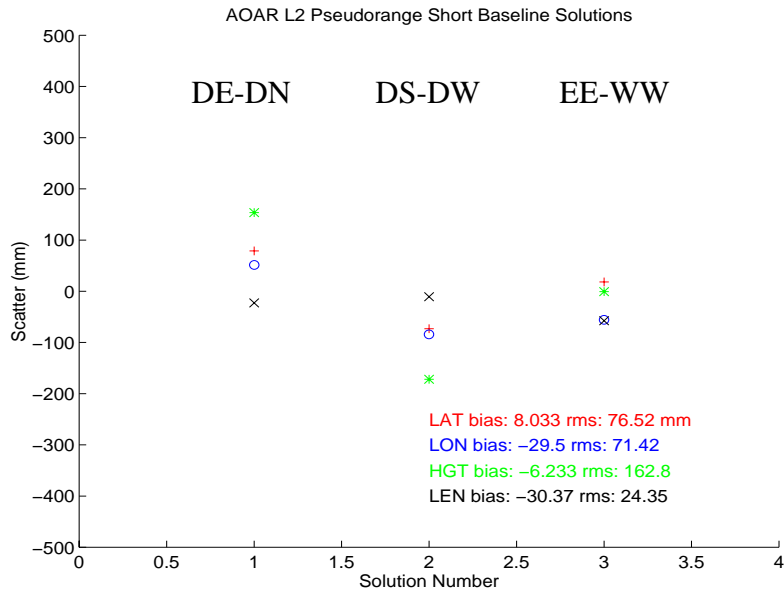


Figure 2.30: L2 pseudorange short baseline solutions for the AOAR receiver. The symbols are the same as in Figure 2.26.

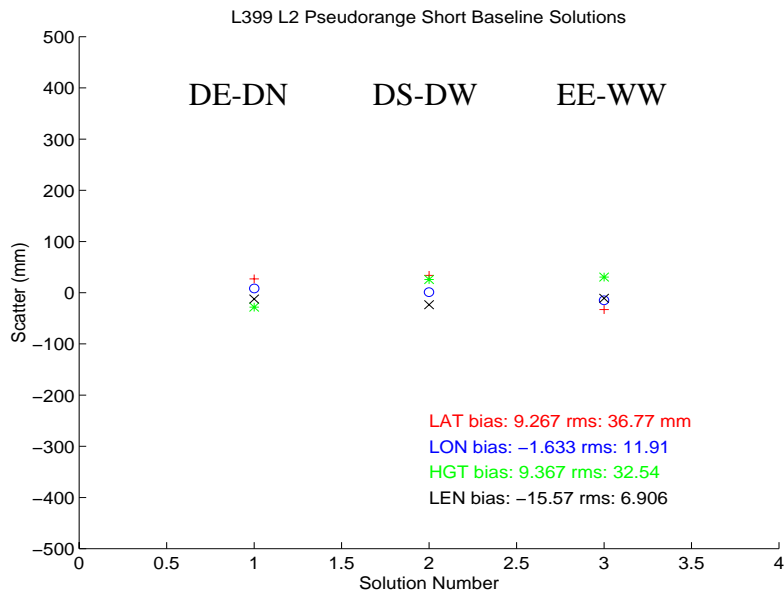


Figure 2.31: L2 pseudorange short baseline solutions for the L399 receiver. The symbols are the same as in Figure 2.26.

## 2.8 L3 Pseudorange Solutions

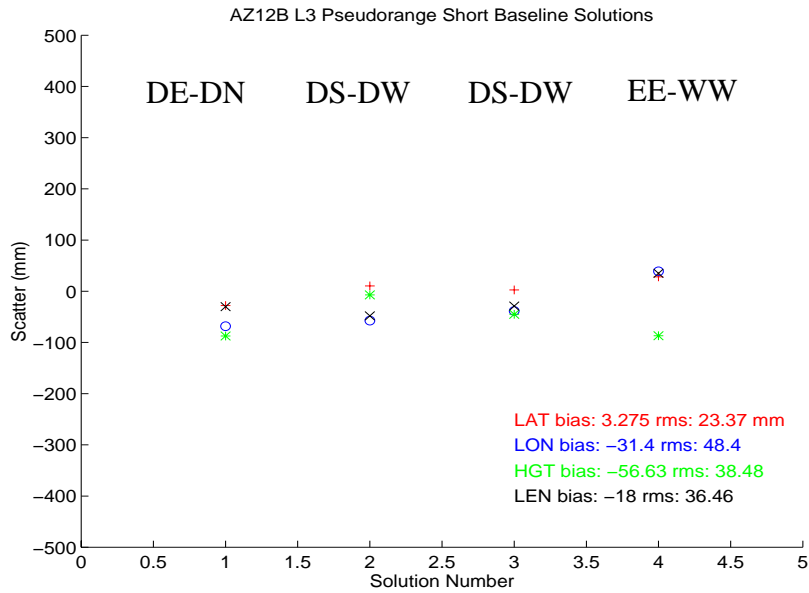


Figure 2.32: L3 pseudorange short baseline solutions for the AZ12B receiver. The red plus signs (+) represent latitude, the circles (o) represent longitude, the asterisk (\*) represent height, and the crosses (x) represent length. The average and rms of each component has been computed for all the solutions.

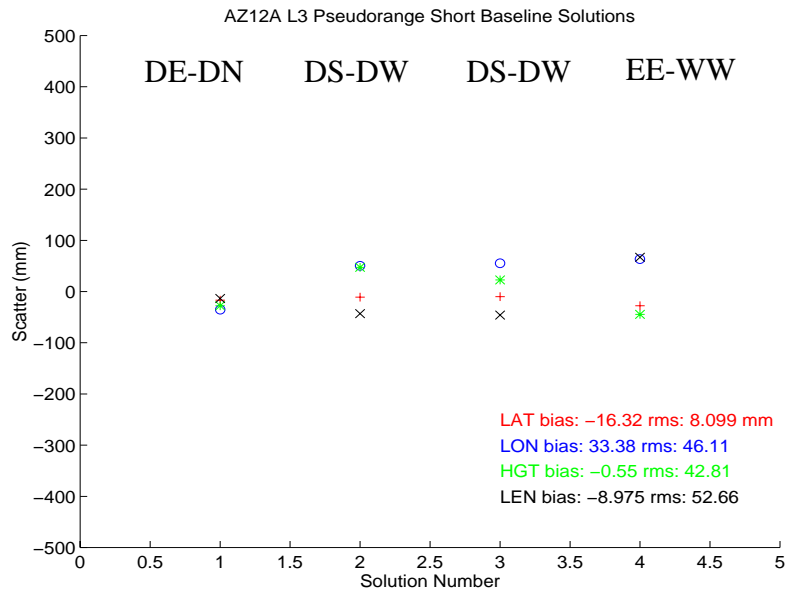


Figure 2.33: L3 pseudorange short baseline solutions for the AZ121A receiver. The symbols are the same as in Figure 2.32.

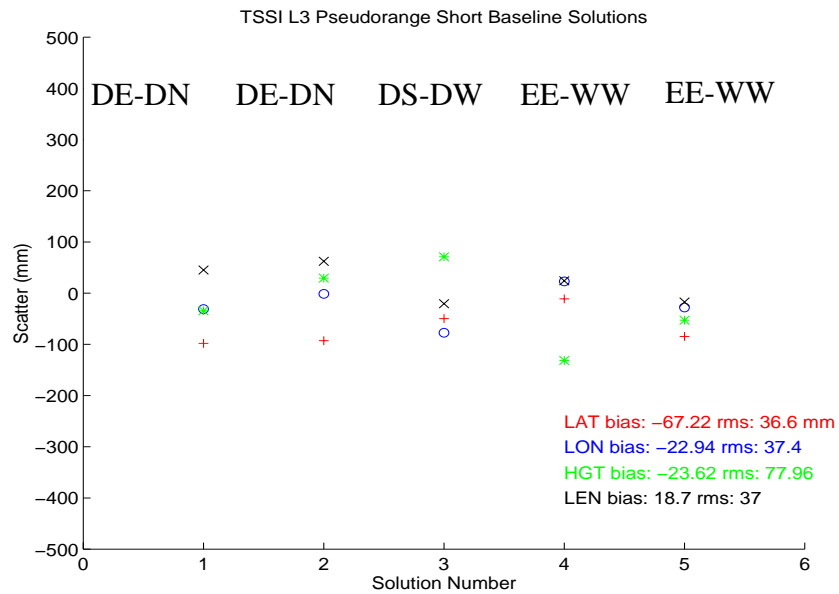


Figure 2.34: L3 pseudorange short baseline solutions for the TSSI receiver. The symbols are the same as in Figure 2.32.

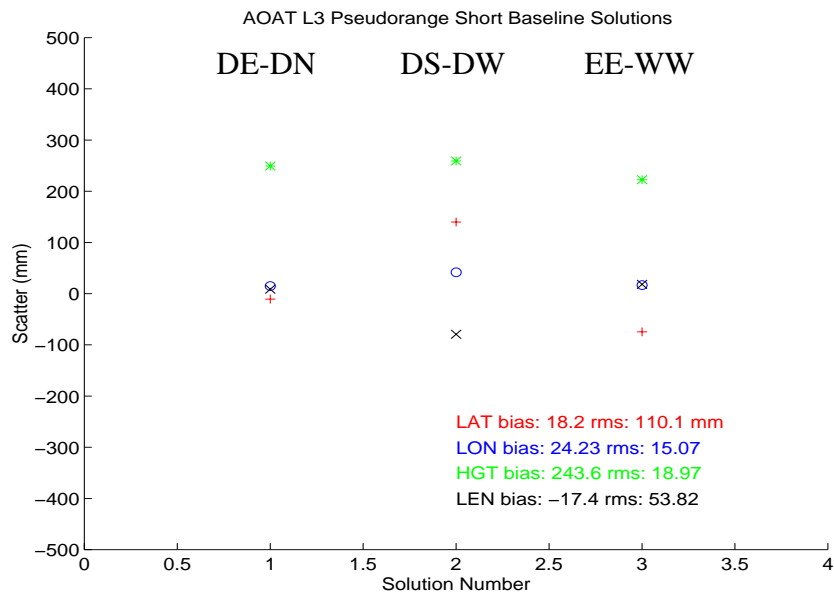


Figure 2.35: L3 pseudorange short baseline solutions for the AOAT receiver. The symbols are the same as in Figure 2.32.

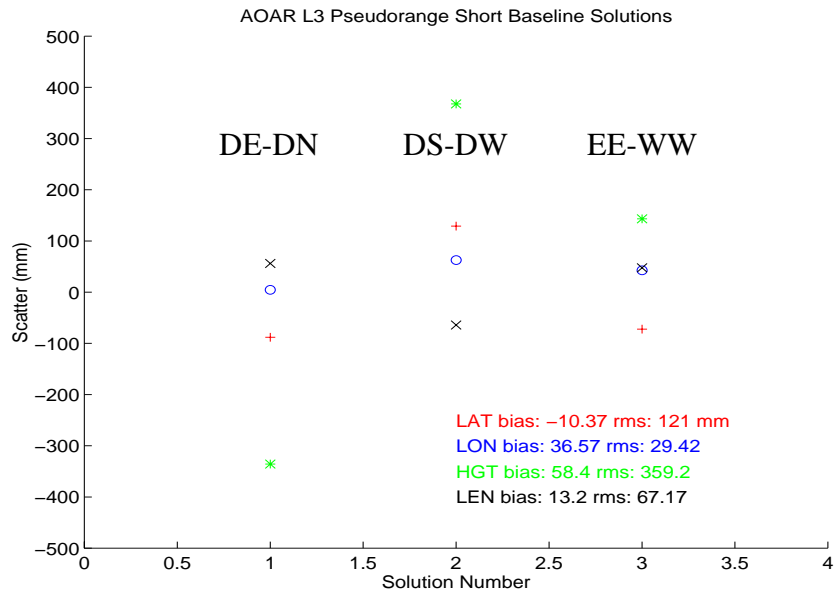


Figure 2.36: L3 pseudorange short baseline solutions for the AOAR receiver. The symbols are the same as in Figure 2.32.

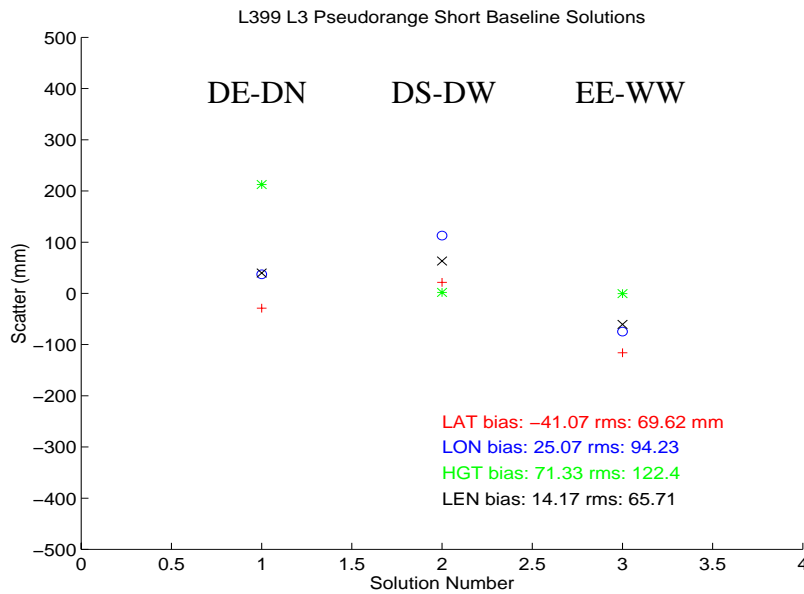


Figure 2.37: L3 pseudorange short baseline solutions for the L399 receiver. The symbols are the same as in Figure 2.32.

### 3. Summary of quality check results

Each receiver occupied five test markers with four 20 hour sessions per marker; and had one session of data collected with an AOA choke-ring antenna with an eight-way splitter for mixed-receiver tests. UNAVCO's quality check program (QC) was run for each rinex file and the average QC variables are given in the tables with receivers arranged alphabetically. QC scans rinex files and compiles statistics about the data, including: counts of observations, counts of LLI (loss of lock indicator) flags in the file, counts of slips according to selected detection parameters, and average MP1 and MP2. MP1 is a linear combination of P1, L1 and L2, MP2 is a linear combination of P2, L1, and L2. MP1 and MP2 reflect multipath plus receiver noise. QC also creates plot files of the ionosphere delay, first derivative of ionosphere delay, MP1, MP2, and elevation for each SV. (See 3-12, 3-13 for defining equations.) L1 and L2 refer to the phase measurements for the two GPS frequencies, and P1 and P2 refer to the pseudorange measurements.

QC statistics were compiled for a low elevation (0-10 degrees) subset of the data, and for 1 second data sample files, as well as for the complete data sets, to examine how the receivers perform under adverse conditions.

The average number of points tracked given in the tables is the average number of points with complete(L1, L2 plus P1, P2) observations. The average number of possible observations was 21014. The number of possible observations below 10 degrees was about 4500. For an eight-channel receiver the maximum number of points possible was approximately 19120. The number of points tracked is an important quality check variable.

**Table 3.1: SUMMARY OF QC VARIABLES (0-90 degrees)**

RECEIVER [# OF CHANNELS]	# OF POINTS	MP1	MP2	L1 LLI COUNTS < 10° / > 10°	L2 LLI COUNTS < 10° / > 10°
ASHTECH Z-XII3 [12]	19545.5	0.51	0.52	2.6 / 0.0	29.1 / 0.6
ASHTECH Z-XII3 w/ Ashtech. rinex tran. [12]	19552.9	0.17	0.17	13.2 / 0.1	5.5 / 0.0
LEICA SR399E [9]	18375.5	0.39	0.52	14.5 / 4.2	90.2 / 13.6
AOA RASCAL [8]	18392.1	0.46	1.10	0.0 / 0.0	90.0 / 17.0
TRIMBLE 4000 SSI [12]	19510	0.37	1.05	41 / 7.3	117.4 / 19.0
AOA TURBOROGUE SNR-8000 [8]	18321.1	0.49	0.97	2.8 / 5.8	24.7 / 77.1

1: Zero counts indicates that no LLI flags were written to the rinex files for the specified elevation range and frequency.

**Table 3.2: SUMMARY OF LOW ELEVATION QC VARIABLES (0-10 DEGREES)**

RECEIVER	# OF POINTS	MP1	MP2	L1 LLI COUNTS < 5° / > 5°	L2 LLI COUNTS < 5° / > 5°
ASHTECH Z-XII3	3227.9	0.97	0.99	2.3 / 0.3	27.5 / 1.6
ASHTECH Z-XII3 w/ Ash-tech rinex trans.	3229.7	0.31	0.30	11.8 / 1.8	5.5 / 0.0
LEICA S399E	2177	0.75	1.04	11.3 / 3.2	47.7 / 42.5
AOA RASCAL	2407.91	0.85	2.17	0.0 / 0.0	64.9 / 25.1
TRIMBLE 4000 SSI	3136.2	0.68	2.21	23.7 / 17.3	95.3 / 22.1
AOA TURBOROGUE SNR-8000	2467.8	0.71	1.77	4.9 / 0.9	55.4 / 21.7

2: Zero counts indicates that no LLI flags were written to the rinex files for the specified elevation range and frequency.

AOA Rascal and Turborogue SNR-8000 receivers have many more slips at low elevations than are indicated by LLI (loss of lock indicator) flags in the rinex files. AOA recommends not using data collected below 20 degrees and the QC results verify problems at low elevations. The Rascal rinex files do not have any L1 LLI flags.

The Ashtech translator does some slip fixing/testing and smooths the pseudorange values. The Ashtech translator shows fewer L2 LLI flags but more L1 LLI flags than the Bern rinex translator. The number of slips the QC program detects based on its slip criteria (not the number of LLI flags it counts from the rinex files) is the same for both translations of the Ashtech data. The MP1 and MP2 values are seen to be smaller with the Ashtech translator because of the receiver-generated smoothing applied by the Ashtech translator.

The Leica SR399E translator also applies some smoothing of pseudorange values (as can be seen in following MP1 and MP2 figures). We note that the tested receiver data collection unit mistakenly had older firmware with a 1 cycle discretization in the pseudorange sampling and the unusual steps in the MP1 and MP2 figures. This problem is discussed by Leica engineers in Appendix E.

**Table 3.3: 1 Second epoch QC Variables (Average of Two 1 Hour files for each receiver)**

RECEIVER	MP1 < 10° / > 10°	MP2 < 10° / > 10°	L1 LLI COUNTS < 10° / > 10°	L2 LLI COUNTS < 10° / > 10°
ASHTECH Z-XII3	0.95 / 0.31	1.07 / 0.32	6.0 / 0.0	3.0 / 0.0
ASHTECH Z-XII3 w/ Ash. rinex trans.	0.14 / 0.03	0.15 / 0.03	6.0 / 0.0	3.0 / 0.0
LEICA SR399E	0.35 / 0.04	0.48 / 0.06	0.0 / 0.0	9.0 / 5.0
AOA RASCAL	0.48 / 0.33	1.46 / 0.72	0.0 / 0.0	7.5 / 11.5
TRIMBLE 4000 SSI	0.57 / 0.19	1.75 / 0.40	3.0 / 6.0	4.5 / 6.5
AOA TURBOROGUE SNR-8000	0.62 / 0.24	1.56 / 0.69	0.0 / 0.0	7.0 / 0.5

3: Zero counts indicates that no LLI flags were written to the rinex files for the specified elevation range and frequency.

For both one second and 30 second epoch intervals the Trimble 4000 SSI has the lowest unsmoothed MP1, with the Ashtech Z-XII3 having the lowest smoothed and unsmoothed MP2. The Rascal and Rogue SNR-8000 show lower average MP1 and MP2 below 10 degrees for the high rate data; but this is an artifact caused by the high number of slips these receivers had at low elevations when no Signal to Noise Ratio (SNR) was applied and the fact that the QC program resets MP1 and MP2 to zero when a slip is detected. The Rascal and TurboRogue SNR-8000 slipped thousands of times below 20 degrees during the 1 hour high rate runs when no minimum SNR cut-off was applied. When a SNR of five (cut-off value to eliminate the slips) was applied, only 10% of the TurboRogue SNR-8000 and 20% of the Rascal data below 20 degrees were accepted.

Figure 3.1: Low elevation traces (below 10 degrees) for each SV at mark DEB2. All receivers are seen to track down to zero degrees at times. Ability to maintain lock below 10 degrees does vary.

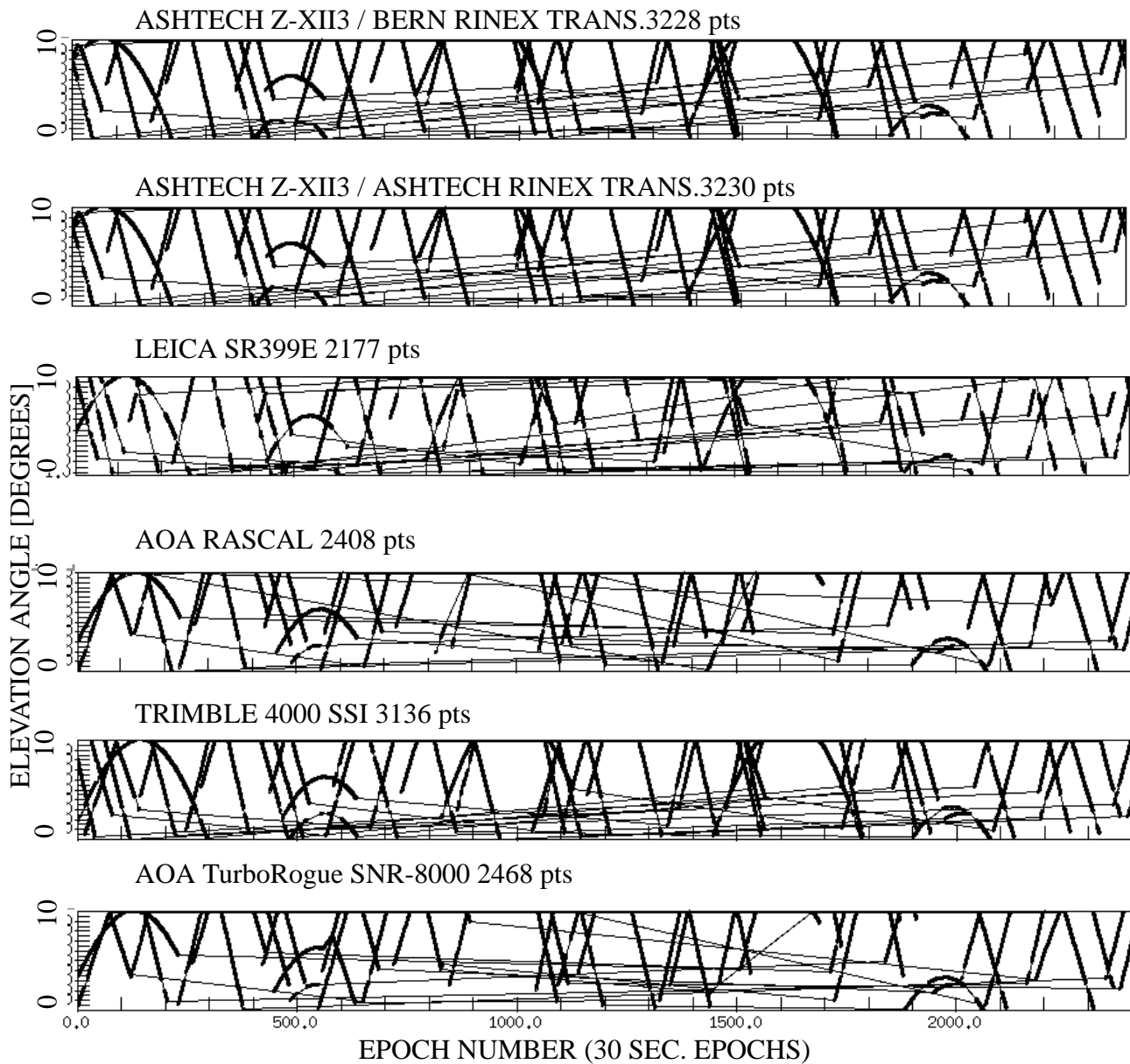


Figure 3.2: Low Elevation(0-10 degrees) IOD (Ionospheric delay derivative) and Elevation traces for SV 9 day 243. The IOD shows phase noise as well as actual rate of change of the ionosphere delay. Lower frequency features that are repeated for different receivers are actual ionospheric activity, while the high frequency oscillation reflects receiver phase noise. For instance, both the Ashtech and Trimble receivers show peaks at the 60th epoch, the other receivers are not tracking SV 9 at the 60th epoch. The Ashtech rinex translation is not shown because it gives the same elevation and ionosphere derivative as the Bern rinex translation of the Ashtech file.

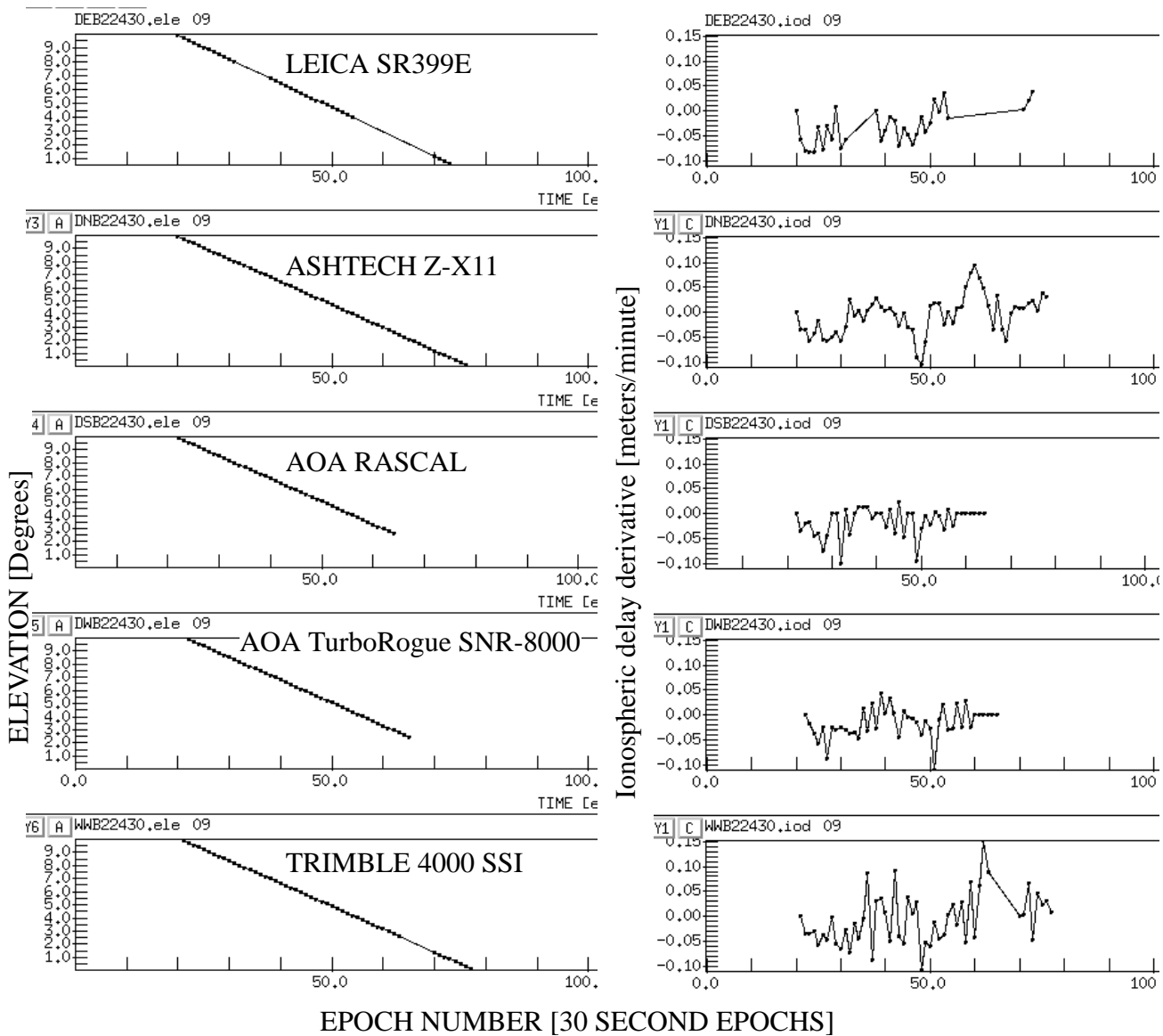


Figure 3.3: 30 second low elevation (0-10 degree) MP1 and MP2 traces for SV 9 day 243. The Leica SR399E has flat MP1 and MP2 traces, because, like the Z-XII3 with the Ashtech translator, the pseudoranges are smoothed. The Leica SR399E trace shows a large jump. The SR399E, AOA Rascal and AOA TurboRogue SNR-8000 low elevation MP1 and MP2 traces show a lot of these jumps. MP2 is shown below MP1 for each Receiver.

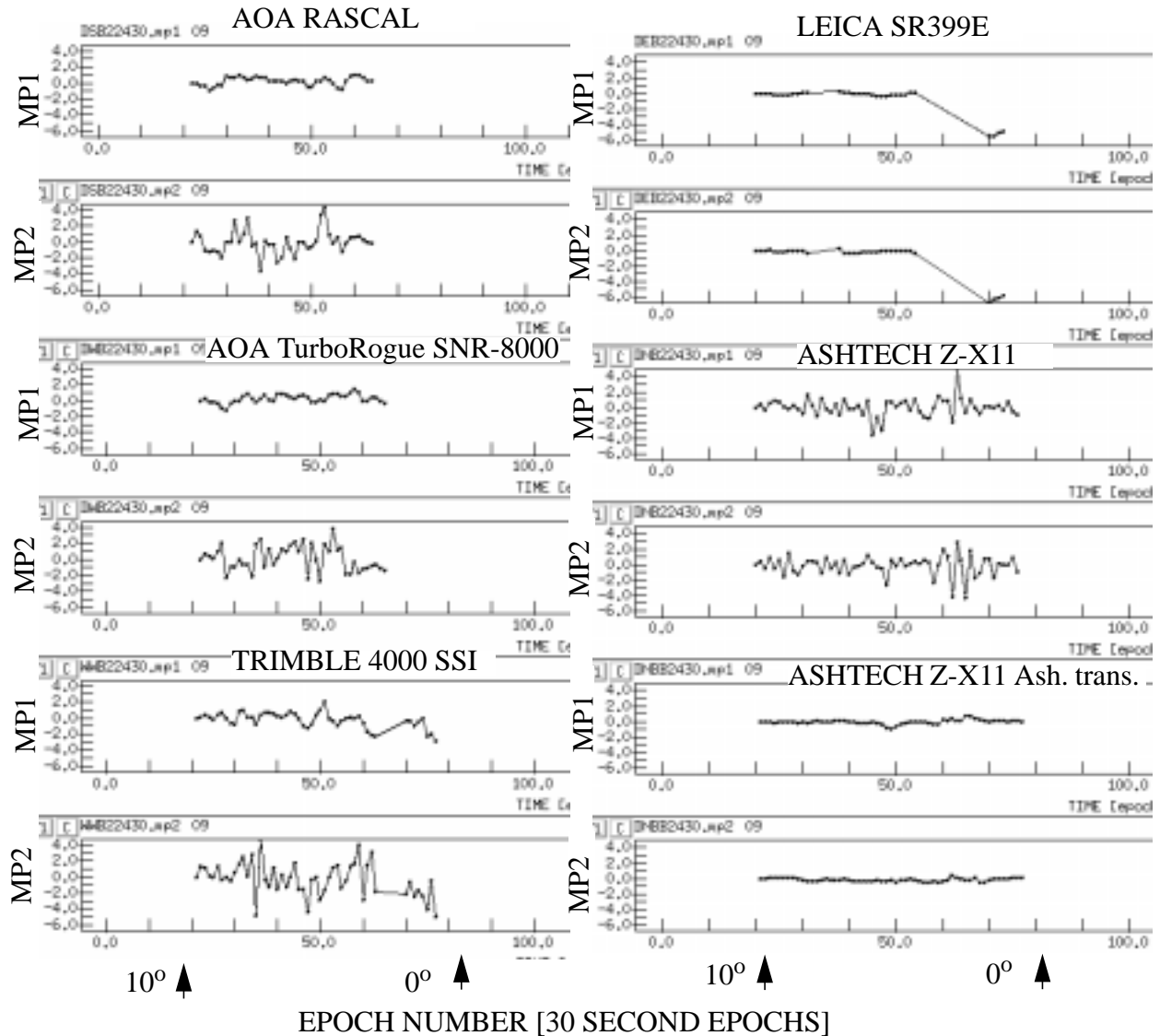


Figure 3.4: 30 second normal elevation range(10-90) IOD and elevation traces from each receiver for SV 1 on day 240. The AOA TurboRogue SNR-8000 and AOA Rascal have the lowest phase noise at high elevations. At low elevations the Ashtech Z-XII3 has the lowest phase noise. An Ionospheric signal can be seen from epochs 0-150, the phase noise is represented by the width of the line.

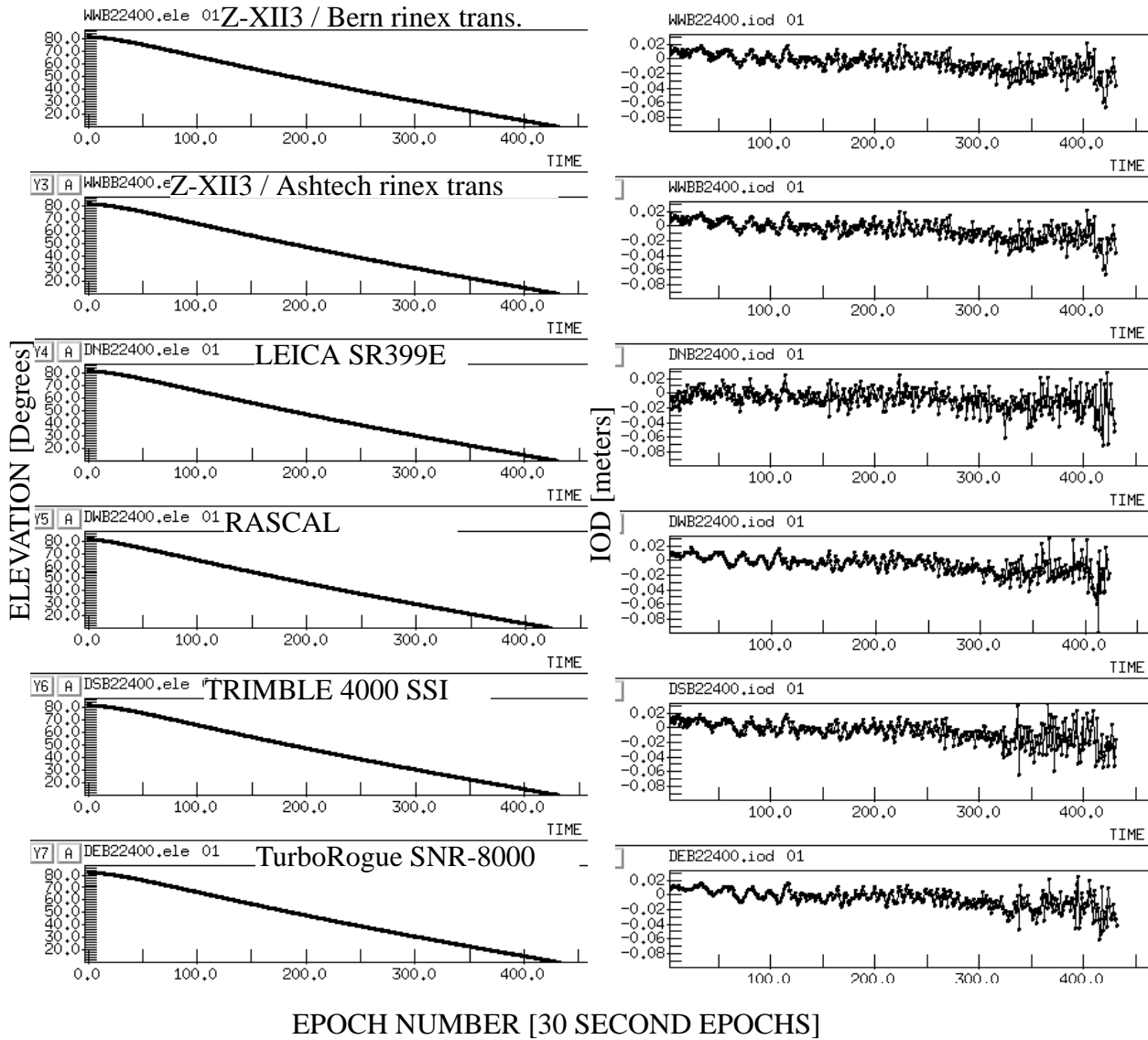


Figure 3.5: 30 second data normal elevation range (10-90) MP1 and MP2 traces for SV1 on day 140. Note that the MP1 traces have twice the scale of the MP2 traces. The Leica SR399E trace is much smoother than expected from the average values in table 1. This is caused by the 1 cycle discretization of the smoothing. It can also be seen that the TurboRogue SNR-8000 and the Rascal have the lowest unsmoothed MP1 and MP2 at high elevations; but get increasingly noisy toward lower elevations.

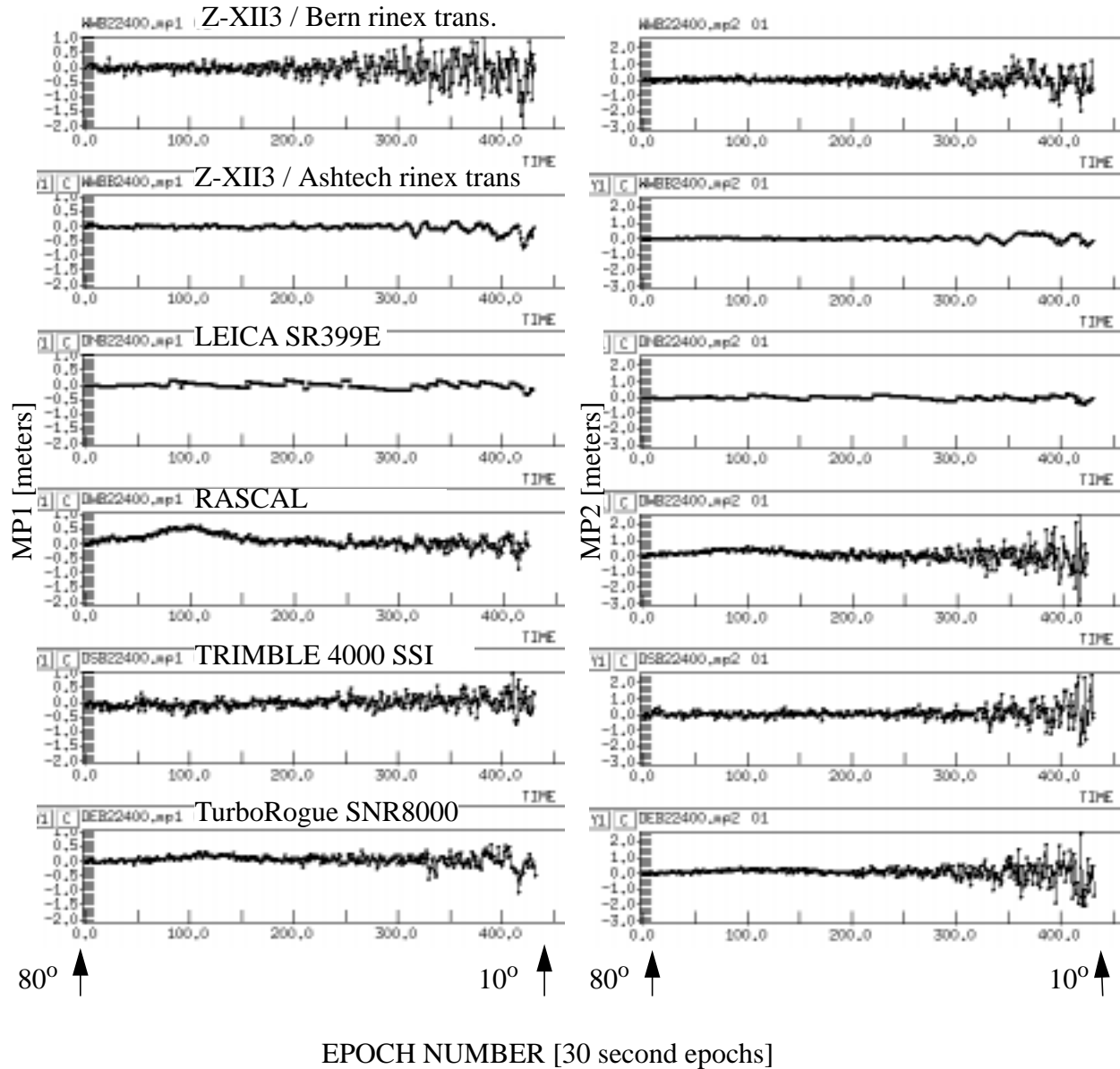




Figure 3.7: 1 second data IOD traces; normal elevation range, SV 25. The Trimble 4000 SSI has the best high elevation phase noise at the high data rate. The AOA TurboRogue SNR-8000 and AOA Rascal show the highest phase noise at high data rate.

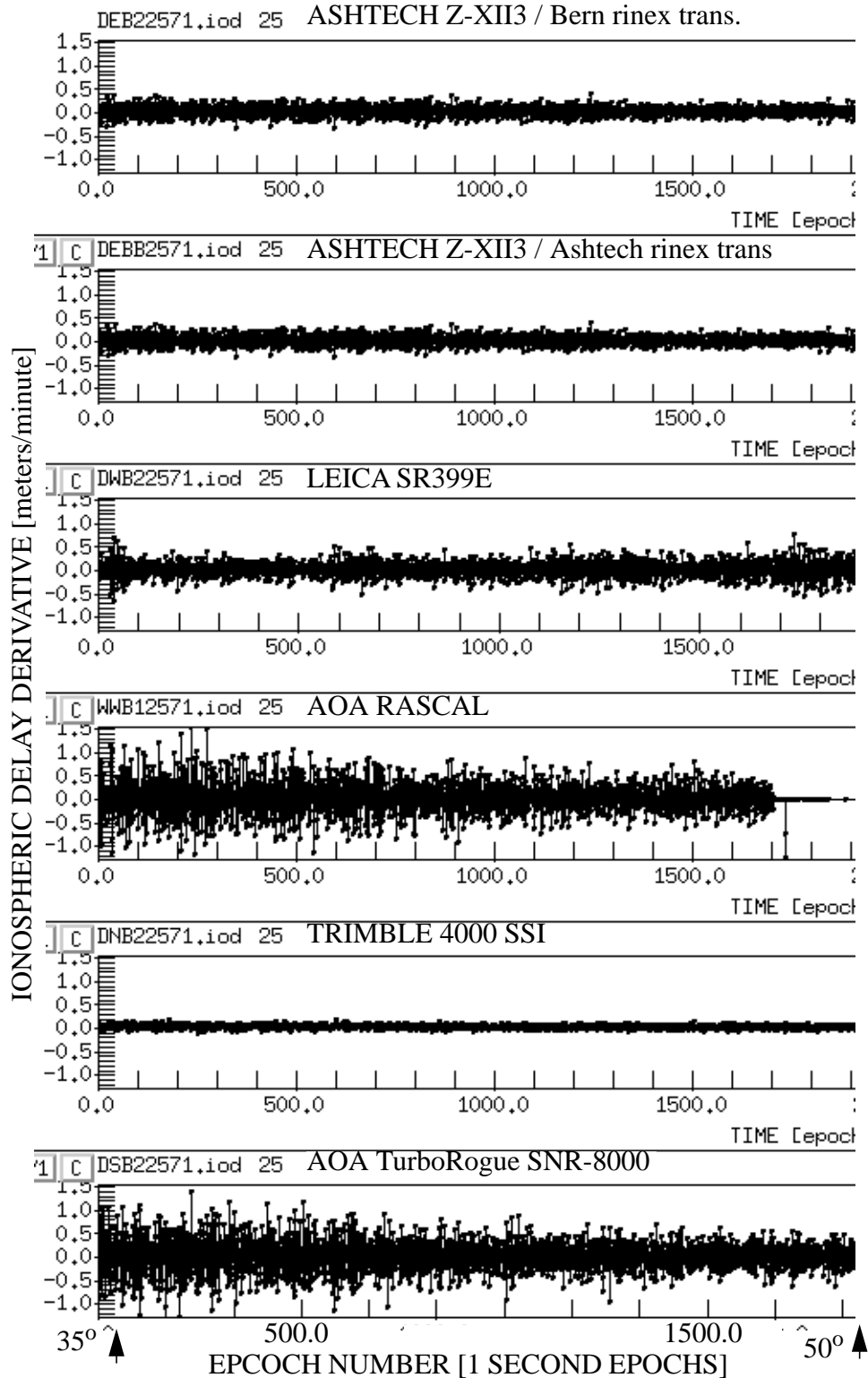
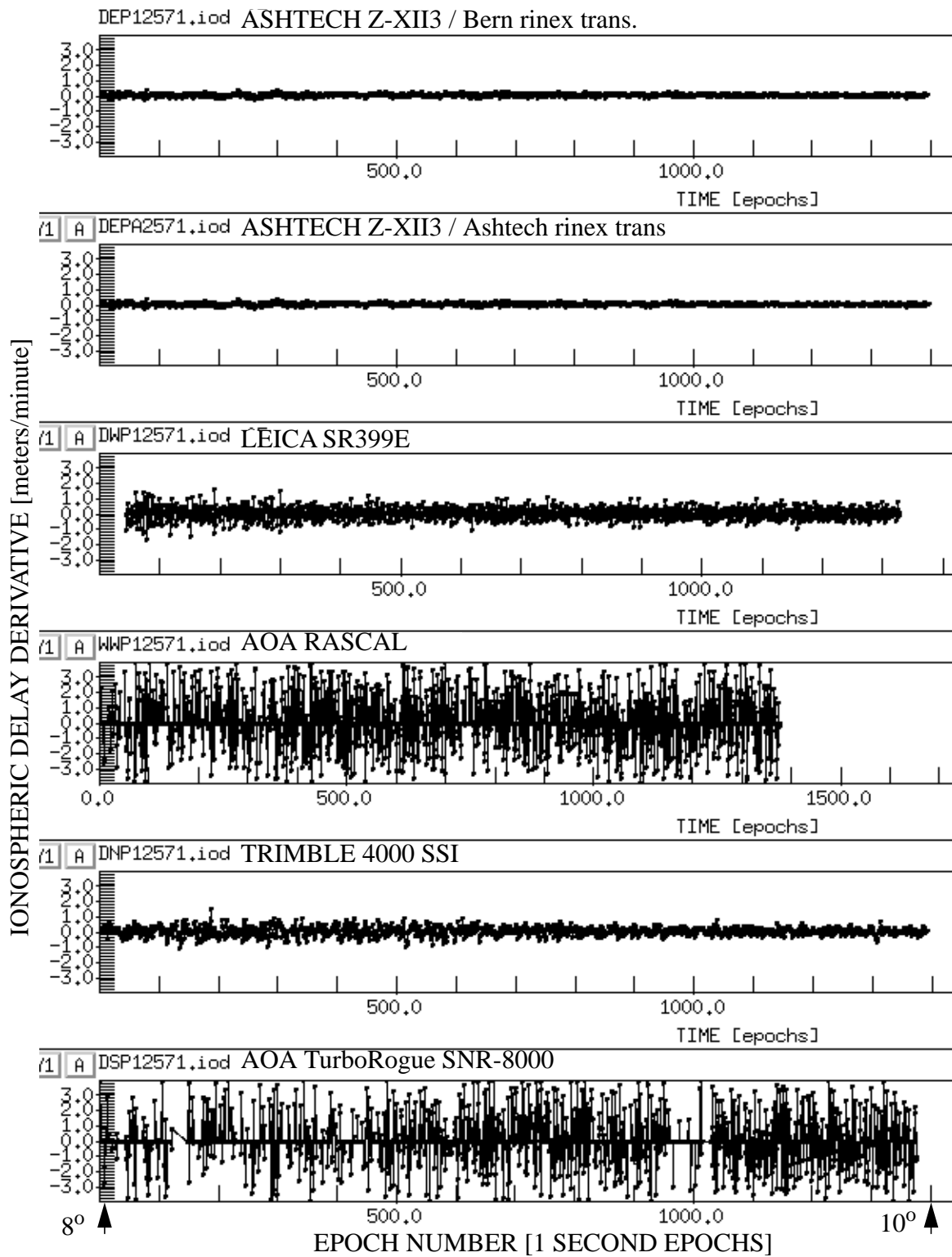


Figure 3.8: Low Elevation 1 second data IOD traces for SV 5 on day 257. Ashtech Z-XII3 receiver has best low elevation phase noise. The points at 0.0 meters are resets applied by the QC program whenever a slip was detected. No minimum signal to noise ratio was applied



## Derivation of MP1 and MP2:

First we describe the pseudorange measurements as:

$$p_i = \mathfrak{R} + c(dt - dT) + I_i + \mathfrak{S} + MPp_i \quad (\text{eqn 1})$$

and the phase measurements as:

$$\Phi_i = \mathfrak{R} + c(dt - dT) + \lambda_i N_i - I_i + \mathfrak{S} + MP\Phi_i \quad (\text{eqn 2})$$

Where:

$p$  = pseudo-range observation in meters

$\mathfrak{R}$  = distance between satellite and receiver in meters

$c$  = speed of light in meters/sec

$dt$  = satellite clock error in sec

$dT$  = receiver clock error in sec

$I$  = ionospheric range error in meters

$\mathfrak{S}$  = tropospheric range error in meters

$N$  = integer cycle ambiguity

$MPp$  = pseudo-range multipath

$MP\Phi$  = phase multipath

$i$  = observation frequency,  $i = 1 \equiv L1; i = 2 \equiv L2$

$f_1$  = Frequency of L1;  $f_1 = 1.57542 \text{GHz}$

$f_2$  = Frequency of L2;  $f_2 = 1.2276 \text{GHz}$

$\lambda_1$  = Wavelength of L1;  $\lambda_1 \cong 19.03 \text{cm}$

$\lambda_2$  = Wavelength of L1;  $\lambda_2 \cong 24.42 \text{cm}$

IOD, or first derivative of ionospheric delay is defined as:

$$\frac{f_1^2}{f_1^2 - f_2^2} \times ((L2 - L1)_i (L2 - L1)_{i-1}) \quad (\text{eqn 3})$$

By taking advantage of the fact that the ionospheric delay for L1 and L2 are related as

$$I_2 = \alpha I_1; \left( \alpha \equiv \left( \frac{f_1}{f_2} \right)^2 \right) \quad (\text{eqn 4})$$

We can solve the phase measurement equation for the ionospheric delay. First we will solve for  $I_1$ :

$$\frac{(\Phi_1 - \Phi_2)}{(\alpha - 1)} = I_1 + \frac{(\lambda_1 N_1 - \lambda_2 N_2)}{(\alpha - 1)} + \frac{(MP\Phi_1 - MP\Phi_2)}{(\alpha - 1)} \quad (\text{eqn 5})$$

This equation combined with the phase equation for L1 (eqn 2) gives us the phase range equation:

$$\Phi_1 + \frac{(\Phi_1 - \Phi_2)}{(\alpha - 1)} = \mathfrak{R} + c(dt - dT) + \mathfrak{S} + b_1 + m\Phi_1 \quad (\text{eqn 6})$$

Where  $B_1$  is the phase bias term defined as:

$$b_1 = \lambda_1 N_1 + \frac{(\lambda_1 N_1 - \lambda_2 N_2)}{(\alpha - 1)} \quad (\text{eqn 7})$$

and  $M\Phi_1$  is the phase multi-path term defined as:

$$m\Phi_1 = MP\Phi_1 + \frac{(MP\Phi_1 - MP\Phi_2)}{(\alpha - 1)} \quad (\text{eqn 8})$$

The phase range equation (eqn 6) is a linear combination of the L1 and L2 phase observables that gives us the range to the satellite along with receiver/satellite clock errors, tropospheric errors, a bias term and a phase multipath term.

Combining the equation for ionospheric delay (eqn 5), the phase range equation (eqn 6) and the pseudo-range equation (eqn 1) gives us:

$$p_1 - \left(1 + \frac{2}{\alpha - 1}\right)\Phi_1 + \left(\frac{2}{\alpha - 1}\right)\Phi_2 = MPp_1 + B_1 + M\Phi_1 \quad (\text{eqn 9})$$

Where  $B_1$  is the bias term defined as:

$$B_1 = -(\lambda_1 N_1 - \lambda_2 N_2) - b_1 = -\left(1 + \frac{2}{\alpha - 1}\right)\lambda_1 N_1 + \left(\frac{2}{\alpha - 1}\right)\lambda_2 N_2 \quad (\text{eqn 10})$$

and  $M\Phi_1$  is the phase multi-path term defined as:

$$M\Phi_1 = -(MP\Phi_1 - MP\Phi_2) - m\Phi_1 = -\left(1 + \frac{2}{\alpha - 1}\right)MP\Phi_1 + \left(\frac{2}{\alpha - 1}\right)MP\Phi_2 \quad (\text{eqn 11})$$

MP1 is then defined as the linear combination obtained (eqn 9):

$$MP1 \equiv p_1 - \left(1 + \frac{2}{\alpha - 1}\right)\Phi_1 + \left(\frac{2}{\alpha - 1}\right)\Phi_2 \quad (\text{eqn 12})$$

Performing similar operation for L2, we get the following equations:

$$p_2 - \left(\frac{2\alpha}{\alpha - 1}\right)\Phi_1 + \left(\frac{2\alpha}{\alpha - 1} - 1\right)\Phi_2 = MPp_2 + B_2 + M\Phi_2 \quad (\text{eqn 13})$$

$$B_2 = -\left(\frac{2\alpha}{\alpha - 1}\right)\lambda_1 N_1 - \left(\frac{2\alpha}{\alpha - 1} - 1\right)\lambda_2 N_2 \quad (\text{eqn 14})$$

$$M\Phi_2 = -\left(\frac{2\alpha}{\alpha - 1}\right)MP\Phi_1 - \left(\frac{2\alpha}{\alpha - 1} - 1\right)MP\Phi_2 \quad (\text{eqn 15})$$

$$MP2 \equiv p_2 - \left(\frac{2\alpha}{\alpha - 1}\right)\Phi_1 + \left(\frac{2\alpha}{\alpha - 1} - 1\right)\Phi_2 \quad (\text{eqn 16})$$

Looking at multipath equations for L1 (eqn 9) and L2 (eqn 13), we see that the MP equations contain two terms in addition to the multipath values. The first term is a bias term ( $B_i$ ) that arises from the unknown phase ambiguities. QC fixes this value to be the first MP value calculated for a satellite. This is not strictly true, but brings the MP values to near zero values. What is of interest from the MP values is its structure over time, not the DC bias term. The second addition term ( $M\Phi_1$ ) comes from the phase multi-path. Since the phase multipath is much smaller in magnitude than the P-code multipath, the MP values are dominated by P-code multipath.

## 4. Power Tests

### 4.1 Power Consumption

These tests were performed using a Fluke 45 Dual Display Multimeter. The receivers were connected to a 12 volt 17 Amp-hr Powersonic battery (see figure 4.1), except for the AOA Rascal receiver which was run of its 6VDC power supply. The multimeter measured the voltage of the battery and the current draw of the receiver. The readings from the multimeter were logged every 15 seconds for 10 minutes. The power consumption was calculated by multiplying current and voltage and taking the mean of all the readings. The results are summarized in Table 4.1 below. The precision of each individual sample is better than 0.001%. The variation of repeated sets of measurements was found to be approximately 5% (or a range of 0.3 to 0.9 watts).

The receivers were tracking with zero degree elevation mask and 30 seconds sampling rate. They were tracking 6-9 satellites when the power readings were taken. The temperature was ambient room temperature. On the last power consumption test, the antenna was left connected to the receiver and tracking was either terminated (AOA Rascal, AOA Turborogue, and Leica SR399E) or all the satellites disabled (Trimble 4000 SSi and Ashtech Z-12). This represents the minimum power consumption.

**Table 4.1: Power Consumption (Watts)**

	AOA Rascal	AOA Turborogue SNR-8000	Trimble 4000 SSi	Ashtech Z-12	Leica SR399E
Manufacturer specification	< 5	17	10.5	12	12
Tracking with backlight on (maximum power use)	7.41	17.09	12.45	13.65	13.67
Tracking with backlight off	7.00	15.09	11.60	11.32	13.54
Antenna connected, not tracking with backlight off (minimum power use)	6.01	13.06	8.87	11.41	3.96

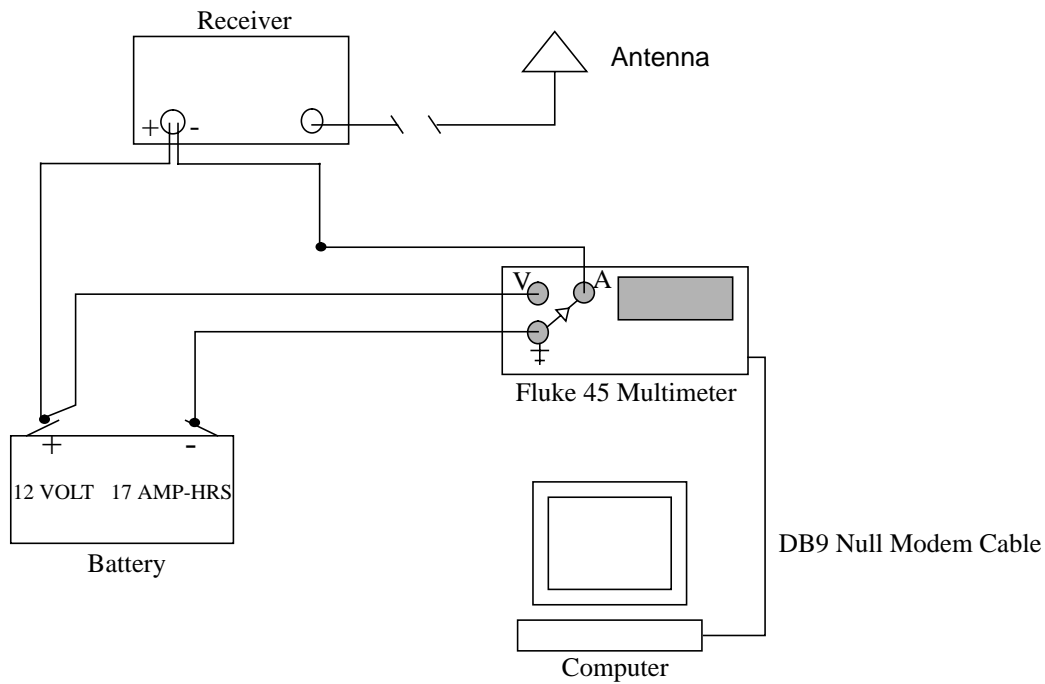


Figure 4.1: Power Test Set Up

## 4.2 Mid-Survey Power Failure Tests

A series of tests were undertaken to determine the receiver failure responses to power failures occurring in mid-survey. This is an important concern for remote operations where an operator is not present to manually restart the survey. Three types of failures were simulated and the recovery times to full data logging were measured. In the first two cases the power was quickly disconnected resulting in a sudden drop in voltage. The receivers were then reconnected after less than 1 sec (a “glitch”) and after 10 sec.

The third test simulated a gradual loss in power such as might occur if the receiver is running on batteries with AC power supply or solar panel. In the event of an extended external power failure, the battery capacity is gradually run down and when the voltage drops to a minimum level needed to operate the receiver, the receiver either fails or is shutdown by the receiver’s internal operating system. Power recovery would occur quickly if attached to A/C or more slowly if powered by solar panels. Results are summarized in the Table 2 below.

Two types of failure modes were observed. With the first type of failure (fail 1), the receiver returns to a powered-up condition, but the receiver does not track or log and a manual power off and on is needed to resume tracking and logging. This would be fatal for an unattended remote operation without two-way communications, such as a receiver setup in the backcountry. If communications recover, however, it would be possible to remotely restart the survey and datalogging with fail 1 on the AOA Rascal using a password not typically available to the user. With the second type of failure (fail 2), the receiver stays off and no further communications with the receiver are possible. It is not possible to continue the survey without manually powering on the receiver.

Note that when the Leica 399 is used with a PC as a local controller/logger using WILDBASE, the survey will restart after a power failure, but returns to receiver defaults rather than user supplied parameters.

**Table 4.2: Power Fail Responses of Receivers**

	Receiver	Power Glitch	10 sec Fail	Low Battery Fail	Comments
Recovery Time /Minutes	Ashtech Z-12	1.0	1.0	1.0	Creates new file with duplicate file name for each fail.
	AOA Turborogue SNR-8000	4.0	4.0	4.0	
	AOA Rascal	2.5	2.5	Fail 1	
	Trimble 4000SSi	1.0	1.0	1.0	With "low battery override option" installed
	Trimble 4000SSE	1.0	1.0	Fail 2 (see comment->)	Does not power up after low-battery fail. "Low battery override option" is available for SSE, but was not tested.
	Leica 399	Fail 2	Fail 2	N/D	Does not power up after any power fail. Requires manual restart and loses all timer programming.

Power Glitch

External power cycled as quickly as possible.

Low Battery Fail

Supply voltage allowed to slowly fall below manufacturers minimum.

Recover Time

Time for receiver to power-up and resume tracking and data logging.

N/D

NO Data. Test not performed.

Fail 1

Receiver powered up but lost all memory of previous almanac and tracking parameters. Receiver would not track or log without manually powering receiver off then on again. Since receiver was still powered on after the failure it may be possible to restart via a communications port, but this requires a special password typically not available to user.

Fail 2

Receiver fails to power up after interruption. No recovery without manual restart.

## 5. GPS Receiver Download Speed Comparison:

### 5.1 Purpose:

The time to download a GPS receiver is important since a fast download will reduce staff time, phone bills and computer resource needs. Shorter download times also allow improved quality assurance, through an increased likelihood of a safe and complete download. The time to download a file is not dependent on just throughput speeds, commonly indicated by baudrate setting or by typical actual throughput in characters (or bytes) per second. Download times are also dependent on each receivers download file size, communications port baudrate setting, the download method and the computer and communications system used.

This report is intended as a sampling of typical download times of several receivers and a discussion of related issues for determining procedures or equipment that could achieve the best possible results. These tests were performed many times with some hardware and software flag changes to attempt to represent each receivers best possible relative results using available equipment and software. Also, calls to technical support were made to each manufacturer to clarify performance or operational issues, and responses of most manufacturers to the early draft version of this report have been considered and incorporated where appropriate.

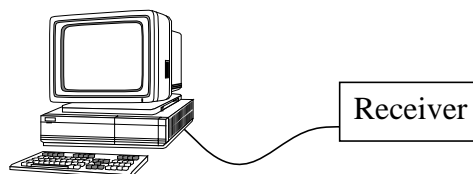
### 5.2 Description:

Download tests were performed on the different receivers using the various software<sup>1</sup> provided or recommended by the manufacturers. The tests were performed with several different computers to explore the effects of different hardware. Three test suites were performed to simulate typical UNAVCO user scenarios: direct connection downloads, phone modem downloads, and radio modem downloads.

Please note that these are relative comparison tests. Each test suite was performed on uniform equipment but the times will vary according to the equipment used. By no means, do we claim that these speeds are the fastest possible although we tried to optimally configure each system.

In the **direct connection** test, each receiver was connected directly to a computer using manufacturer provided cables and downloaded to a hard drive.

Direct Connection

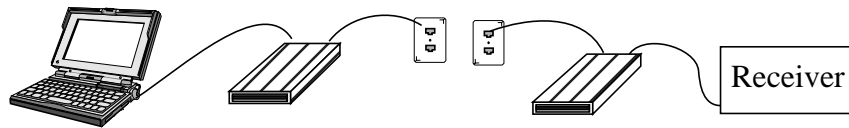


---

1. The software used for the various downloads was HOSE v. 5.3.00 (Ashtech), REMOTE v. 5.000 (Ashtech), WILDBASE v. 1.0a (Leica), SKI v. 1.09b (Leica), RFILE v. 2.6 (Trimble), 4000 v. 3.11 (Trimble), GETFILE v. 1.04 (Trimble), and Procomm Plus v. 2.01 (for Rascals and TurboRogues).

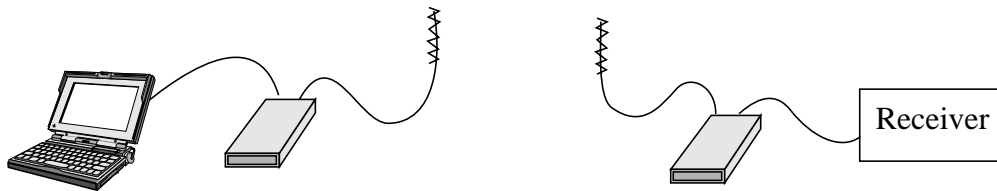
In the **phone modem connection** test, each receiver was attached directly to a Telebit Worldblazer phone modem, which was dialed from a computer attached to another Telebit Worldblazer phone modem. Various modem configurations were tested, including vendors suggested settings to determine the optimal settings for each receiver.

Phone Modem Connection



In the **radio modem** test, each receiver was attached directly to a Freewave Wireless Data Transceiver (DGR-115), which transmitted signals to a computer attached to another Freewave radio modem. The radio modems were placed in different buildings 100 meters apart. The transmission was sent through the windows of the buildings which are known to attenuate the signal due to a metalized reflective coating. Transmission statistics were recorded and indicated a connection similar to those experienced in field use. The placement of the radio modems did not change between the tests.

Radio Modem Connection



### 5.3 Summary of Measurements:

The tables that follow report the best times and throughput speeds recorded for each download test suite. Download timing tests were performed by downloading selected large files from the receiver to a PC. File size measured in bytes from a directory listing on the PC after the download and the time elapsed on a stopwatch to download the file were recorded. The effective throughput in characters per second (CPS) was measured by dividing this file size by the recorded time. The time to download a 24 hour file<sup>1</sup> was calculated by dividing a typical number of bytes in an average 24 hour file<sup>1</sup> by the fastest actual download speed measured. These tests were done for sev-

---

1. Average file size for 24 hours of observation, with 30 second sampling, and 0 degree elevation cutoff for each receiver.

Ashtech Z-XII3 (after a “hose” download):2.4983 MB  
 Ashtech Z-XII3 (after a “remote” download):0.7844 MB  
 Leica SR399E:0.9588 MB  
 AOA Rascal (Conan Binary format):0.4416 MB  
 Trimble 4000 SSI (after a “4000” download):1.8768 MB  
 Trimble 4000 SSI (after a “getfile” or “rfile” download):0.8088 MB  
 AOA TurboRogue (Conan Binary format):0.4416 MB

eral receiver port baudrate settings, but only the fastest results were included in the tables. For a more complete list of the tests performed, see Appendix C.

*Note that the highest baud setting possible on the receiver does not always produce the fastest download.* This may result from communication errors at higher baud settings and the need for more bytes to be resent. The receiver with the highest throughput is not necessarily the fastest one to download, because the file sizes differ between receivers.

For the **direct connection** test, the Ashtech Z-XII3 had the highest throughput but the Trimble 4000 SSI had the fastest download, as shown in Table 5.1 on page 5-3. Note that the proprietary remote programs (rfile, getfile, and remote) have much slower throughputs than the standard download programs (4000 and hose) even during a direct connection, non “remote” download.

**Table 5.1: Direct Connection<sup>a</sup>**

Receiver	Download Software	Baud Setting	CPS	Time to download 24 hr. file - sec. [min]
Trimble 4000 SSI	4000	57600	12570	149 [2:29]
Ashtech Z-XII3	hose	115200	15939	157 [2:37]
Trimble 4000 SSI	rfile -f	57600	3948	205 [3:25]
Trimble 4000 SSE <sup>b c</sup>	rfile -f	57600	3800	212 [3:32]
Trimble 4000 SSI	rfile	57600	3174	255 [4:15]
Trimble 4000 SSE	rfile	57600	2994	270 [4:30]
Trimble 4000 SSE	getfile	57600	2950	274 [4:34]
AOA TurboRogue <sup>d</sup>	pcplus-xmodem	19200 <sup>e</sup>	1267	348 [5:48]
Ashtech Z-XII3 <sup>f</sup>	remote	115200	2211	355 [5:55]
AOA Rasca <sup>g</sup>	pcplus-xmodem	38400	1112	397 [6:37]
Leica SR399E	SKI	38400	1971	486 [8:06]

- a. Direct Connection tests were performed on a CompuAdd 486DX, 25 MHz, desktop computer, with 4 MB RAM and an 8250 UART.
- b. Initially, the Trimble SSI used for the download test did not have the remote download option, so a Trimble SSE-RC was substituted for the tests requiring that option. According to Trimble, this should not have effected the times.
- c. An additional 90 seconds are required to convert file from rfile and getfile downloads to standard Trimble format. An additional 2 minutes are required to convert the standard Trimble files to the rinex format.
- d. An additional 3 minutes are required to convert the conan binary file to the rinex format.
- e. In this test, the 19200 baud download was slightly faster than the 38400 baud download.

- f. An additional 2 minutes are required to convert the file from remote download to standard Ashtech format.  
An additional 2 minutes are required to convert the standard Ashtech files to the rinex format.
- g. An additional 3 minutes are required to convert the conan binary file to the rinex format.

For the **phone modem** tests, the AOA TurboRogue had the highest throughput and the fastest download, as shown in Table 5.2 on page 5-4. The information in this table has also been optimized to only show the best times we achieved. The AOA receivers download using the XMODEM protocol and are able to take advantage of a rare but useful *spoofing* capability of some modems, which allows significant savings on long distance calls compared to the other receivers.

**Table 5.2: Phone Modem Connection<sup>a</sup>**

Receiver	Download Software	Protocol	Baud Setting	CPS	Time to download 24 hr file - sec. [min]
AOA TurboRogue	pcplus-xmodem	PEP	19200 <sup>b</sup>	1113	397 [6:37]
AOA Rascal	pcplus-xmodem	PEP	19200 <sup>c</sup>	1043	424 [7:04]
Ashtech Z-XII3	remote	PEP	38400 <sup>d</sup>	943	832 [13:52]
Trimble 4000 SSI	rfile -f	v.32	9600 <sup>e</sup>	929	871 [14:31]
Trimble 4000 SSI	rfile	v.32bis	57600	710	1139 [18:59]
Trimble 4000 SSI	getfile	v.32bis	57600	671	1205 [20:05]
Trimble 4000 SSE	getfile	v.32bis	57600	488	1657 [27:37]
Trimble 4000 SSE	rfile	v.32bis	57600	481	1681 [28:01]

- a. Phone Modem tests were performed on an AST 486DX, 25 MHz, laptop computer, with 4 MB RAM and an 8250 UART.
- b. In this test, the 19200 baud download was slightly faster than the 38400 baud download.
- c. In this test, the 19200 baud download was slightly faster than the 38400 baud download.
- d. The remote program changed the modem settings to this baudrate. As noted in section 5.3, the download time likely could be reduced by up to 40% (from 13:52 to 8:30) by using newest firmware and data type 3.
- e. In this test, the 9600 baud download was faster than the 57600 baud download. Trimble representatives note that faster times have been measured by adjusting modem parameters and using their newest software

The AOA Rascal downloaded the fastest over our **radio modem** connection, as shown in Table 5.3 on page 5-5. The Trimble 4000 program downloaded at the highest throughput.

**Table 5.3: Radio Modem Connection<sup>a</sup>**

Receiver	Download Software	Baud Setting	CPS	Time to download 24 hr file - sec. [min]
AOA Rascal	pcplus-xmodem	19200 <sup>b</sup>	958	461 [7:41]
Trimble 4000 SSI	getfile	57600	1848	517 [8:37]
AOA TurboRogue	pcplus-xmodem	38400	854	517 [8:37]
Trimble 4000 SSI	4000	57600	3156	595 [9:55]
Trimble 4000 SSE	getfile	57600	1035	781 [13:01]
Trimble 4000 SSE	4000	57600	2301	816 [13:36]
Trimble 4000 SSI	rfile	57600	836	967 [16:07]
Ashtech Z-XII3	remote	38400 <sup>c</sup>	730	1075 [17:55]
Trimble 4000 SSE	rfile	57600	581	1392 [23:12]
Ashtech Z-XII3	hose	38400 <sup>d</sup>	1751	1427 [23:47]

- a. Radio Modem tests were performed on an AST386SL, 25 MHz, laptop computer with a 387 math coprocessor, with 4 MB RAM and an 8250 UART.
- b. In this test, the 19200 baud download was slightly faster than the 38400 baud download.
- c. The download crashed at higher baud rates, on our tests. Also see section 5.3 and footnotes for the Ashtech in Table 5.2. Vendor claims that 3 minute downloads are achievable with modern PC's and on-site support or training.
- d. The download crashed at higher baud rates, on this particular computer.

#### 5.4 Related Issues/Discussion:

Any receiver that can be controlled using DOS or Windows software should also be capable of remote operation using commonly available remote control software (i.e. PCAnywhere, Carbon Copy, Reach Out Remote Control), but our tests focused on receivers which included remote control capability without additional software or hardware purchases. However some researchers may find this method to their advantage due to familiarity with DOS, the ease of use of off the shelf software, and the added flexibility from having an on-site computer near the receiver. If we had tested this mode of operations, we believe that the download times would have been among the fastest, but the added complexity of operating a “remote” computer was outside of the scope of this test.

The Leica SR399E receiver was therefore not included in the phone modem or radio modem tests because remote control and operation of the Leica SR399E is intended to be in conjunction with a

DOS compatible computer using remote control software (i.e. PCAnywhere...) and due to lack of time to pursue in depth the features of the necessary WILDBASE software. In order to operate Leica receivers in a remote situation, i.e. retrieving data through a modem, the Leica Sensor must be previously programmed with the desired scenario and directly attached to a computer via one of the computer's two serial ports. The computer must be configured to run WILDBASE through Windows upon power up. The Leica Sensor can then download data to the locally attached computer. To allow remote access the computer must simultaneously run a communications program (i.e. PCAnywhere...) in host mode on the computer's other serial port. The speed of remote transfer will then depend on the capabilities of the remote communication software and its interaction with the modem, the baud setting, the file transfer protocol, and the communications/computer equipment.

In all AOA TurboRogue and AOA Rascal downloads, the Conan Binary format was used but other choices could affect download times.

In all Ashtech Z-X113 downloads, we are not certain which downloads used type 0 or type 3 formats which could affect measured download times by 40%. We did not distinguish which type was downloaded since type 3 was not documented in the manual provided with our test receivers. Since some surveys were collected data in type 3 mode we cannot definitively see or compare the differences. (In this paper we use the term "data types" for what Ashtech terminology refers to as "Ranger Modes". The data types are described more in section 5.6 under "Raw Data File Formats"). During our tests we consulted with Ashtech technical support several times about the exact differences between the data types, and we discussed the differences with other users of Ashtech receivers. We received conflicting responses describing the differences between type 0 and type 3 which we attributed to the newly updated firmware in our test receivers and lack of supporting documentation (i.e. "...type 3 data is both compressed and omits information that is redundant for a continuously operating GPS site", versus "...type 3 data is only compressed and contains all of the information that is in type 0"). At press time other Ashtech users with the new firmware report observing the beneficial effects of the compressed type 3 data, but we were unable to confirm the improved download speeds from our data and we did not have a receiver available to repeat the tests. We conclude that Ashtech download times are probably capable of up to 40% less time than we measured, and this is noted in Table 5.2/5.3 footnotes.

The Leica SR399E and the AOA TurboRogue have removable PC-Card (also known as PCMCIA or flash card) memory. Removal of the PC-Cards is another method of rapidly downloading a receiver. We did not report on this download method, but we note that users can benefit from the option of simply visiting the site and swapping PC-Cards - effectively a very rapid download.

The Trimble rfile software reportedly can soon be upgraded to a version that supports flow control and can achieve significantly higher flow rates than we were able to obtain. Newer firmware will reportedly support higher baud rate settings and allow download speeds to increase as baud rate settings are increased.

On some receivers the firmware can be upgraded remotely. However we did not evaluate the effectiveness of the feature.

## 5.5 Conclusions:

This test suite measured relative download speeds between GPS receivers in three typical scenarios faced by geodetic researchers. We found a wide range in times to download across the three scenarios. Much of the wide variation is not just receiver dependent but believed to also be due to the type of modem, modem protocol, computer and software protocol used to transfer data - a complex set of interdependencies that most researchers would probably prefer to be solved prior to making a purchase. Although our measurements were taken with the latest equipment and software supplied by each vendor, the rapid pace of development requires that purchases not be made only based on these test results but rather after conferring with the vendors regarding capabilities at the time of purchase. Remote communications to a GPS site can be expensive in both phone bills and time to install and configure a reliable system. Additional documentation and support from vendors regarding effective control and downloading of remote sites is needed.

For direct downloads the time to download took less than ten minutes for all receivers and therefore should not be a serious issue when determining which receiver to purchase. The download throughput speeds were repeatable within a narrow range for each receiver/software test, and the results should be easily matched by any researcher using any of the receivers with a modern computer. The option of swapping PC-Cards to "download" is available on some receivers, too.

In the radio and phone modem tests the download speeds varied significantly between different brands of receivers and even within the same brand but with different software used for the downloads. The fastest throughput from the phone modem tests was 1,113 characters per second - a factor of ten slower than the fastest direct download. More importantly, the receivers and modem had to be tuned to achieve optimal results rather than just "setting the baudrates to the highest value." In almost all cases, the receivers surprisingly performed better when port speeds were set to a value below the receivers maximum possible port speed, which emphasizes the need for additional system integration and documentation. Cost effective methods for retrieving data over high cost phone lines (long distance international or cellular) must be determined in advance or else unexpectedly high cost could be incurred - over \$8,000 of yearly phone charges (at \$1.00/minute) separate the fastest and slowest download times for one day of 30-second epoch GPS data. Although not shown in the tables, we believe that problems with communications over cellular and international telephone lines have similar performance issues. It may be less expensive in the long term to download a receiver directly to a computer locally at the site (using automated software) and then to retrieve the data from that computer over the modem using commercially available software. This could be faster because protocol spoofing, higher baud settings, and higher modulation speeds could be employed. These configurations will vary in different cellular or international regions with different line qualities. For researchers whose data does not require daily or near real time analysis, exchanging disks or PC-Cards by mail with a distant operator would be cost effective.

These tests show that significant receiver performance variations exist between direct download connections and phone modem or radio modem connections. Researchers should examine particular needs (on-site downloads by software or PC-Card swapping, remote control software capabilities and interface, near real time data access requirements versus phone bills) and balance the issues with the vendors support for specific capabilities before purchasing a receiver.

## 5.6 Receiver Options Related to Downloading:

### Memory Options:

Ashtech Z-XII3:	256 kB buffer plus 1 MB, 3 MB, 4 MB, 6 MB, 10 MB, 20MB, 40 MB internal PC-Card
Leica SR399E:	512 MB, 1 MB, 2 MB, or 4 MB removable SRAM cards <sup>1</sup> , or 1 MB internal memory
AOA Rascal:	2 MB, 4 MB, or 8MB internal flash memory
Trimble 4000 SSI:	256 kB buffer plus 1 MB, 2.5 MB, 5 MB, 10 MB, 20 MB, or 40 MB internal PC-Cards
AOA TurboRogue:	128 kB buffer plus 1 MB, 4 MB, or 10 MB removable PC-Cards

### Data Storage Hours<sup>2</sup>:

Ashtech Z-XII3:	1 MB - 29.25 hr.	10 MB - 292.5 hr.
Leica SR399E:	1 MB - 36 hr.	4 MB - 144 hr.
AOA Rascal:	1 MB - 33 hr.	8 MB - 264 hr.
Trimble 4000 SSI:	1 MB - 52 hr.	20 MB - 1040 hr.
AOA TurboRogue:	1 MB - 33 hr.	40 MB - 1320 hr.

### Baud Rate Settings:

Ashtech Z-XII3:	300, 600, 1200, 2400, 4800, 9600, 19200, 38400, 57600, 115200
Leica SR399E:	300, 600, 1200, 2400, 4800, 9600, 19200
AOA Rascal:	300, 600, 1200, 2400, 4800, 9600, 19200, 38400
Trimble 4000 SSI:	50, 110, 300, 600, 1200, 2400, 4800, 9600, 19200, 38400, 57600
AOA TurboRogue:	300, 600, 1200, 2400, 4800, 9600, 19200, 38400, (57600 and 115200 available as option)

### Data Deletion after Receiver Memory if Full:

Ashtech Z-XII3:	Receiver stops recording when full until data is deleted by operator or REMOTE software.
Leica SR399E:	Data can be deleted after a specified number of days with WILDBASE.
AOA Rascal:	Memory stops recording when full until data is erased by operator.
Trimble 4000 SSI:	Continuous logging option, where data logging will wrap around when the memory is full, overwriting the oldest data files. The feature can be turned on or off.
AOA TurboRogue:	Wrap on flashcard can be turned on or off.

### Number of Satellites Tracked:

Ashtech Z-XII3:	12
Leica SR399E:	9
AOA Rascal:	8 or 12

- 
1. Leica's SRAM cards should be upgraded to PC-Card Flash RAM cards by the end of the year.
  2. Based on 5 SVs present and 30 second epochs. These numbers are from the receiver operator manuals, or updated from vendor technical support contacts.

Trimble 4000 SSI: 12  
AOA TurboRogue: 8

### **Sample Rates:**

Ashtech Z-XII3: 0.5 - 999.5 seconds in 0.5 intervals, with option for 0.25 intervals.  
Leica SR399E: 1 - 60 seconds in 1 second intervals.  
AOA Rascal: 1, 3 - 3600 seconds in 1 second intervals.  
Trimble 4000 SSI: 0.5 - 900.0 seconds in 0.5 second intervals.  
AOA TurboRogue: 1, 3 - 3600 seconds in 1 second intervals.

### **Ports:**

Ashtech Z-XII3: 2 power, 4 serial ports, 1 antenna, 1 ext. ref., 1 camera in, 1PPS  
Leica SR399E: 1 sensor/power, 1 sensor/power/NMEA, 1 RTCM in/out  
AOA Rascal: 1 power, 2 serial ports, 1 antenna  
Trimble 4000 SSI: 3 power, 2 I/O ports, 1 AUX port, 1 antenna, 1 ext. ref.  
AOA TurboRogue: 1 power, 2 serial ports, 1 antenna, 1 5MHz in and 1 out, 1PPS out

### **Flow Control:**

Ashtech Z-XII3: XON/XOFF  
Leica SR399E: Handshake supported in the future.  
AOA Rascal: None  
Trimble 4000 SSI: None, XON/XOFF, RTS/CTS (port 2)  
AOA TurboRogue: None, RTS/CTS (by changing wires on cable)

### **Transfer Protocol:**

Ashtech Z-XII3: hose (xmodem-1k) and remote (xmodem-1k)  
Leica SR399E: SKI (proprietary)  
AOA Rascal: xmodem  
Trimble 4000 SSI: 4000 (proprietary) and rfile (proprietary)  
AOA TurboRogue: xmodem

### **Downloading Environments Supported:**

Ashtech Z-XII3: DOS.  
Leica SR399E: Windows.  
AOA Rascal: DOS, Windows, UNIX, Macintosh.  
Trimble 4000 SSI: DOS and UNIX.  
AOA TurboRogue: DOS, Windows, UNIX, Macintosh

### **Raw Data File Formats:**

Ashtech Z-XII3: Type 0 (all position and phase information), Type 1 (position and code phase information), Type 2 (position information), Type 3 (all position and phase information), Binary, ASCII.  
Leica SR399E: Rinex, Leica Proprietary.  
AOA Rascal: Conan Binary, TurboBinary, Conan Ascii, Turbo Ascii, Long Turbo Binary, Tone Binary, Clonex Obs File, Clonex Nav File, Spread Sheet.  
Trimble 4000 SSI: Trimble Proprietary.

AOA TurboRogue: Conan Binary, TurboBinary, Conan Ascii, Turbo Ascii, Long Turbo Binary, Tone Binary, Clonex Obs File, Clonex Nav File, Spread Sheet.

**Other:**

Ashtech Z-XII3: Download requires a math coprocessor.

Leica SR399E: Continuous operations and automatic restarts after power fails require the running WILDBASE on a computer co-located with the sensor.

AOA Rascal: The manual states<sup>1</sup> inability to simultaneously track and download except at low data rates. Our test receiver did not track and download simultaneously. The manufacturer states that this was due to earlier software versions, but their current production models can simultaneously track and download at the highest rates.

**5.7 Remote Operation Capabilities:**

Some researchers need to access the receiver through phone modem connections. Proper operations include at least the ability to query the receiver to determine its operational status, to download data files through the modem, and to change various receiver parameters.

The following table describes the programs used to download a receiver through a modem and the process of changing the receiver parameters through a modem.

**Table 5.4: Remote Operation Capabilities**

	Ability to download through remote two-way communications.	Ability to change receiver configuration through remote access.
Ashtech Z-X113	Ashtech's REMOTE program.	Ashtech's REMOTE program or any communications program.
AOA TurboRogue	Any communications program.	Any communications program.
AOA Rascal	Any communications program.	Any communications program.
Leica SR399E	The sensor must operate in conjunction with a computer. The computer must run WILDBASE and a separate communications program in host mode on Windows.	Remote control possible with a remote control software such as PCAnywhere.

---

1. AOA Rascal Operators Manual, p. 16

**Table 5.4: Remote Operation Capabilities**

	Ability to download through remote two-way communications.	Ability to change receiver configuration through remote access.
Trimble 4000 SSI	Trimble's RFILE or GETFILE programs.	Trimble's YELLOWBOX program which displays a virtual receiver front panel.



Static Survey RMS Baseline Scatter from LGHN station TO (in meters):

STAT	BASE.LENGTH	D(LAT)	D(LON)	D(HGT)	D(LGT)
B322	630	0.0006	0.0002	0.0017	0.0000
K405	1296	0.0000	0.0013	0.0020	0.0006
R440	2217	0.0051	0.0002	0.0144	0.0052
Y320	2274	0.0018	0.0016	0.0072	0.0022

The scatter is typically less than 1.8 mm in the horizontal components and 7.2 mm in the height with the exception of R440 which is 5.1 mm in Latitude and 14.4 mm in height. As noted, this station is next to a utility pole and, as will be shown below, the scatter is also larger in the real-time results for this site.

Baseline lengths were from 0.7 kilometers to 2.4 kilometers. As an option, points out to about 10 kilometers were included in the static observations and these points were available to the manufacturers to try if they chose to do so. The shorter lengths were decided on to avoid making the real time system's accompanying radio packages an issue in the test. All manufacturers were asked to use the types of radio systems which they would offer in a baseline GPS price package. Optional, more powerful, radios are available for use with any receiver system.

A static evaluation of GPS equipment was conducted concurrently with the real time work on NOAA's Table Mountain Facility. The real time test was not conducted there because use of radios at Table Mountain is prohibited by law. It was agreed that a fair evaluation could be made by running a circuit through the four points along Route 36 three times. At each visit to a point the operator would make three different position determinations with respect to a known base station using real time phase measurements. The position determinations were based on three different initialization techniques as follows:

- (1) Initialization on the fly
- (2) Initialization using a known position for the point where data was being collected
- (3) Initialization on an unknown point

This yielded 9 positions per point per manufacturer and with three manufacturers this brought the number of positions yielded per point to 27. From this information it is possible to compare the following:

- (1) Real time positions against results of the static survey
- (2) Receiver specific real time position repeatability based on the three different methods of initialization cited above (presented as a standard error below)
- (3) Overall repeatability based on all derived values for a point

(4) Performance of different makers' systems at sites characterized by signal interference caused by obstructions such as utility poles.

Each manufacturer collected the data for the test at approximately the same time of day on Monday, Wednesday and Thursday during the week of September 17, 1995 in order to have results under similar satellite geometry conditions. The satellite constellation had between five and eight satellites during the observations. The operators collected three data points per observation mode and collected data for at least five seconds after ambiguities were resolved. Horizontal and vertical precision parameters were set at 1.5 centimeters and 2 centimeters respectively in the receivers. While traveling by car between each point the units were forced to lose lock on all satellites each time station locations were changed. Receivers were operated with default data acquisition parameters as follows:

BASE STATION			ROVER STATION	
	Elevation Mask	Update Rate	Elevation Mask	Update Rate
Ashtech	13°	1 second	13°	1 second
Leica	15°	2 second	15°	2 second
Trimble	13°	1 second	13°	1 second

#### 6.4 Comments:

There are two inconsistencies in the data from the test. Both are related to the known point initialization. Trimble and Leica used the first on-the-fly occupation of each point as the basis of all of their subsequent known point determinations. Ashtech on the other hand only operates in an on-the-fly mode, which is to say Ashtech does not have either "initialize from a known point" or "initialize from an unknown point" feature. Therefore, the recourse for Ashtech was to force a loss of lock between every observation they made. The effect of these inconsistencies should be very minor.

At the time Trimble ran over the course, weather conditions could be described as moderate with light rain. On Leica's test day, it was raining, sleeting and quite cold for summer. The equipment functioned better than the participants that day. The weather does not affect the data, although the chance of operator setup error is always greater in inclement weather conditions. By the time Ashtech ran the course, there were four inches of snow on the ground, although it was not snowing during the observations.

#### 6.5 Comparison of Results:

The observed baseline vectors were provided on floppy disks in DX, DY, and DZ in meters from the base station at LGHN. We then converted the values to DN, DE and DU in local coordinates (local to LGHN) in order to separate vertical from horizontal components for purposes of comparison. The raw XYZ and derived NEU components are given in Appendix D. A summary of averaged results and standard errors is also given in Appendix D and is plotted in Figure V-1 below.

The RMS scatter for the horizontal components (9 observations/site/manufacturer) was less than

8 mm and more typically less than 5 mm. The vertical scatter was less than 17 mm in all cases and more typically less than 7 mm. Overall, the scatter between observations taken with the three different types of initialization at each occupation was less than the scatter between reoccupations of the site. This suggests that setup error or change of satellite constellation was more of a contribution to the scatter than initialization method.

The agreement between the average real-time results and the static results was typically better than 7 mm in the North, 2 mm in East and 10 mm in the vertical components. All average observations fell within manufacturer minimum standard error (one sigma) specifications of  $\pm 10$  mm horizontal and  $\pm 20$  mm vertical when accounting for static solution uncertainties. The solutions between manufacturers agreed generally to better than 1 centimeter except for station R440 near the utility pole where the scatter was slightly larger.

Overall, the data collected on the spot exceeded input precision minimums. All of the evaluated units not only repeated well with each other and static solutions, they also all locked on to the satellites and resolved ambiguities within a matter of seconds and therefore, speed of operation was not an issue.

## Real-time GPS Baseline Statistics

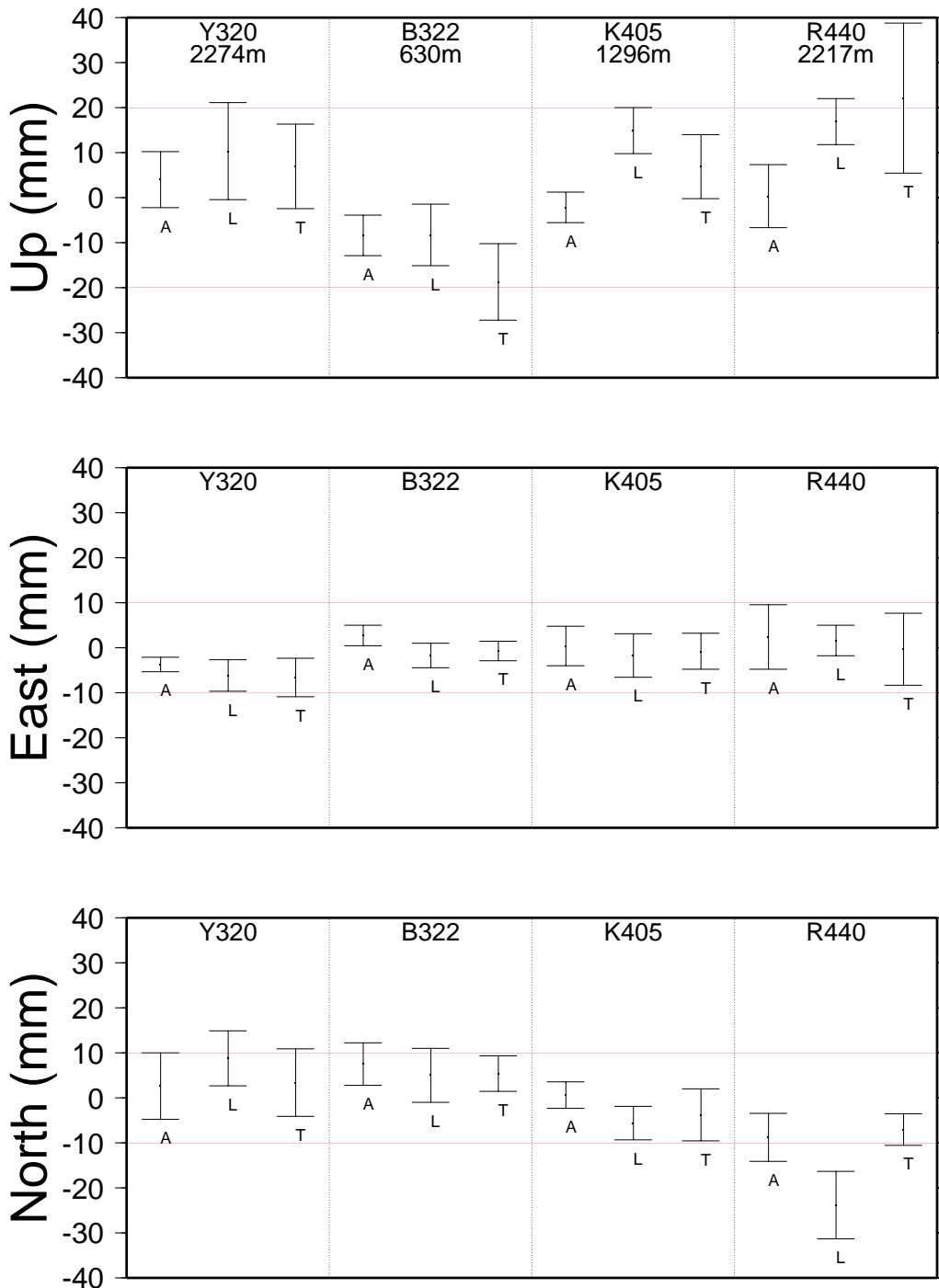


Figure 6.1: Comparison of baseline component between real-time kinematic and static survey results for 4 stations. Shown are the average of 9 solutions (3 independent visits, 3 obs/visit) and one standard deviation scatter. A = Ashtech, L= Leica and T = Trimble. The manufactures minimum error specification is shown with horizontal lines (+-10 mm horizontal, +- 20 mm vertical).

A comparison of published receiver specifications is given in Appendix C. For the UNAVCO demonstration, the manufacturers used the following equipment:

LEICA

BASE STATION	Sensor SR399E.....Firmware Version 3.04 AT303 External Antenna.... with ground plane CR344 Controller.....Firmware Version 3.20 RFM96W 2 watt Pacific Crest 2 watt Radio Modem
ROVER SATATION	Sensor SR399E.....Firmware Version 3.04 AT303 External Antenna....without ground plane CR344 Controller.....Firmware Version 3.20 RFM96W 2 watt Pacific Crest 2 watt Radio Modem
Processing Software	SKI 2.0b

TRIMBLE

BASE STATION	4000 SSI Receiver Compact L1/L2... with ground plane TDC1 Data Collector Trimtalk 900 Radio Modem
ROVER SATATION	4000 SSI Receiver Compact L1/L2....without ground plane TDC1 Data Collector Trimtalk 900 Radio Modem
Processing Software	GPSurvey 2.0

ASHTECH

BASE STATION	Ashtech Z-12 RTZ Ashtech Geodetic Antenna Husky FS/2 Data Controller RFM96W 2 watt Pacific Crest 2 watt Radio Modem
ROVER SATATION	Ashtech Z-12 RTZ Ashtech Hydro Antenna....without ground plane Husky FS/2 Data Controller RFM96W 2 watt Pacific Crest 2 watt Radio Modem
Processing Software	PRISM II

## 6.6 Persons Contacted:

Name	Organization & Job Title Address Internet	telephone fax
Ellis Veatch	Ashtech Technical Services 1170 Kifer Road Sunnyvale, CA 94086 Internet ellis@ashtech.com	408-524-1504 408-524-1500
Dave Hull	Colorado Sales Representative for Survey Systems Leica Inc. 2 Inverness Drive East Suite 106 Denver, CO 80112 Internet 76026.3605@compuserve.com	303-799-9453 303-799-4809
Andrew Hurley	GPS Product Specialist Leica Inc. 2 Inverness Drive East Suite 106 Denver, CO 80112 Internet 76323,3017@compuserve.com	303-799-9453 303-799-4809
Bryn Fosburgh	New Survey Product Specialist Trimble Navigation Limited 880 West Maude Ave Building 8 Sunnyvale, CA 94086	800-827-8000 x 8372 or 608-846-7974
Randy Hurt	Colorado Sales Representative for Survey Systems Trimble Navigation Limited 1839 Kiowa Trail Elizabeth, CO 80107 Internet randy_hurt@trimble.com	303-646-9864
Brennan O'Neill	Technical Support to Sales Representative Trimble Navigation Limited P O Box 191 Manitou Springs, CO 80829 Internet brennan_o'neill@trimble.com	719-685-1736 719-685-4280
Dave Ross	Chief of Operations Trimble Navigation Limited 2203 Timberloch Place	713-363-4700 713-292-8876

Suite 250  
 The Woodlands, TX 77380  
 Internet dave\_ross@trimble.com

Dr. Joan Yau GPS Product Specialist 604-278-3898  
 Leica Inc. 604-278-3558  
 15-13520 Crestwood Place  
 Richmond, BC V6X 2W7  
 Canada  
 Internet 75471,1655@compuserve.com

John Stenmark Manage, Product Support 303-799-9453  
 Leica Inc. 303-799-4809  
 2 Inverness Drive East  
 Suite 106  
 Englewood, CO 80112  
 Internet 73770,1616@compuserve.com

## 6.7 Summary of Features and specifications for Real-time Surveying Systems based on Manufacturers Brochures

	TRIMBLE	LEICA	ASHTECH
<b>BASE PACKAGE</b>			
Receiver frequency	• Site Surveyor SSI Receiver	• SR399 GPS Sensor /Antenna	• Z-12 RTZ GPS receiver/dual-
Base Antenna (700718B)	• Geodetic Antenna Kit (Compact L1/L2 with grndpln)	• SR399E Sensor	• L1/L2 Antenna/grnd pln
Roving Antenna	• Traverse Antenna Kit (Compact L1/L2)	• AT202 External Antenna	• Antenna - L1/L2 (700700A)
Antenna Grnd Pln	• Removable antenna ground plane	• Ground Plane for AT202 External Antenna	N/A
Data Collector	• TDC1 handheld Survey Controller	• CR344 Controller	• Husky FS/2 Data collector
Firmware	• RTK Firmware (OTF)	• RT-SKI firmware for GPS controller	• RTZ Firmware
exchanged in order to	• RTK is add-on option	• RT-SKI is add-on option	Receiver firmware must be
RTZ			switch from static mode to
Receiver standard firmwarization while moving)		• Automatic on-the-fly (initialization while moving)	• Automatic on-the-fly (initial-
Receiver firmware options	• Automatic on-the-fly (initialization while moving)		
Radio System (Crest)	• TRIMTALK 900 (0.3 watt) (repeater included)	• RFM96 Radio modem (2)watt amp (Pac Crest)	• 2 watt radio modem (Pac
	• 5db radio antennas	• Omni mobile whip antenna 5db	• antenna
	<i>A license is required for any radio broadcasting over 1/2 watt.</i>		
<b>TECHNICAL SPECIFICATIONS</b>			
Modes after ambiguity res)	• Rapid Static (immediately after ambiguity res)	• Rapid Static (immediately after ambiguity res)	• Rapid Static (immediately
immediately after	• On-the-fly (moving mode, immediately after initialization)	• On-the-fly (moving mode, immediately after initialization)	• On-the-fly (moving mode, initialization)
	• Stop and go (moving mode)	• Stop and go (moving mode)	• Stop and go (moving mode)
	• Kinematic (moving mode)	• Kinematic (moving mode)	• Kinematic (moving mode)
Accuracy	• 1cm + 2ppm horizontal	• 1cm + 2ppm horizontal	• 1cm + 2ppm horizontal
	• 2cm + 2ppm vertical	• 2cm + 2ppm vertical	• 2cm + 2ppm vertical
	<i>Based on favorable multipath, atmospheric conditions and proper antenna alignment</i>		
Measurement rate measurement	• 0.5 second per independent measurement (default measuring time: 1.0 sec)	• 1 second per independent measurement (default measuring time: 1.0 sec)	• 1 second per independent
Position latency	• 1 second	• 2 to 3 seconds	• 1 second
Range	• Up to 10km depending on radios used	• Up to 10km	• Up to 10km
Initialization mode	• Automatic while stationary	• Rapid static	• On the fly
	• Two known points	• On known point	

Initialization time ellipses obscured) known points).	<ul style="list-style-type: none"> <li>• &lt; 1 min (typical after all satellites obscured)</li> <li>• &lt; 10 sec. (typical with 2 known points).</li> </ul>	<ul style="list-style-type: none"> <li>• On the fly</li> <li>• &lt; 1 min (typical after all satellites obscured)</li> <li>• &lt; 10 sec. (typical with 2 known points).</li> </ul>	<ul style="list-style-type: none"> <li>• &lt; 1 min (typical after all sat- ellites obscured)</li> <li>• &lt; 10 sec. (typical with 2 known points).</li> </ul>
<i>Times are a function of the number of satellites visible, obstructions, baseline length, multipath and environmental effects.</i>			
Q C display	<ul style="list-style-type: none"> <li>• Displays RMS of position fix</li> </ul>	<ul style="list-style-type: none"> <li>• Displays RMS of position fix</li> </ul>	<ul style="list-style-type: none"> <li>• Displays RMS of position fix</li> </ul>
Tracking L2 P-code, operational	<ul style="list-style-type: none"> <li>• 9 channels L1 C/A code, L1/L2 P-code,"</li> <li>• L1/L2 full cycle carrier. Fully operational during P-code encryption. (12 channels optional)</li> </ul>	<ul style="list-style-type: none"> <li>• 9 channels L1 C/A code, L1/L2 P-code,</li> <li>• L1/L2 full cycle carrier. Fully operational during P-code encryption.</li> </ul>	<ul style="list-style-type: none"> <li>• 9 channels L1 C/A code, L1/ L2 P-code.</li> <li>• L1/L2 full cycle carrier. Fully operational during P-code encryption.</li> </ul>
Datalogging	<ul style="list-style-type: none"> <li>• Internal memory not standard; data is logged in optional survey controller or optional internal memory</li> </ul>	<ul style="list-style-type: none"> <li>• Optional 1MB in controller</li> <li>• 0.5 MB and 2 MB PCMCIA cards</li> </ul>	
Start-up start	<ul style="list-style-type: none"> <li>• &lt; 2 minutes from power on to survey start</li> <li>• &lt; 30 seconds with recent ephemeris</li> </ul>		<ul style="list-style-type: none"> <li>• 2 minutes to first data, cold</li> <li>• &lt; 30 seconds warm start</li> </ul>
Communications max	<ul style="list-style-type: none"> <li>• Dual RS 232 ports for radio input and data collector control. Baud rates up to 38,400 baud rate on port 1 and 57,600 baud on port 2.</li> </ul>		<ul style="list-style-type: none"> <li>• 2 RS-232 ports 115200 bps</li> </ul>
Post-processed survey firmware surveying options planning, quality control, work adjustment (TERRAMODEL)	<ul style="list-style-type: none"> <li>• Internal memory and static survey firmware for post-processed surveying</li> <li>• GPSurvey software for mission planning, automatic data processing, quality control, database management, network adjustment</li> <li>• using TRIMNET Plus software and outputs to mapping software (TRIMMAP)</li> </ul>	<ul style="list-style-type: none"> <li>• Internal memory and static survey firmware for post-processed surveying</li> <li>• SKI software for mission planning, automatic data processing, quality control, database management, network adjustment</li> <li>• outputs to mapping software (LISCAD)</li> </ul>	<ul style="list-style-type: none"> <li>• Internal memory and static for post-processed surveying</li> <li>• PRISM software for mission automatic data processing, database management, net- using PNAV software and outputs to mapping software</li> </ul>
Other software	<ul style="list-style-type: none"> <li>• Trimble 4000 download</li> <li>• TRIMCONTOUR (USA) contours for TRIMMAP</li> <li>• QUICKPLAN mission planning</li> <li>• (3) TRIMTALK 900 program disks to (change channels)</li> </ul>		
<b>QUERY BASE STATUS</b>	<ul style="list-style-type: none"> <li>• battery</li> <li>• memory</li> <li>Receiver sends info from base</li> </ul>	<ul style="list-style-type: none"> <li>• battery</li> <li>• memory</li> <li>Operator finds info in a menu in controller</li> </ul>	<ul style="list-style-type: none"> <li>• no</li> <li>• no</li> </ul>

## **7. UNAVCO ARI Antenna Tests**

C Rocken, C. Meertens, J. Braun, M. Exner, B. Stephens

Test Result Summary

October, 1995

### **7.1 Abstract**

As GPS receivers routinely demonstrate sub-mm zero-baseline results, GPS antenna performance is a limiting error source and increasingly important for the highest accuracy GPS applications. Therefore, the UNAVCO facility tested several geodetic antennas. First we operated different antennas in the field on short baselines and compared the obtained GPS results with ground truth. Next we placed all the tested antenna types in the anechoic chamber operated by Ball Aerospace (Ball). The tested antennas were: Ashtech Choke-ring (Ashtech CR), AOA Choke-ring T (AOA CR), Trimble Geod L1/L2 GP (Trimble GEOD), Leica SR399 External (Leica), and AOA Rascal (AOA Rascal). In the Ball anechoic chamber we measured antenna phase center variations and antenna amplitude (gain) patterns as a function of direction. The resulting phase patterns from our chamber tests were applied to field data from mixed antenna (and receiver) baselines and results were compared to ground truth. We find that, using our anechoic chamber values, data from the different tested antennas can be mixed with an accuracy of about 5 mm in the vertical and 3 mm in the horizontal components when the ionospheric free linear combination L3 of the GPS carriers is processed. L1 and L2 solutions are generally better. If we process the same L3 data but also estimate a tropospheric delay parameter every hour the vertical accuracy is still about 15 mm or better for most tested antenna pairs. The horizontal accuracy is not significantly affected by the tropospheric estimation.

### **7.2 Introduction**

Antenna performance is important for high-accuracy GPS surveys. GPS analysis software computes the range from the point of signal reception at the receiving antenna to the point of signal transmission at the satellite transmitting antenna. The effective “point of signal reception” is also called the antenna phase center. Antenna chamber measurements can be used to determine this phase center. However, knowledge of the phase center alone is not sufficient for computing the exact GPS signal range. This range also varies with the direction of the signal and thus additional antenna-specific correction terms, which are a function of azimuth and elevation must be applied.

Antenna chamber tests can be used to determine the phase centers and the additional direction-dependent correction. This is done by “illuminating” a GPS antenna from all directions and measuring the phase change as a function of direction to the source. Then a least-squares approach can be used to determine the phase center which is the point about which the direction-dependent correction terms are minimized. The residuals of this least-squares estimation of the phase center are thus the direction - dependent corrections that the GPS software must apply. The technique to estimate the phase centers of the antenna and the direction-dependent correction is described in a paper by Kolesnikoff (1994).

In this paper we talk about phase centers and phase patterns. It is important to understand however that these two sets of numbers together describe the antenna. The phase center in this report is defined as the point in space about which the direction dependent corrections (or the phase pattern) are at a minimum. One could to define other points as phase centers as long as the direction dependent corrections are modified accordingly. One reasonable alternative phase center could be the intercept point between the top of the ground plane and the vertical axis of rotation of the antenna. Phase patterns could without much difficulty be computed with respect to this point. This is not generally done, however, because the phase patterns would not be minimized and they would generally be less symmetric, than the patterns used in this test.

There are several important differences between these recent UNAVCO/Ball chamber tests and those conducted previously for the high-accuracy GPS community by Schupler and Clark.

- (a) We ran the antennas in the chamber with LNAs - as used in GPS field applications.
- (b) The chamber source was varied in frequency to simulate spread spectrum conditions by measuring at 9 frequencies for L1 and L2 each, and then weighing the measurements to simulate the spread spectrum modulation characteristic of GPS P-code.
- (c) We stepped in 5 degrees through the azimuth and elevation directions, thus there are 72 azimuth steps. The measurements were taken to +/- 120 degree elevation. Thus considering the 9 frequencies for each map ~ 38,000 phase observation were taken for each L1 and L2 correction map and phase center.
- (d) A laser was used for finding the center of rotation about which the GPS antenna is spun.

These differences could be the cause for differences in both the phase centers and the direction-dependent maps that we present here and those published earlier.

### 7.3 Application of Antenna Chamber Results in GPS Software

Assume a GPS antenna is setup at a known height and well-aligned above a geodetic benchmark at  $\vec{X}_{mark}$ . Assume further that we know the phase centers and corresponding correction maps for both GPS frequencies. Then the range  $R$  to a GPS satellite at position  $\vec{X}_{sat}$  is computed as:

$$R = \left| \vec{X}_{mark} + \vec{X}_{ref} + \vec{X}_{phas} + \delta(\Phi, \Theta) \hat{e}_{\Phi, \Theta} - \vec{X}_{sat} \right| \quad (1)$$

Here  $\vec{X}_{ref}$  is the vector from the benchmark to a known physical antenna reference point (ARP) such as defined, for example, by the IGS,  $\vec{X}_{phas}$  is the vector from the ARP to the chamber-determined phase center,  $\delta(\Phi, \Theta)$  is the direction dependent correction as a function of satellite elevation and azimuth angles  $\Phi$  and  $\Theta$ .  $\hat{e}_{\Phi, \Theta}$  is the unit vector from the phase center in the direction of the GPS satellite.

Phase centers and corresponding direction-dependent corrections are determined for the L1 and the L2 frequencies separately. When GPS analysis software is processing the ionosphere-free linear com-

bination of the GPS carrier data then the linear combination of the L1 and L2 correction term has to be applied to the phase center coordinates and direction dependent correction terms as well, according to:

$$R = \left| \hat{X}_{mark} + \hat{X}_{ref} + A \cdot \hat{X}_{phas_{L1}} - B \cdot \hat{X}_{phas_{L2}} + (A \cdot \delta(\Phi, \Theta)_{L1} - B \cdot \delta(\Phi, \Theta)_{L2}) \cdot \hat{e}_{\Phi, \Theta} - \hat{X}_{sat} \right| \quad (2)$$

Here  $A=f1^2/(f1^2-f2^2)=2.546$ , and  $B = f2^2/(f1^2-f2^2)=1.546$ , with  $f1$  and  $f2$  the L1 and L2 carrier frequencies. Note that we made the (very good) approximation that the unit vector from the L1 phase center to the satellite is the same as the unit vector from the L2 phase center.

It is important to note that  $\hat{X}_{phas}$  and  $\delta(\Phi, \Theta)$  for a specific antenna are not unique. If one changes, for example the location of the phase center to  $\overrightarrow{X}_{phas}^*$ , then the direction-dependent correction map can be transformed to  $\delta^*(\Phi, \Theta)$  so that the condition  $\hat{X}_{phas} + \delta(\Phi, \Theta) \hat{e}_{\Phi, \Theta} = \overrightarrow{X}_{phas}^* + \delta^*(\Phi, \Theta) \hat{e}_{\Phi, \Theta}$  holds. The geodetic results obtained with the “\*” corrections should be identically the same as results obtained with the original values. The phase center for this study was chosen as the point that minimizes the residuals (direction-dependent corrections). It is however also possible to define other points of the antenna as phase center if the direction-dependent terms are transformed appropriately.

#### 7.4 Horizontal Phase Centers - Rotation Tests and Antenna Chamber results

Since 1989 the UNAVCO facility has determined horizontal phase centers directly from GPS field experiments. For these experiments we determined the relative vector between two antennas for different relative antenna, orientations. These tests, also known as antenna rotation tests, yield the horizontal offset of the antenna phase centers from the antenna’s vertical axis of rotation.

In the past the antenna phase center offsets, determined in the field from antenna rotation tests did not agree with values determined by antenna chamber experiments. Figure 7.1 summarizes the location of all horizontal phase centers, estimated from the UNAVCO/Ball antenna chamber tests.

# UNAVCO/BALL Anechoic chamber

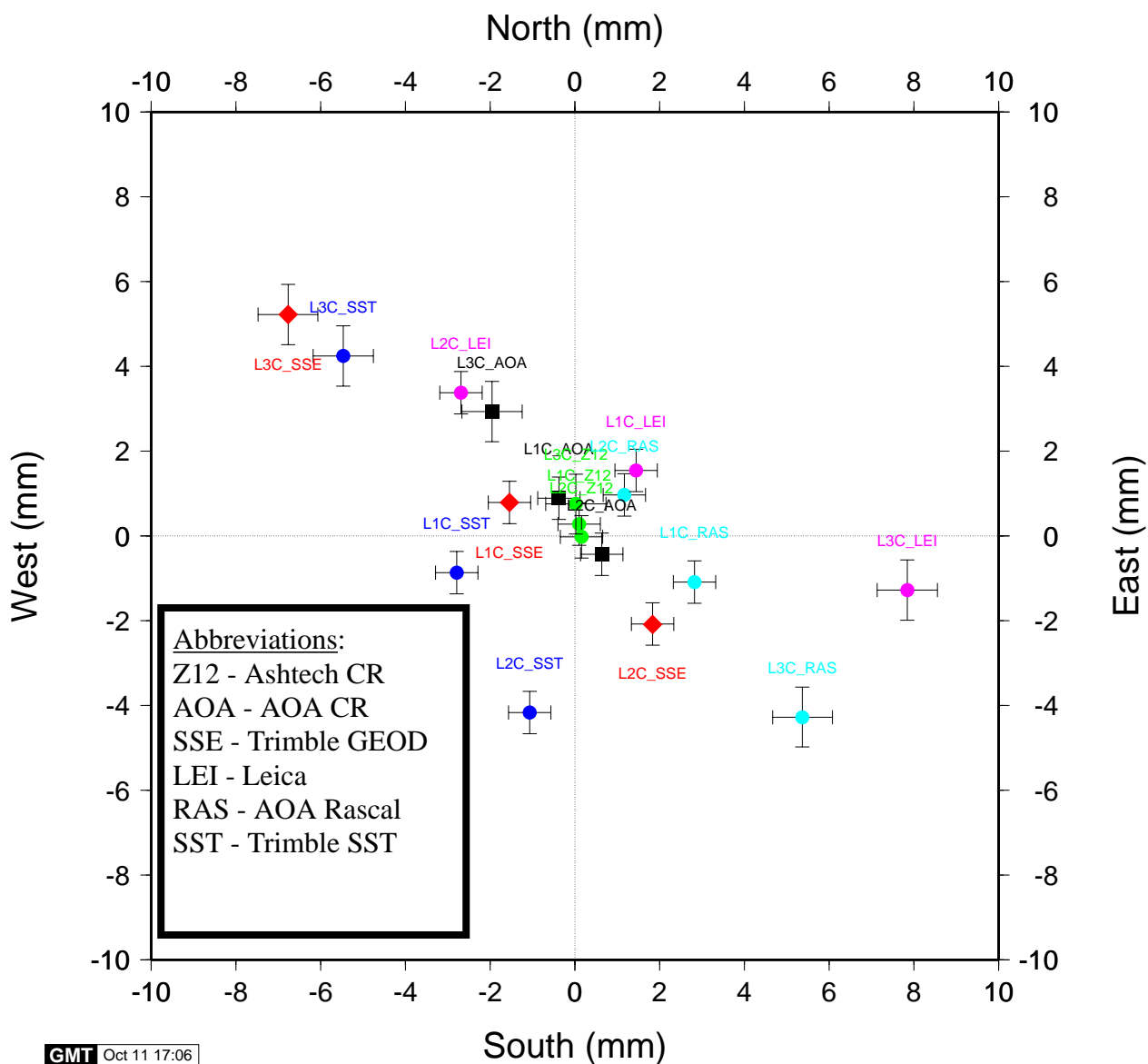


Figure 7.1: shows the horizontal phase center location for the antennas tested during the UNAVCO/Ball antenna chamber tests. The zero-point of this plot is the axis of rotation of these antennas. Phase centers for the L1,L2 and ionospheric free L3 linear combinations are shown. Error bars are +/- 0.5 mm based on estimates from Ball engineers. L1C, L2C and L3C show the locations of the L1, L2 and L3 phase centers as determined in the chamber for different antennas.

The most recent horizontal phase centers as determined during the UNAVCO/Ball tests agree well with our field rotation results as is shown for the AOA Choke-ring T and the Trimble GEOD antenna in Figure 7.2.

# ANTENNA PHASE CENTERS

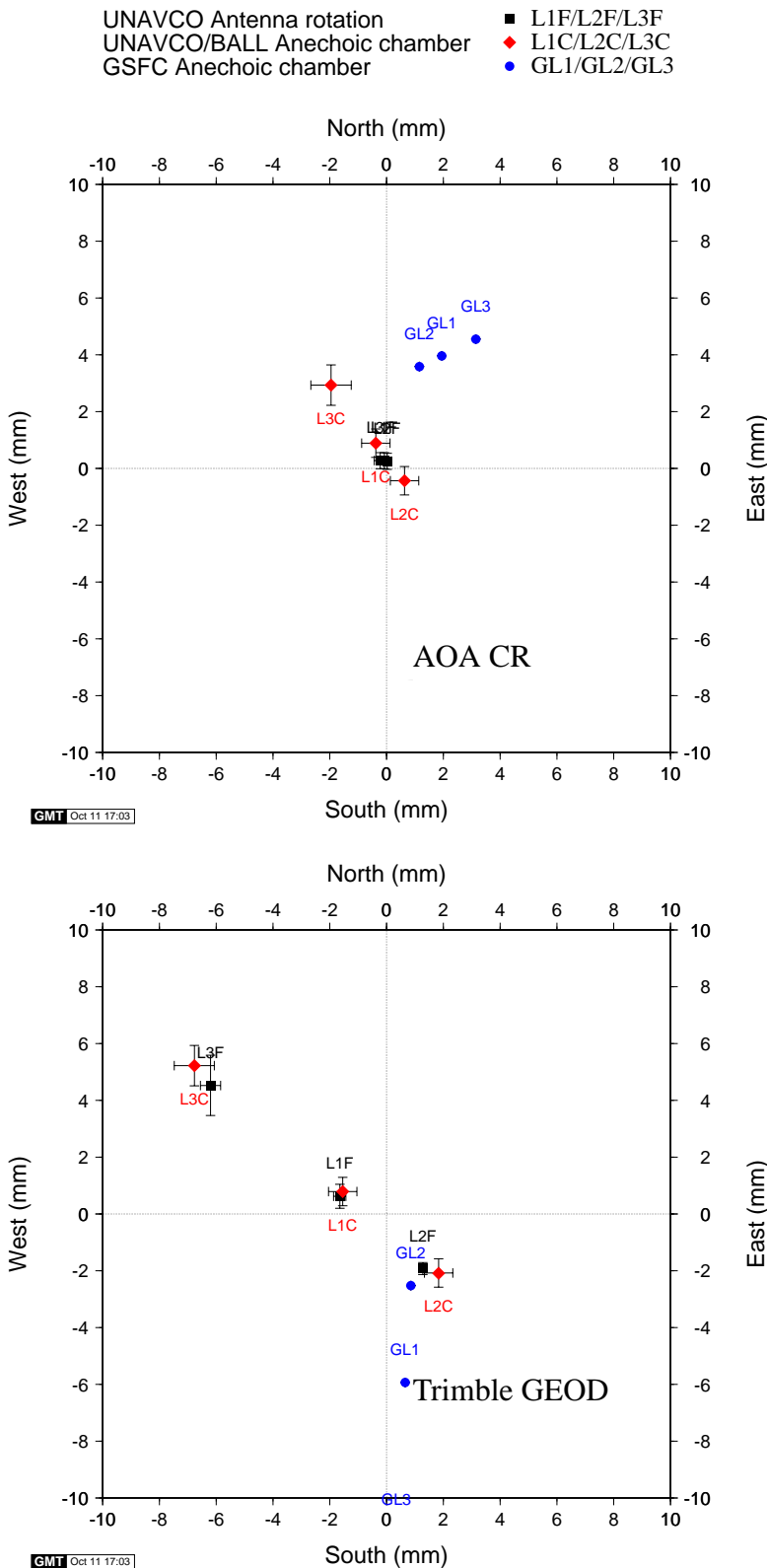


Figure 7.2: Horizontal phase center locations. In the top panel phase center locations for the AOA CR antenna are shown; in the bottom results for the Trimble GEOD are shown.

In these plots we compare the locations that were estimated from 3 experiments. 1) UNAVCO antenna rotation tests, 2) UNAVCO/Ball antenna chamber tests, 3) Goddard/Bendix antenna chamber tests are shown for comparison with previous results. Good agreement can be seen for the L1 and L2 UNAVCO rotation and antenna chamber results.

Small ~ 0.5 mm errors in L1 and L2 phase center locations are amplified when the L3 linear combination is formed.

## 7.5 Test of the UNAVCO/Ball Antenna Chamber Results

During the ARI receiver tests conducted on the UNAVCO test range on Table Mountain, 10 miles north of Boulder, Colorado, a large data set of mixed receiver/antenna baseline data was collected on known GPS baselines. This data was used to validate the UNAVCO/Ball correction values.

Antenna phase center corrections are especially important in two cases: (a) when different antenna designs are mixed, and (b) when very long baselines are surveyed with GPS. For short baselines and two antennas of identical design the effect of the antenna phase center variations cancels when the GPS single difference (SD) between observations of the same satellite from the two sites are formed. The reason for this cancellation is that  $\vec{X}_{phas_{antenna1}} = \vec{X}_{phas_{antenna2}}$  and  $\delta(\Phi, \Theta)_{antenna1} = \delta(\Phi, \Theta)_{antenna2}$  for same antennas, and for short baselines  $\vec{e}_{\Phi, \Theta_{antenna1}} = \vec{e}_{\Phi, \Theta_{antenna2}}$ . For mixed baselines the first two conditions do not hold. Elevation and azimuth from the two antennas to the GPS satellite are not identical at ends of long baselines. Thus phase center patterns are important in the long baseline case, even if identical antennas are used. Figures 3 and 4 show the L1 and L2 phase center patterns from the UNAVCO/Ball tests.

In the case of mixed antenna baselines, errors are incurred if the phase centers and corresponding phase patterns are not known accurately. Unknown differences in the phase patterns between two antennas can have systematic signatures. These systematic differences, when unmodelled, can be interpreted by the GPS analysis software falsely as a tropospheric delay. If this happens, the consequence is typically a corrupted tropospheric estimation and a large error in the vertical component of the estimated baseline vector.

In the ideal case antenna phase center corrections should, when applied during GPS processing according to the equations above, result in baseline coordinates that (a) agree with ground truth, (b) are identical for L1, L2 and the L3 ionosphere-free linear combination, and (c) are not affected by the estimation of tropospheric parameters at the sites. Antenna mixing problems result in errors that can be identified if any of these three conditions do not hold.

Using data from the ARI tests and the Bernese GPS software we tested how well the requirements (a), (b) and (c) were met for mixed baselines between the following receiver/antenna pairs:

<u>Pair Number</u>	<u>Pair Description</u>
(1)	Ashtech Z-XII3 / Ashtech CR (with dome) (antenna part number 700936(B))
(2)	AOA Rogue SNR-8000 / AOA CR (antenna part number 7490582-1)
(3)	AOA Rascal / AOA CR (antenna part number 7490582-1)
(4)	Leica SR399 / Leica (antenna part number AT202)
(5)	Trimble 4000 SSI / Trimble GEOD (antenna part number 23033-00)

We tested several different phase center correction methods:

<u>Name of Test</u>	<u>Phase Center Description</u>
Ball_0	Use only the UNAVCO/Ball phase centers and do not apply direction-dependent corrections.
Ball_1	Use UNAVCO/Ball phase centers and apply elevation-dependent corrections, independent of azimuthal direction. These elevation-dependent corrections were determined by averaging over all azimuthal directions.
Ball_2	Use UNAVCO/Ball phase centers and apply full azimuth and elevation dependent corrections (full map).
Ball_3	Same as Ball_1 but the chamber correction values for the Ashtech CR (with dome) had been replaced with the values determined in the chamber for the AOA CR Choke-ring antenna. This test was done to test if antenna mixing results improve when we assume that the Ashtech CR and AOA CR antennas are identical.
Ball_4	Same as Ball_1 but this time we replaced the chamber determined values for the AOA CR antenna with those estimated in the chamber for the Ashtech CR (with dome). This test was done to test if antenna mixing results improve when we assume that the Ashtech CR and AOA CR antennas are identical
Schup_0	Correction values distributed by Schupler and Clark during the IUGG meeting in Boulder Colorado, July, 1995. Phase centers were applied only, no elevation dependent corrections were applied.
Schup_2	Same as Schup_0 but phase centers and elevation dependent corrections were applied.

Each of these 7 different phase center correction schemes was tested. The purpose of Ball\_0 was for comparison with the other methods to assess the importance and effect of the direction-dependent corrections. Ball\_1 was tested because it is generally easier (and faster) to apply elevation-dependent corrections only. Ball\_2 was tested to examine if there is any advantage in using the full map (elevation and azimuth dependent) as opposed the azimuth-averaged map from Ball\_1.

From the results computed with the Ball\_1 and Ball\_2 phase center corrections we noticed that there were mixing problems between the Ashtech CR (with dome) and AOA CR antennas. Thus we decided to test if these antennas would mix better when using the same phase centers and the same direction dependent terms for both. This was done for Ball\_3 by simply replacing the elevation-dependent terms for the Ashtech CR with those of from the AOA CR antenna. In Ball\_4 we did the opposite and replaced the values for the AOA CR antenna with those from the Ashtech choke ring antenna.

The results that we obtained, using the correction terms distributed by Schupler and Clark in the Summer of 1995 were tested under the Schup\_0 and Schup\_2 runs. Schupler and Clark did not determine any corrections for the Ashtech CR (with dome) and Leica antennas. Thus for the Schup\_ tests we applied the AOA CR numbers to the Ashtech CR. Further we used the UNAVCO/Ball correction values for the Leica.

Between three and nine baselines were formed for each of the 10 possible ways of mixing the tested receiver and antenna pairs, resulting in 45 baseline files. Each of these files contained 20 hours of 30-sec GPS data, about 11,000 GPS observations. For each of the 7 phase center correction methods we processed each baseline 6 times in the following ways:

<u>Process-Name</u>	<u>Process Description</u>
L1_NOTROP	Process L1 phase data, estimate baseline vector only, carrier phase ambiguities are resolved and fixed to integer values.
L2_NOTROP	Same as L1_NOTROP for the L2 carrier frequency
L3_NOTROP	Same as L1_NOTROP for the ionosphere-free linear combination
L1_TROP	Process L1 phase data, estimate baseline vector, plus one tropospheric delay parameter every hour. Carrier phase ambiguities are resolved and fixed to integer values.
L2_TROP	Same as L1_TROP for the L2 carrier frequency
L3_TROP	Same as L1_TROP for the ionosphere-free linear combination

The results from these tests, for the vertical baseline component are shown in this report.

## **7.6 Results**

A total of 1890 baseline solutions were computed, each involving approximately 11,000 GPS observations. Below we summarize the most important results for the UNAVCO/Ball phase center maps from this analysis.

### **L1\_NOTROP**

Use of phase centers plus the full phase center maps from the UNAVCO/Ball chamber tests, results in vertical baseline errors of no more than 3 mm for any of the 10 possible mixing combinations. Application of the correction maps indicates improvement in all cases over just using the phase center offsets. A slight improvement can be seen when the full (Ball\_2 solutions) map is used over just using elevation-dependent corrections (Ball\_1 solution).

## L2\_NOTROP

All solutions for the Ball\_2 run show vertical mixing errors of better than 5 mm (Figure 7, left panel). Application of the Ball phase center maps increases mixing problems in some cases. Mixing between Ashtech CR and AOA CR is made worse when the direction dependent correction terms are applied. Best overall mixing performance is achieved for the Ball\_4 solution - all results appear to mix at the 2 mm level.

## L3\_NOTROP

All solutions mix to 5 mm or better when the full Ball\_2 phase map is applied. It is interesting to note that the Trimble GEOD antenna mixes better with the AOA CR antenna than the Ashtech CR. This is especially surprising because the Ashtech CR is a very close copy of the AOA CR. Generally Ball\_2 results (Figure 8, left panel) are better than Ball\_1 results (Figure 5, left panel), indicating that full phase center maps should be used.

The mixing error between these two Choke-ring antennas can be reduced if we set the Ashtech correction values to the values determined for the AOA CR (Ball\_3 results, Figure 9, left panel). However if we do this, the Ashtech CR mixes worse with the Leica antenna.

## L3\_TROP

This is probably the most important and also most demanding solution. Most important because this is the mode in which GPS data for geodetic research have to be processed, most demanding because the effect of any small errors in  $\hat{X}_{phas}$  and  $\delta(\Phi, \Theta)$  are amplified by forming the L3 linear combination by a factor of about 3.1. In addition the tropospheric estimation tends to increase the effect of errors in the phase center and correction map on the baseline vertical, as can be seen when comparing left and right panels in Figures 5-10.

When using the full correction map (solution Ball\_2) we see that all antennas except for the Leica can be mixed with the Trimble GEOD antenna at about the 5 mm level. The Trimble GEOD and Leica mix still shows errors of about 15 mm. It is interesting to note that once again the Ashtech CR and AOA CR mixing results are biased by about 12 mm. This effect is reduced to about 10 mm when we use the same phase center and same phase patterns for the two versions of the Choke-ring antenna. Thus no matter what we do, our analysis indicates that there is a mixing problem between Ashtech's Choke-ring antenna and the AOA CR antenna on the order of 1 cm.

The overall best mixing solutions for L3\_TROP processing are obtained for the Ball\_4 calculations, when only the mixing errors between the Ashtech CR and the Leica antenna are significantly larger than 10 mm (Figure 10, right panel).

## 7.7 Ashtech CR Antenna Dome Tests

The Ashtech CR antenna comes with a conical compressed styrofoam dome that covers the antenna. Our short mixed baseline results indicated that this antenna shows significant biases when mixed with the AOA CR antenna. These biases were observed when we assumed the AOA CR and

Ashtech CR antennas to be identical and they were not reduced when we applied the different patterns from the chamber tests. To determine if the conical dome could cause solution biases, the Ashtech CR antenna and Z12 receiver system (AZ12) was tested with and without the dome. Two AZ12s, and an Allen Osborne SNR-8000 Turborogue antenna and receiver system (AOAT) collected data at three of the marks on Table Mountain for two days. On the first day, the domes were attached to the Ashtech CR antennas, on the second day they were removed. Baselines were computed between all three marks for both days. These two systems have very similar antennas, and they should produce solutions that are close to ground truth.

## 7.8 Results of the Dome Tests

The height solutions for the two baselines using an AOAT system at one end of the baseline and an AZ12 system at the other end are presented in table 7.1. From the table, it can be seen that when the dome is attached, the L1 solu-

**Table 7.1: AOA CR - Ashtech CR Mixed Baseline Height Solutions Compared To Ground Truth**

Frequency (Baseline)	Ashtech CR With Dome		Ashtech CR Without Dome	
	No Troposphere Estimated	Troposphere Estimated	No Troposphere Estimated	Troposphere Estimated
L1 (DNDS)	1.2 (mm)	5.7 (mm)	0.6 (mm)	1.0 (mm)
L1(DNDW)	0.1	3.6	-0.7	-1.0
L2(DNDS)	1.3	0.2	-0.2	-0.9
L2(DNDW)	0.4	-0.4	-1.0	-2.0
L3(DNDS)	1.0	14.2	1.8	3.9
L3(DNDW)	-0.7	9.9	-0.1	0.5

tions estimating an hourly troposphere parameter are different from ground truth by up to 5.7 millimeters. This height error is amplified in the L3 solutions (14.2 and 9.9 millimeters) for both test baselines. The solutions without troposphere estimates have a scatter of less than 2.0 millimeters for all solutions (L1, L2, L3) with and without the dome.

The height results from the baseline computed with an AZ12 system at each end of the marks are presented in table 7.2. While the solutions when estimating troposphere parameters are not as close to ground truth as the solu-

**Table 7.2: AZ12 - AZ12 Unmixed Baseline Height Solutions Compared To Ground Truth**

Frequency (Baseline)	AZ12 With Dome		AZ12 Without Dome	
	No Troposphere Estimated	Troposphere Estimated	No Troposphere Estimated	Troposphere Estimated
L1(DSDW)	-0.8 (mm)	-3.0 (mm)	-0.8 (mm)	-3.0 (mm)
L2(DSDW)	-0.3	-2.1	-0.4	-2.4

**Table 7.2: AZ12 - AZ12 Unmixed Baseline Height Solutions Compared To Ground Truth (Continued)**

Frequency (Baseline)	AZ12 With Dome		AZ12 Without Dome	
	No Troposphere Estimated	Troposphere Estimated	No Troposphere Estimated	Troposphere Estimated
L3(DSDW)	-1.4	-4.5	-1.6	-4.0

tions without troposphere estimates, the problem is not as large as the AOAT-AZ12 mix. The problem is less than 5.0 millimeters for all solutions. There also does not appear to be one frequency that is off significantly more than the other. The solutions without the troposphere estimate have a scatter of less than 2.0 millimeters for all solutions. This is similar to the mixed baselines without troposphere estimates

Because the larger height biases occur when the dome is attached to an antenna at one end of the baseline, it appears that it is causing the problem. When both antennas have the dome attached, the bias may difference out. It is also possible that there is a receiver mixing problem in the AOAT-AZ12 baselines. The next set of measurements will involve measuring a baseline with two AZ12 systems. One end of the baseline will have the dome attached during the entire test, the other mark will have the dome removed for half of the solutions.

## 7.9 Conclusions and Future Work

We have characterized several important GPS antennas in the Ball Aerospace antenna chamber and tested these chamber corrections with mixed antenna data, collected in the field. Our results show that the antenna characteristics determined in the Ball anechoic chamber can be used to significantly reduce antenna mixing errors (see Figures 5-10, comparison of Ball\_0 with Ball\_1,2,3,4 results). Mixing problems between AOA CR and the Trimble GEOD are reduced to several mm in the vertical, even for the L3 linear combination when tropospheric parameters are estimated. This compares to mixing errors of more than 50 mm that we reported prior to the UNAVCO/Ball tests. Mixing errors in the vertical for any combination of the tested antennas is at a level below 20 mm. Horizontal mixing errors seem to be reduced to about the 3 mm-level.

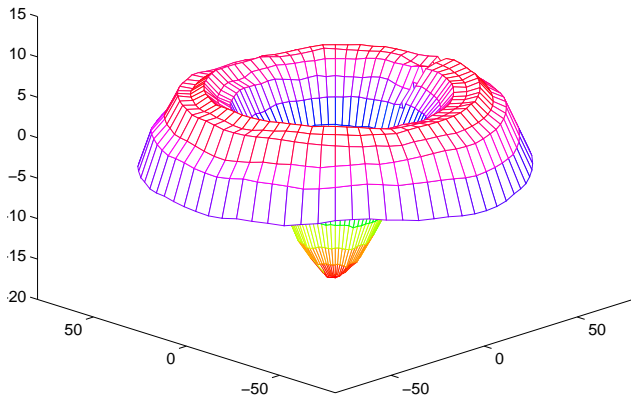
While the corrections greatly improve results for many antenna pairs over older correction values and over no correction values at all, they are not at the desired 1 mm-level yet. Especially the estimation of tropospheric parameters still affects the baseline results significantly. We believe that this may be caused by site multipath. UNAVCO tests (Antenna Height test report available on the UNACO home page, <http://www.unavco.ucar.edu/>) have shown that even with identical antennas the antenna setup height can affect solutions by 1-2 cm in the vertical when tropospheric parameters are estimated. A corresponding report (The Role of Multipath in Height Tests at Table Mountain; also available on the UNAVCO home page) shows that multipath is the likely reason for this effect. Antenna chamber tests determine antenna patterns in a multipath-free environment. These patterns, when applied in a field environment, will not describe the pattern of the antenna which is affected by the site. Thus, in order to achieve mixing of antennas at the mm-level in the vertical when tropospheric parameters are computed, multipath must be reduced or the effect of multipath on the chamber patterns must be better understood.

An alternative approach is to avoid mixing of antennas by using a “Standard Antenna”. This approach would greatly reduce antenna errors, but it will not completely solve the problem because of setup and site-specific multipath and its systematic effect on baseline coordinates. Long baseline problems will also remain unless the phase patterns for each site is well-known.

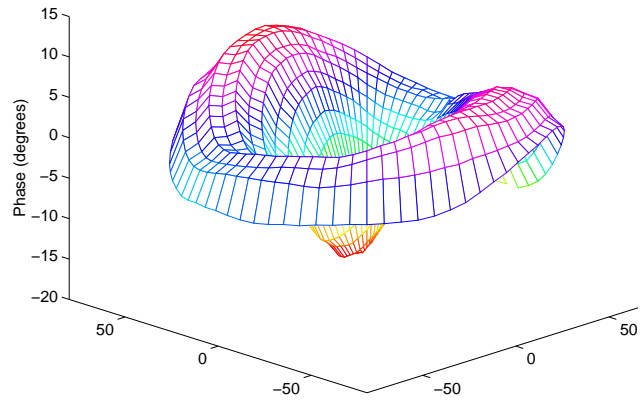
This report also shows that antennas are quite sensitive even to slight modifications. The Ashtech CR and the AOA CR antennas have identical physical dimensions. They differ only in the design of their Low Noise Amplifiers (LNAs) and in the dome, recommended for use with the Ashtech CR. Our tests indicate that use of this dome alone can cause mixing problems at the 1-cm level in the vertical direction.

In summary, errors due to antenna mixing have been reduced, when compared to ground truth, to the 5-20 mm range in the vertical, using the UNAVCO/Ball chamber correction values. To further improve these errors to the 1-mm level we believe that site specific multipath effects must be reduced either through improved antenna designs, or by correcting for these effects in software.

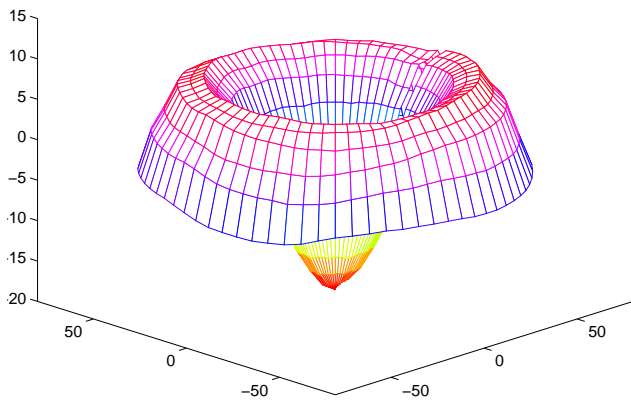
AOA CR L1



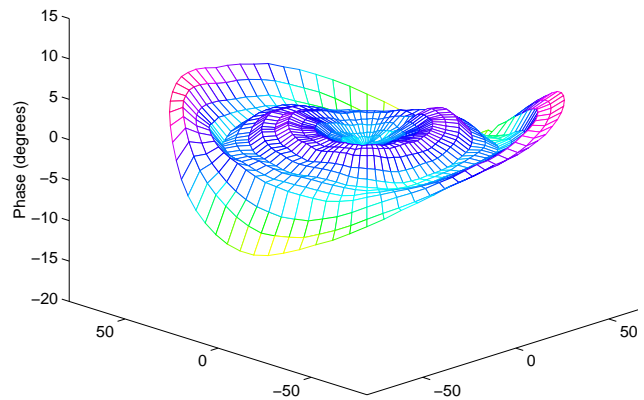
Leica L1



Ashtech CR L1



AOA Rascal L1



Trimble GEOD L1

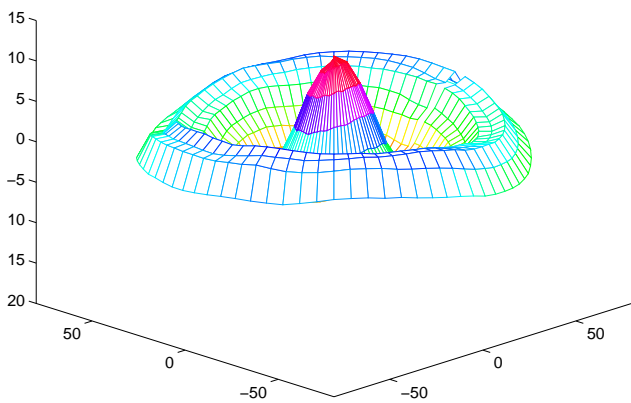
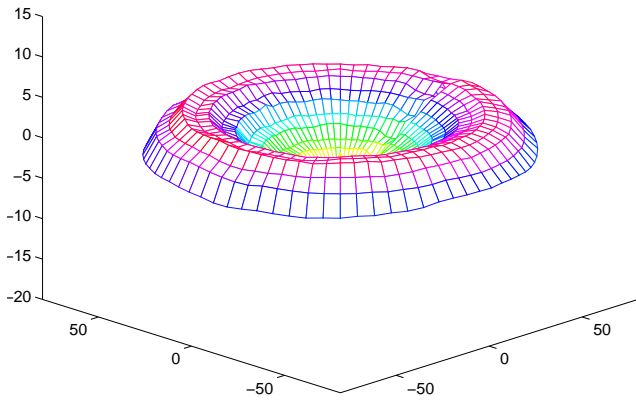
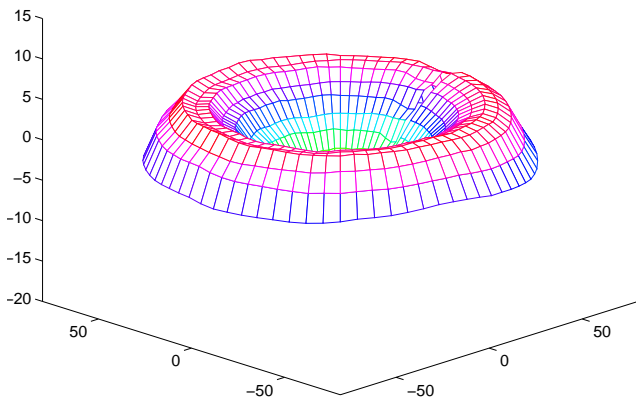


Figure 7.3: Diagrams of the L1 phase variations  $\delta(\Phi, \Theta)$  as function of azimuth and elevation for several tested antennas. Phase variations are shown in units of degrees phase (10 degrees L1 phase  $\sim$  5 mm). Each of the “sombbrero plots” shows zenith values in the center and values for 10 degrees above the horizon at the edges. Circular contour lines are shown in 5 degree elevation steps.

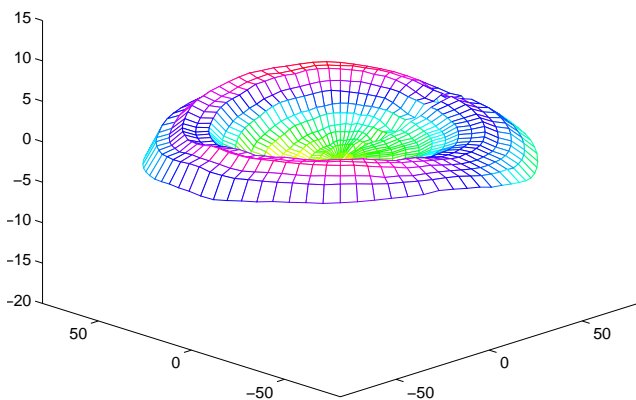
AOA CR L2



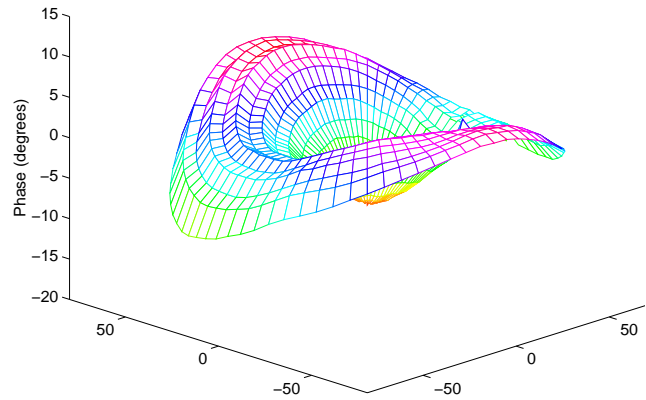
Ashtech CR L2



Trimble GEOD L2



Leica L2



AOA Rascal L2

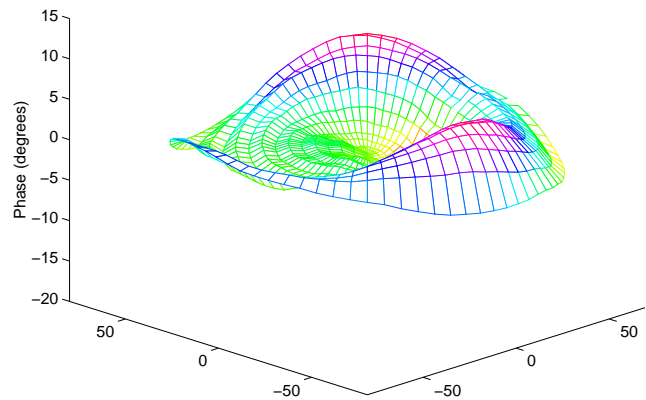
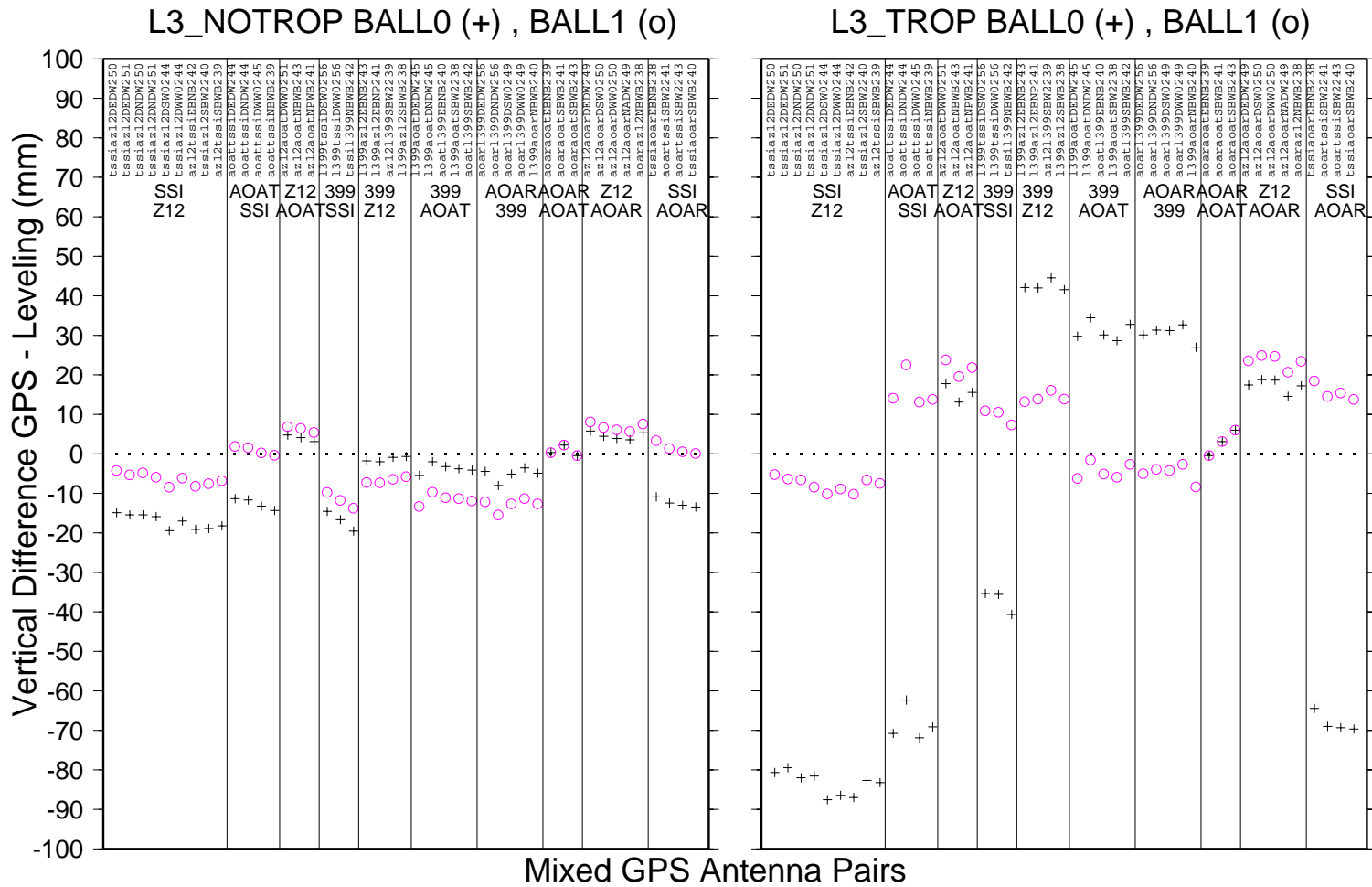
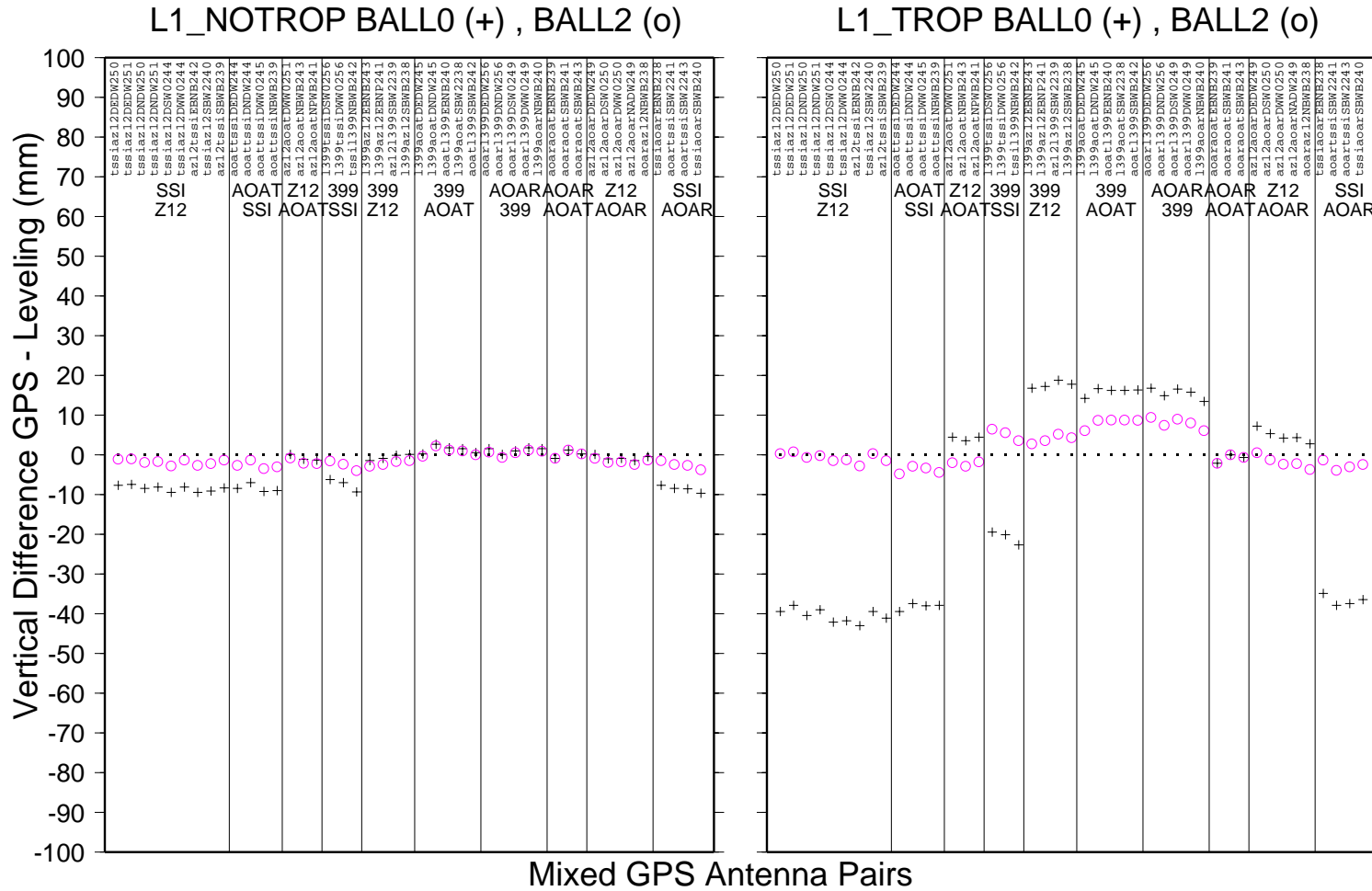


Figure 7.4: Diagrams of the L2 phase variations  $\delta(\Phi, \Theta)$  as function of azimuth and elevation for several tested antennas. Phase variations are shown in units of degrees phase (10 degrees L2 phase  $\sim$  6. mm). Each of the “sombbrero plots” shows zenith values in the center and values for 10 degrees above the horizon at the edges.



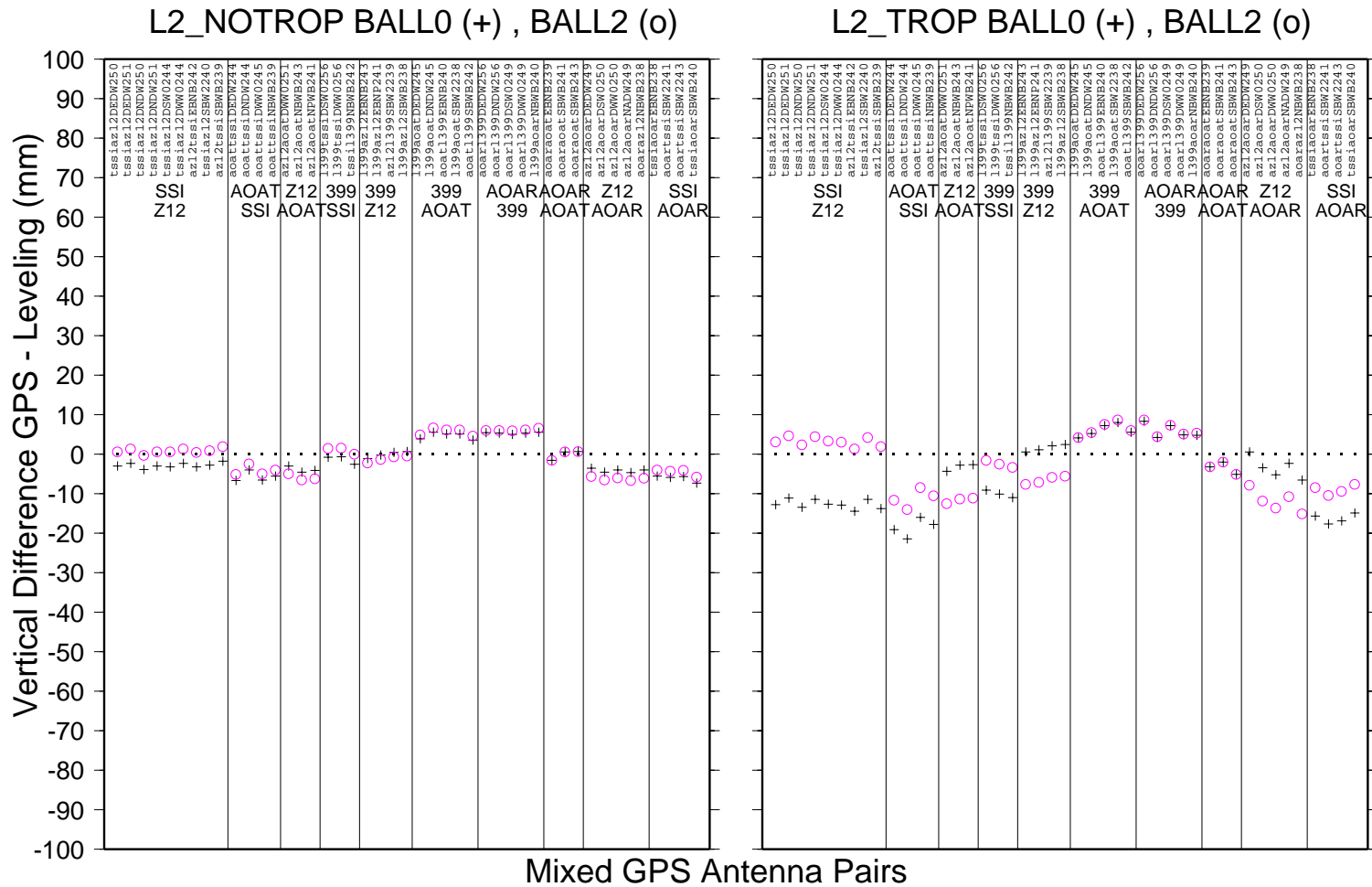
GMT Oct 23 18:02

Figure 7.5: Summary of mixed baseline results for the Ball\_1 (o symbols) processing mode in comparison with Ball\_0 +/- symbols). Ionospheric free L3 solutions are shown with tropospheric estimation (right panel) and without tropospheric estimation (left panel). The columns, separated by vertical lines show the 10 different antenna mixes. The dots at the zero-line correspond to ground truth from levelling.



GMT Oct 23 18:02

Figure 7.6: Summary of mixed baseline results for the full map Ball\_2 (o symbols) processing mode in comparison with Ball\_0 +/- symbols). L1 solutions are shown with tropospheric estimation (right panel) and without tropospheric estimation (left panel). The columns, separated by vertical lines show the 10 different antenna mixes. The dots at the zero-line correspond to ground truth from levelling.



**GMT** Oct 23 18:03

Figure 7.7: Summary of mixed baseline results for the full map Ball\_2 (o symbols) processing mode in comparison with Ball\_0 +/- symbols). L2 solutions are shown with tropospheric estimation (right panel) and without tropospheric estimation (left panel). The columns, separated by vertical lines show the 10 different antenna mixes. The dots at the zero-line correspond to ground truth from levelling.

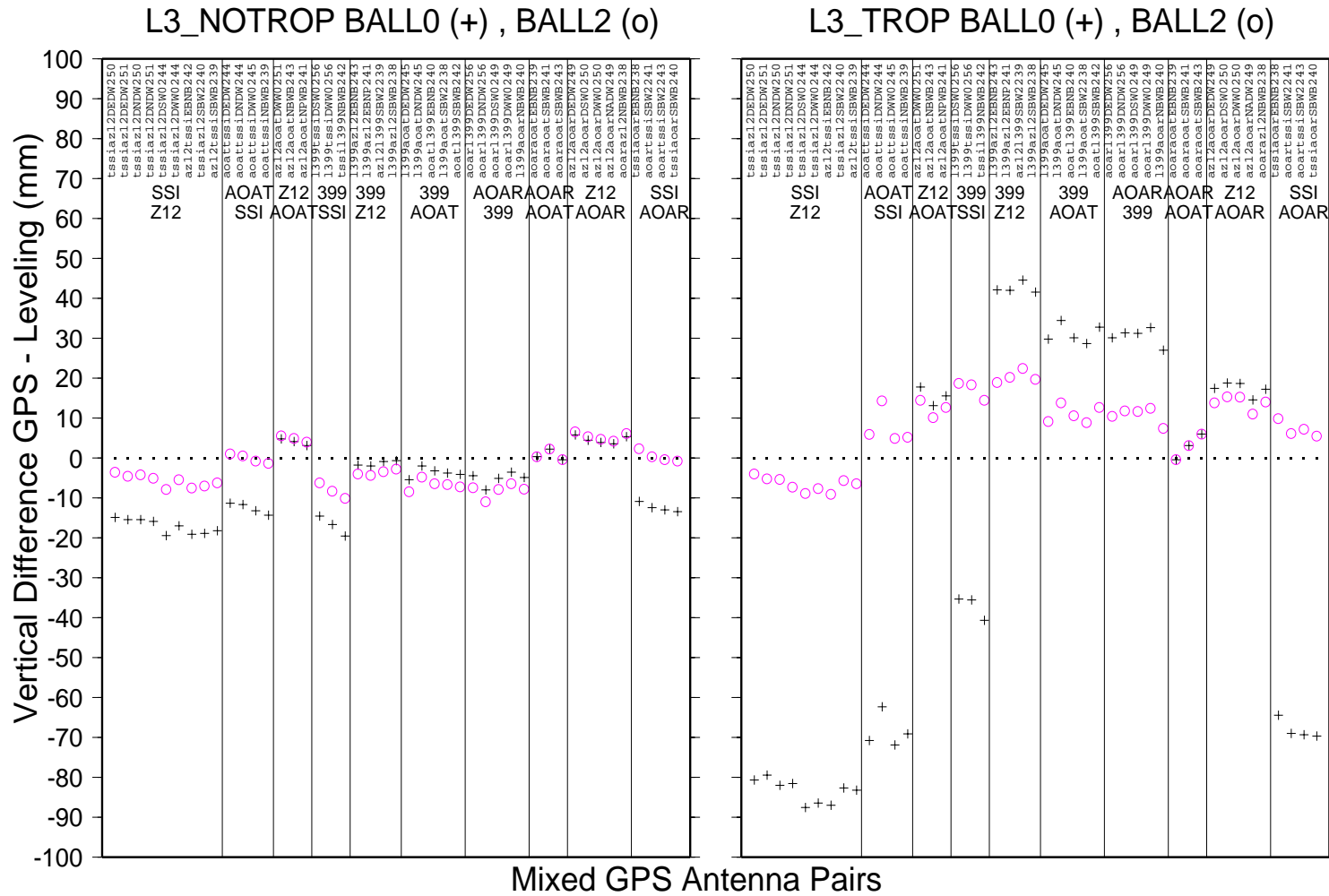
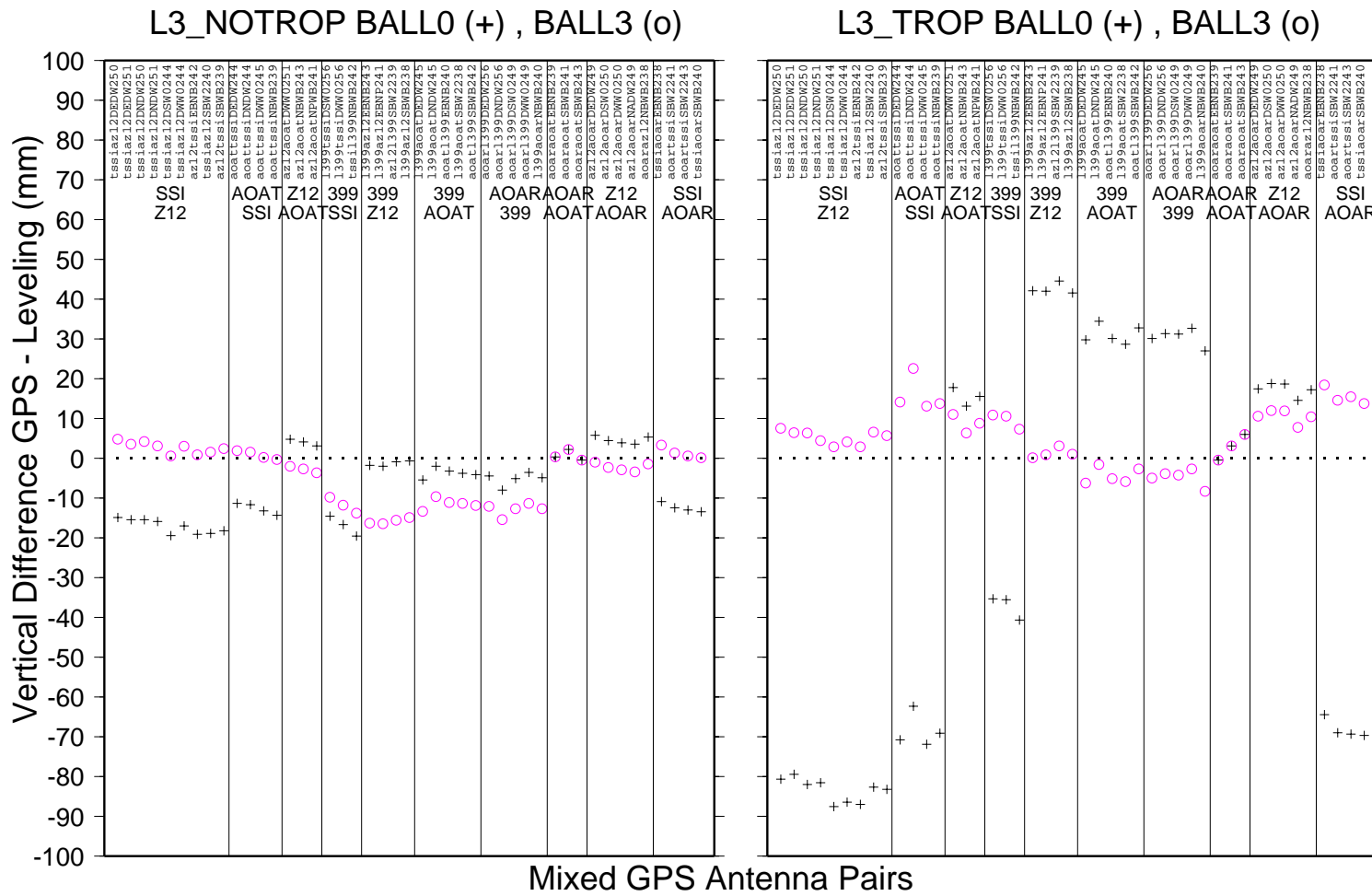
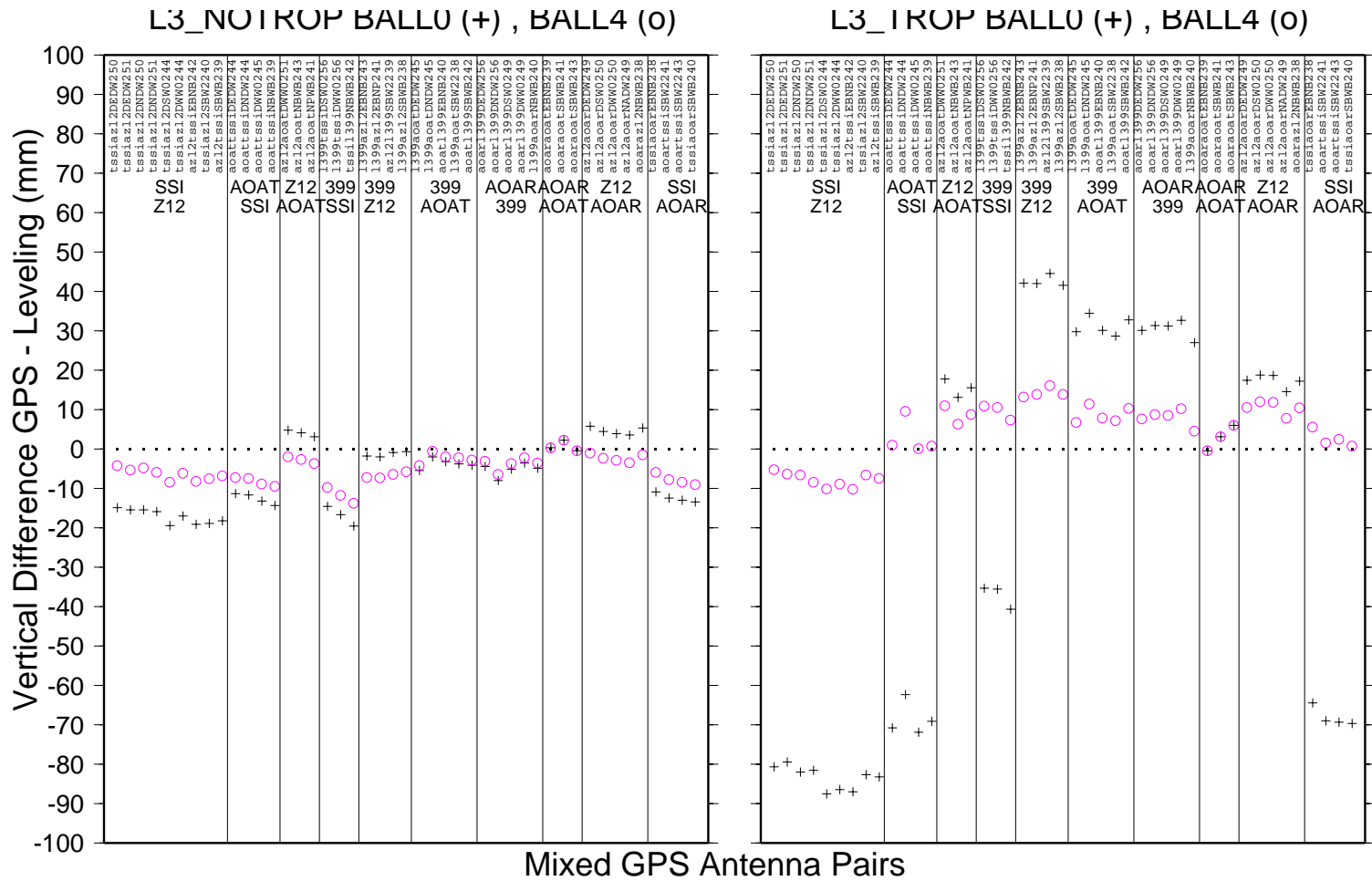


Figure 7.8: Summary of mixed baseline results for the full map Ball\_2 (o symbols) processing mode in comparison with Ball\_0 +/- symbols). Ionosphere free L3 solutions are shown with tropospheric estimation (right panel) and without tropospheric estimation (left panel). The columns, separated by vertical lines show the 10 different antenna mixes. The dots at the zero-line correspond to ground truth from levelling.



GMT Oct 23 18:04

Figure 7.9: Summary of mixed baseline results for Ball\_3 (o symbols) processing mode in comparison with Ball\_0 +/- symbols). Ionosphere free L3 solutions are shown with tropospheric estimation (right panel) and without tropospheric estimation (left panel). The columns, separated by vertical lines show the 10 different antenna mixes. The dots at the zero-line correspond to ground truth from levelling.



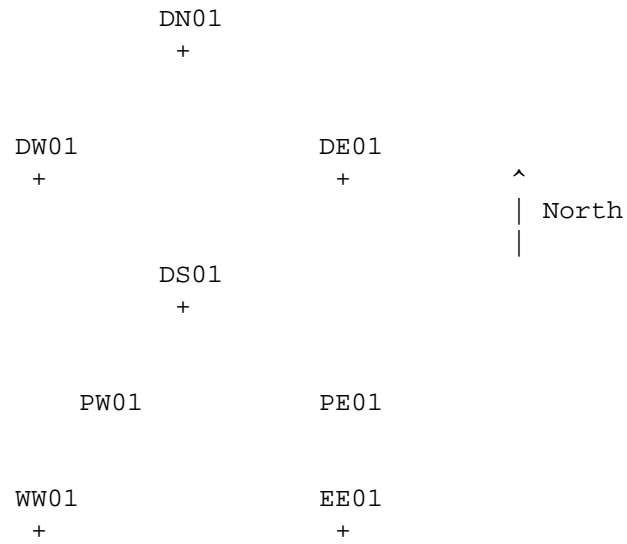
GMT Oct 23 18:05

Figure 7.10: Summary of mixed baseline results for Ball\_4 (o symbols) processing mode in comparison with Ball\_0 +/- symbols). Ionosphere free L3 solutions are shown with tropospheric estimation (right panel) and without tropospheric estimation (left panel). The columns, separated by vertical lines show the 10 different antenna mixes. The dots at the zero-line correspond to ground truth from levelling.

## Appendix A.

### Sketch of Relative Location of Marks

\*\*\*\*\*



### Coordinates of Marks

\*\*\*\*\*

LOCAL GEODETIC DATUM: WGS - 84

STATION NAME	X (M)	Y (M)	Z (M)
DE01	-1283324.2669	-4712974.8025	4090244.6509
DN01	-1283327.1182	-4712971.7753	4090247.3114
DS01	-1283328.2540	-4712976.4440	4090241.7175
DW01	-1283331.1012	-4712973.2709	4090244.5048
WW01	-1283334.8038	-4712987.0348	4090227.9889

EE01                    -1283329.8315   -4712988.7843   4090227.4005

Naming Conventions Used in RINEX names and RINEX "MARKER NAME" fields

\*\*\*\*\*

All marker names in RINEX files are four character abbreviations

First two characters define mark

DE01	DE
DN01	DN
DW01	DW
DS01	DS
WW01	WW
EE01	EE

Third character defines whether RX was powering antenna

P	receiver is powering antenna
B	receiver

Fourth character designates which port in signal splitter receiver connected

1	DC through (powering antenna)
2	DC block (not powering antenna, second port)
3	DC block (not powering antenna, third port)
4	DC block (not powering antenna, fourth port)
etc.	

Example:

MARKER NAME

DNB2	Mark DN01, DC blocked, through splitter port 2
WWP1	Mark WW01, DC through, through splitter port 1

RINEX NAME

DNB22390.950	Observation file for mark DN01, DC blocked, port2, day239
WWP12490.950	Observation file for mark WW01, DC through, port1, day249

List of Receivers Participating and their abbreviation

\*\*\*\*\*

Trimble 4000 SSItssi  
Ashtech Z-12                az12  
Leica 399E                 1399  
Allen Osborne SNR-8000aoat  
Allen Osborne Rascalaoar

Zerobaseline Observation Schedule-(Standard Surveying)

\*\*\*\*\*

Location: Table Mountain

30 second sampling  
0 degree elevation cutoff  
20 hour surveys  
minimum 1 satellite tracking

DAY	SESS	DN01	DE01	DW01	DS01WW01EE01
242	001	tssi	az12	1399	aoataoar
238	002	aoar	tssi	az12	1399aoat
239	003	aoat	aoar	tssi	az121399
240	004	1399	aoat	aoar	tssiaz12
243	005	az12	1399	aoat	aoartssi

Short Baseline Observation Schedule-(Standard Surveying)

\*\*\*\*\*

Location: Table Mountain

30 second sampling  
0 degree elevation cutoff  
20 hour surveys  
minimum 1 satellite tracking

DAY	SESS	DN01	DE01	DW01	DS01WW01EE01
-----	------	------	------	------	--------------

250	006	tssi	tssi	az12	az12aoar	aoar
244	007	aoat	aoat	tssi	tssiaz12az12	
245	008	1399	1399	aoat	aoattssitssi	
256	009	aoar	aoar	1399	1399tssitssi	
251	009a	tssi	tssi	az12	az12aoataoat	
249	010	az12	az12	aoar	aoar13991399	

Zerobaseline Observation Schedule-(Rapid sampling)

\*\*\*\*\*

Location: Table Mountain

1 second sampling  
 0 degree elevation cutoff  
 1 hour surveys  
 minimum 1 satellite tracking

DAY	SES	DN01	DE01	DW01	DS01WW01EE01
-----	-----	-----	-----	-----	-----
257	011	tssi	az12	1399	aoataoar

Single Antenna Zero Baseline Observation Schedule

\*\*\*\*\*

Location: Table Mountain

30 second sampling  
 0 degree elevation cutoff  
 20 hour surveys  
 minimum 1 satellite tracking

DAY	SES	DN01	DE01	DW01	DS01WW01EE01
---	---	-----	-----	-----	-----
2571	012	az12	1399	aoat	aoartssi

## Appendix B. SUMMARY OF OBSERVATIONS AT TABLE MOUNTAIN TEST SITE

August-September 1995

\*\*\*237\*\*\*

SESSION NOT USED! MULTIPLE PROBLEMS WITH RECEIVER SETUPS

DAY	RINEX FILE	MARK	RXSN	RX TYPE	ANTSN	ANT TYPE	VHGT	TRANSLATION PGM
237	DEBB2370.950	DEBB	350	Z-XII3	753	ASHTECH CHOKERING	1.5299	ASHTORIN
237	DEPA2370.950	DEPA	160	ASHTECH Z-XII3	753	ASHTECH CHOKERING	1.5299	ASHTORIN

\*\*\*238\*\*\*

SESSION 002 ZBL TESTS

DAY	RINEX FILE	MARK	RXSN	RX TYPE	ANTSN	ANT TYPE	VHGT	TRANSLATION PGM
238	DEB22380.950	DEB2	11054	TRIMBLE 4000SSI	19949	TRIMBLE GEOD W/GP	1.4601	TRRINEXO V2.6.1 UX
238	DEP12380.950	DEP1	11091	TRIMBLE 4000SSI	19949	TRIMBLE GEOD W/GP	1.4601	TRRINEXO V2.6.1 UX
238	DNB22380.950	DNB2	R2	AOA RASCAL	201	AOA CHOKERING	1.4891	srx v1.3 (5/19/93)
238	DNP12380.950	DNP1	R1	AOA RASCAL	201	AOA CHOKERING	1.4891	srx v1.3 (5/19/93)
238	DSB22380.950	DSB2	000337	SR399	097839	external without GP	1.4332	OBSTORNX
238	DSP12380.950	DSP1	000293	SR399	097844	external without GP	1.4332	OBSTORNX
238	DWB22380.950	DWB2	350	ASHTECH Z-XII3	753	ASHTECH CHOKERING	1.4700	ASRINEXO V2.6.1 UX
238	DWBB2380.950	DWBB	350	Z-XII3	753	ASHTECH CHOKERING	1.4700	ASHTORIN
238	DWP12380.950	DWP1	160	ASHTECH Z-XII3	753	ASHTECH CHOKERING	1.4700	ASRINEXO V2.6.1 UX
238	DWPA2380.950	DWPA	160	Z-XII3	753	ASHTECH CHOKERING	1.4700	ASHTORIN
238	WWB22380.950	WWB2	107	TURBOROGUE	200	AOA CHOKERING	1.4619	srx v1.3 (5/19/93)
238	WWP12380.950	WWP1	106	TURBOROGUE	200	AOA CHOKERING	1.4619	srx v1.3 (5/19/93)

\*\*\*239\*\*\*

SESSION 003 ZBL TESTS

DAY	RINEX FILE	MARK	RXSN	RX TYPE	ANTSN	ANT TYPE	VHGT	TRANSLATION PGM
239	DEB22390.950	DEB2	R2	AOA RASCAL	201	AOA CHOKERING	1.4604	SRX V1.3 (5/19/93)

239	DEP12390.950	DEP1	R1	AOA RASCAL	201	AOA CHOKERING	1.4604	srx v1.3 (5/19/93)
239	DNB22390.950	DNB2	107	TURBOROGUE	200	AOA CHOKERING	1.4891	srx v1.3 (5/19/93)
239	DNP12390.950	DNP1	106	TURBOROGUE	200	AOA CHOKERING	1.4891	srx v1.3 (5/19/93)
239	DSB22390.950	DSB2	LP00350	ASHTECH Z-XII3	11753	ASHTECH CHOKERING	1.4468	ASRINEXO V2.6.1 UX
239	DSBB2390.950	DSBB	350	Z-XII3	753	ASHTECH CHOKERING	1.4468	ASHTORIN
239	DSP12390.950	DSP1	LP00160	ASHTECH Z-XII3	11753	ASHTECH CHOKERING	1.4468	ASRINEXO V2.6.1 UX
239	DSPA2390.950	DSPA	160	Z-XII3	753	ASHTECH CHOKERING	1.4468	ASHTORIN
239	DWB22390.950	DWB2	A11054	TRIMBLE 4000SSI	019949	TRIMBLE GEOD W/GP	1.4697	TRRINEXO V2.6.1 UX
239	DWP12390.950	DWP1	A11091	TRIMBLE 4000SSI	019949	TRIMBLE GEOD W/GP	1.4697	TRRINEXO V2.6.1 UX
239	WWB22390.950	WWB2	000337	SR399E	097839	external without GP	1.4362	OBSTORNX
239	WWP12390.950	WWP1	000293	SR399E	097844	external without GP	1.4362	OBSTORNX

\*\*\*240\*\*\*\*

SESSION 004 ZBL TESTS

DAY	RINEX FILE	MARK	RXSN	RX TYPE	ANTSN	ANT TYPE	VHGT	TRANSLATION PGM
240	DEB22400.950	DEB2	107	TURBOROGUE	200	AOA CHOKERING	1.4601	srx v1.3 (5/19/93)
240	DEP12400.950	DEP1	106	TURBOROGUE	200	AOA CHOKERING	1.4601	srx v1.3 (5/19/93)
240	DNB22400.950	DNB2	000337	SR399E	097839	external without GP	1.4639	OBSTORNX
240	DNP12400.950	DNP1	000293	SR399E	097844	external without GP	1.4639	OBSTORNX
240	DSB22400.950	DSB2	A11054	TRIMBLE 4000SSI	19949	TRIMBLE GEOD W/GP	1.4461	TRRINEXO V2.6.1 UX
240	DSP12400.950	DSP1	A11091	TRIMBLE 4000SSI	19949	TRIMBLE GEOD W/GP	1.4461	TRRINEXO V2.6.1 UX
240	DWB22400.950	DWB2	R2	AOA RASCAL	201	AOA CHOKERING	1.4700	srx v1.3 (5/19/93)
240	DWP12400.950	DWP1	R1	AOA RASCAL	201	AOA CHOKERING	1.4700	srx v1.3 (5/19/93)
240	WWB22400.950	WWB2	350	ASHTECH Z-XII3	753	ASHTECH CHOKERING	1.4609	ASRINEXO V2.6.1 UX
240	WWBB2400.950	WWBB	350	Z-XII3	753	ASHTECH CHOKERING	1.4609	ASHTORIN
240	WWP12400.950	WWP1	160	ASHTECH Z-XII3	753	ASHTECH CHOKERING	1.4609	ASRINEXO V2.6.1 UX
240	WWPA2400.950	WWPA	160	Z-XII3	753	ASHTECH CHOKERING	1.4609	ASHTORIN

\*\*\*241\*\*\*\*

NO DATA FROM AZ12 RECIEVER SN 350

DAY	RINEX FILE	MARK	RXSN	RX TYPE	ANTSN	ANT TYPE	VHGT	TRANSLATION PGM
241	DEB22410.950	DEB2	000337	SR399	097839	external without GP	1.4357	OBSTORNX
241	DEP12410.950	DEP1	000293	SR399	097844	external without GP	1.4357	OBSTORNX
241	DNP12410.950	DNP1	160	ASHTECH Z-XII3	753	ASHTECH CHOKERING	1.4891	ASRINEXO V2.6.1 UX
241	DNPA2410.950	DNPA	160	Z-XII3	753	ASHTECH CHOKERING	1.4891	ASHTORIN

241	DSB22410.950	DSB2	R2	AOA RASCAL	201	AOA CHOKERING	1.4468	srx v1.3 (5/19/93)
241	DSP12410.950	DSP1	R1	AOA RASCAL	201	AOA CHOKERING	1.4468	srx v1.3 (5/19/93)
241	DWB22410.950	DWB2	0	TURBOROGUE	200	AOA CHOKERING	1.4705	srx v1.3 (5/19/93)
241	DWP12410.950	DEP1	106	TURBOROGUE	200	AOA CHOKERING	1.4705	srx v1.3 (5/19/93)
241	WWB22410.950	WWB2	11054	TRIMBLE 4000SSI	19949	TRIMBLE GEOD W/GP	1.4606	TRRINEXO V2.6.1 UX
241	WWP12410.950	WWP1	11091	TRIMBLE 4000SSI	19949	TRIMBLE GEOD W/GP	1.4606	TRRINEXO V2.6.1 UX

\*\*\*242\*\*\*

SESSION 001 ZBL TESTS

DAY	RINEX FILE	MARK	RXSN	RX TYPE	ANTSN	ANT TYPE	VHGT	TRANSLATION PGM
242	DEB22420.950	DEB2	350	ASHTECH Z-XII3	753	ASHTECH CHOKERING	1.4599	ASRINEXO V2.6.1 UX
242	DEBB2420.950	DEBB	350	Z-XII3	753	ASHTECH CHOKERING	1.4599	ASHTORIN
242	DEP12420.950	DEP1	160	ASHTECH Z-XII3	753	ASHTECH CHOKERING	1.4599	ASRINEXO V2.6.1 UX
242	DEPA2420.950	DEPA	160	Z-XII3	753	ASHTECH CHOKERING	1.4599	ASHTORIN
242	DNB22420.950	DNB2	11054	TRIMBLE 4000SSI	19949	TRIMBLE GEOD W/GP	1.4879	TRRINEXO V2.6.1 UX
242	DNP12420.950	DNP1	11091	TRIMBLE 4000SSI	19949	TRIMBLE GEOD W/GP	1.4879	TRRINEXO V2.6.1 UX
242	DSB22420.950	DSB2	0	TURBOROGUE	200	AOA CHOKERING	1.4468	srx v1.3 (5/19/93)
242	DSP12420.950	DSP1	106	TURBOROGUE	200	AOA CHOKERING	1.4468	srx v1.3 (5/19/93)
242	DWB22420.950	DWB2	000337	SR399	097839	external without GP	1.4513	OBSTORNX
242	DWP12420.950	DWP1	000293	SR399	097844	external without GP	1.4513	OBSTORNX
242	WWB22420.950	WWB2	R2	AOA RASCAL	201	AOA CHOKERING	1.4609	srx v1.3 (5/19/93)
242	WWP12420.950	WWP1	R1	AOA RASCAL	201	AOA CHOKERING	1.4609	srx v1.3 (5/19/93)

\*\*\*243\*\*\*

SESSION 005 ZBL TESTS

DAY	RINEX FILE	MARK	RXSN	RX TYPE	ANTSN	ANT TYPE	VHGT	TRANSLATION PGM
243	DEB22430.950	DEB2	000337	SR399	097839	external without GP	1.4357	OBSTORNX
243	DEP12430.950	DEP1	000293	SR399	097844	external without GP	1.4357	OBSTORNX
243	DNB22430.950	DNB2	350	ASHTECH Z-XII3	753	ASHTECH CHOKERING	1.4886	ASRINEXO V2.6.1 UX
243	DNBB2430.950	DNBB	350	Z-XII3	753	ASHTECH CHOKERING	1.4886	ASHTORIN
243	DNP12430.950	DNP1	160	ASHTECH Z-XII3	753	ASHTECH CHOKERING	1.4886	ASRINEXO V2.6.1 UX
243	DNPA2430.950	DNPA	160	Z-XII3	753	ASHTECH CHOKERING	1.4886	ASHTORIN
243	DSB22430.950	DSB2	R1	AOA RASCAL	201	AOA CHOKERING	1.4468	srx v1.3 (5/19/93)
243	DSP12430.950	DSP1	R1	AOA RASCAL	201	AOA CHOKERING	1.4468	srx v1.3 (5/19/93)
243	DWB22430.950	DWB2	0	TURBOROGUE	200	AOA CHOKERING	1.4700	srx v1.3 (5/19/93)

243	DWP12430.950	DWP1	106	TURBOROGUE	200	AOA CHOKERING	1.4700	srx v1.3 (5/19/93)
243	WWB22430.950	WWB2	11054	TRIMBLE 4000SSI	19949	TRIMBLE GEOD W/GP	1.4606	TRRINEXO V2.6.1 UX
243	WWP12430.950	WWP1	11091	TRIMBLE 4000SSI	19949	TRIMBLE GEOD W/GP	1.4606	TRRINEXO V2.6.1 UX

\*\*\*244\*\*\*

SESSION 007 SHORT BASELINE

DAY	RINEX FILE	MARK	RXSN	RX TYPE	ANTSN	ANT TYPE	VHGT	TRANSLATION PGM
244	DE012440.950	DE01	0	TURBOROGUE	201	AOA CHOKERING	1.4599	srx v1.3 (5/19/93)
244	DN012440.950	DN01	106	TURBOROGUE	200	AOA CHOKERING	1.4886	srx v1.3 (5/19/93)
244	DS012440.950	DS01	11054	TRIMBLE 4000SSI	19949	TRIMBLE GEOD W/GP	1.4462	TRRINEXO V2.6.1 UX
244	DW012440.950	DW01	11091	TRIMBLE 4000SSI	19610	TRIMBLE GEOD W/GP	1.4702	TRRINEXO V2.6.1 UX
244	EE012440.950	EE01	160	ASHTECH Z-XII3	753	ASHTECH CHOKERING	1.4155	ASRINEXO V2.6.1 UX
244	EEA12440.950	EEA1	160	Z-XII3	753	ASHTECH CHOKERING	1.4155	ASHTORIN
244	WW012440.950	WW01	350	ASHTECH Z-XII3	757	ASHTECH CHOKERING	1.4614	ASRINEXO V2.6.1 UX
244	WWA12440.950	WWA1	350	Z-XII3	757	ASHTECH CHOKERING	1.4614	ASHTORIN

\*\*\*245\*\*\*

SESSION 008 SHORT BASELINE + RASCAL ZBL WITH RASCAL ANTENNA

DAY	RINEX FILE	MARK	RXSN	RX TYPE	ANTSN	ANT TYPE	VHGT	TRANSLATION PGM
245	DE012450.950	DE01	000337	SR399	097839	external without GP	1.4357	OBSTORNX
245	DN012450.950	DN01	000293	SR399	097844	external without GP	1.4631	OBSTORNX
245	DS012450.950	DS01	106	TURBOROGUE	201	AOA CHOKERING	1.4466	srx v1.3 (5/19/93)
245	DW012450.950	DW01	0	TURBOROGUE	200	AOA CHOKERING	1.4700	srx v1.3 (5/19/93)
245	EE012450.950	EE01	11091	TRIMBLE 4000SSI	19610	TRIMBLE GEOD W/GP	1.4150	TRRINEXO V2.6.1 UX
245	PE012450.950	PE01	R1	AOA RASCAL	R1	AOA RASCAL	0.0778	srx v1.3 (5/19/93)
245	PW012450.950	PW01	R2	AOA RASCAL	R2	AOA RASCAL	0.0782	srx v1.3 (5/19/93)
245	WW012450.950	WW01	11054	TRIMBLE 4000SSI	19949	TRIMBLE GEOD W/GP	1.4603	TRRINEXO V2.6.1 UX

\*\*\*249\*\*\*

SESSION 010 SHORT BASELINE

DAY	RINEX FILE	MARK	RXSN	RX TYPE	ANTSN	ANT TYPE	VHGT	TRANSLATION PGM
249	DE012490.950	DE01	350	ASHTECH Z-XII3	757	ASHTECH CHOKERING	1.4602	ASRINEXO V2.6.1 UX
249	DEA12490.950	DEA1	350	Z-XII3	757	ASHTECH CHOKERING	1.4602	ASHTORIN

249	DN012490.950	DN01	160	ASHTECH Z-XII3	753	ASHTECH CHOKERING	1.4886	ASRINEXO V2.6.1 UX
249	DNA12490.950	DNA1	160	Z-XII3	753	ASHTECH CHOKERING	1.4886	ASHTORIN
249	DS012490.950	DS01	R2	AOA RASCAL	201	AOA CHOKERING	1.4466	srx v1.3 (5/19/93)
249	DW012490.950	DW01	R1	AOA RASCAL	200	AOA CHOKERING	1.4700	srx v1.3 (5/19/93)
249	EE012490.950	EE01	000293	SR399	097844	external without GP	1.3900	OBSTORNX
249	WW012490.950	WW01	000337	SR399	097839	external without GP	1.4356	OBSTORNX

\*\*\*250\*\*\*\*

SESSION 006 SHORT BASELINE

DAY	RINEX FILE	MARK	RXSN	RX TYPE	ANTSN	ANT TYPE	VHGT	TRANSLATION PGM
250	DE012500.950	DE01	11054	TRIMBLE 4000SSI	19949	TRIMBLE GEOD W/GP	1.4595	TRRINEXO V2.6.1 UX
250	DN012500.950	DN01	11091	TRIMBLE 4000SSI	19610	TRIMBLE GEOD W/GP	1.4888	TRRINEXO V2.6.1 UX
250	DS012500.950	DS01	350	ASHTECH Z-XII3	757	ASHTECH CHOKERING	1.4468	ASRINEXO V2.6.1 UX
250	DSA12500.950	DSA1	350	Z-XII3	757	ASHTECH CHOKERING	1.4468	ASHTORIN
250	DW012500.950	DW01	160	ASHTECH Z-XII3	753	ASHTECH CHOKERING	1.4702	ASRINEXO V2.6.1 UX
250	DWA12500.950	DWA1	160	Z-XII3	753	ASHTECH CHOKERING	1.4702	ASHTORIN
250	EE012500.950	EE01	R2	AOA RASCAL	201	AOA CHOKERING	1.4147	srx v1.3 (5/19/93)
250	WW012500.950	WW01	R1	AOA RASCAL	200	AOA CHOKERING	1.4611	srx v1.3 (5/19/93)

\*\*\*251\*\*\*\*

SESSION 009a SHORT BASELINE + RASCAL SHORT BASELINE WITH RASCAL ANTENNA

DAY	RINEX FILE	MARK	RXSN	RX TYPE	ANTSN	ANT TYPE	VHGT	TRANSLATION PGM
251	DE012510.950	DE01	11054	TRIMBLE 4000SSI	19949	TRIMBLE GEOD W/GP	1.4598	TRRINEXO V2.6.1 UX
251	DN012510.950	DN01	11091	TRIMBLE 4000SSI	19610	TRIMBLE GEOD W/GP	1.4892	TRRINEXO V2.6.1 UX
251	DS012510.950	DS01	350	ASHTECH Z-XII3	757	ASHTECH CHOKERING	1.4469	ASRINEXO V2.6.1 UX
251	DSA12510.950	DSA1	350	Z-XII3	757	ASHTECH CHOKERING	1.4469	ASHTORIN
251	DW012510.950	DW01	160	ASHTECH Z-XII3	753	ASHTECH CHOKERING	1.4702	ASRINEXO V2.6.1 UX
251	DWA12510.950	DWA1	160	Z-XII3	753	ASHTECH CHOKERING	1.4702	ASHTORIN
251	EE012510.950	EE01	363	TURBOROGUE	201	AOA CHOKERING	1.4147	srx v1.3 (5/19/93)
251	PE012510.950	PE01	R1	AOA RASCAL	R1	AOA RASCAL	0.0000	srx v1.3 (5/19/93)
251	PW012510.950	PW01	R2	AOA RASCAL	R2	AOA RASCAL	0.0000	srx v1.3 (5/19/93)
251	WW012510.950	WW01	106	TURBOROGUE	200	AOA CHOKERING	1.4612	srx v1.3 (5/19/93)

\*\*\*256\*\*\*\*

SESSION 009 SHORT BASELINE

DAY	RINEX FILE	MARK	RXSN	RX TYPE	ANTSN	ANT TYPE	VHGT	TRANSLATION PGM
256	DE012560.950	DE01	R1	AOA RASCAL	200	AOA CHOKERING	1.4606	srx v1.3 (5/19/93)
256	DN012560.950	DN01	R2	AOA RASCAL	201	AOA CHOKERING	1.4886	srx v1.3 (5/19/93)
256	DS012560.950	DS01	000337	SR399	097839	external without GP	1.4219	OBSTORNX
256	DW012560.950	DW01	000293	SR399	097844	external without GP	1.4513	OBSTORNX
256	EE012560.950	EE01	11054	TRIMBLE 4000SSI	19949	TRIMBLE GEOD W/GP	1.4143	TRRINEXO V2.6.1 UX
256	WW012560.950	WW01	11091	TRIMBLE 4000SSI	19610	TRIMBLE GEOD W/GP	1.4618	TRRINEXO V2.6.1 UX

## Appendix C. Details of Download Timing Tests

**Table C.1: ARI timing tests**

receiver	computer	physical connection	download software	baud setting	file size (bytes)	time (sec)	cps
Ashtech	1	direct	hose	115200	961652	130	7397
Ashtech	1	direct	hose	115200	575551	45	12790
Ashtech	1	direct	hose	115200	3693112	289	12779
Ashtech	1	direct	hose	115200	3171849	199	15939
Ashtech	1	direct	hose	115200	3164962	199	15904
Ashtech	1	direct	hose	57600	3693112	472	7824
Ashtech	1	direct	remote	115200	1913835	878	2179
Ashtech	1	direct	remote	115200	228330	105	2175
Ashtech	1	direct	remote	115200	305130	138	2211
Trimble SSI	1	direct	4000	57600	2265181	197	11498
Trimble SSI	1	direct	4000	57600	2262513	197	11485
Trimble SSI	1	direct	4000	57600	2262513	180	12570
Trimble SSI	1	direct	rfile	57600	955504	301	3174
Trimble SSI	1	direct	rfile -f	57600	955504	242	3948
Trimble SSE	1	direct	rfile -f	57600	197622	52	3800
Trimble SSE	1	direct	rfile	57600	197622	66	2994
Trimble SSE	1	direct	rfile	57600	197622	66	2994

**Table C.1: ARI timing tests (Continued)**

receiver	computer	physical connection	download software	baud setting	file size (bytes)	time (sec)	cps
Trimble SSE	1	direct	getfile	57600	197622	67	2950
Leica	1	direct	SKI	38400	1182742	600	1971
Leica	1	direct	SKI	38400	1190712	611	1949
Rascal	1	direct	pcplus-xmodem	38400	103424	93	1112
Rascal	1	direct	pcplus-xmodem	19200	103424	95	1089
Rascal	1	direct	procomm-xmod	19200	591360	820	721
Rascal	1	direct	procomm-xmod	19200	503424	591	852
TurboRogue	1	direct	pcplus-xmodem	38400	193920	154	1259
TurboRogue	1	direct	pcplus-xmodem	19200	193920	153	1267
TurboRogue	1	direct	procomm-xmod	19200	499456	480	1041
TurboRogue	1	direct	procomm-xmod	19200	584704	561	1042
Ashtech	2	direct	hose	115200	964590	240	4019
Ashtech	2	direct	hose	57600	924969	136	6801
Trimble SSI	4	direct	4000	57600	1551330	266	5832
Trimble SSI	4	direct	4000	57600	1553886	303	5908
Trimble SSE	3	direct	rfile -f	57600	197622	0	crashed
Leica	4	direct	SKI	38400	804692	476	1691
Rascal	4	direct	procomm-xmod	19200	366080	510	718

**Table C.1: ARI timing tests (Continued)**

receiver	computer	physical connection	download software	baud setting	file size (bytes)	time (sec)	cps
Rascal	4	direct	procomm-xmod	19200	361344	588	615
TurboRogue	4	direct	procomm-xmod	19200	363136	450	807
TurboRogue	4	direct	procomm-xmod	19200	363392	541	672
Ashtech	5	direct	hose	115200	2118040	531	3989
Ashtech	5	direct	hose	115200	2051592	480	4274
Ashtech	5	direct	hose	57600	2130132	229	9302
Ashtech	5	direct	hose	57600	2068081	230	9400
Ashtech	2	modem (PEP)	remote	38400	71662	81	885
Ashtech	2	modem (PEP)	remote	38400	1921002	2038	943
Ashtech	2	modem (PEP)	remote	19200	1921002	2155	891
Trimble SSE	2	modem (PEP)	rfile	57600	197622	1098	180
Trimble SSE	2	modem (PEP)	rfile	38400	197622	1112	178
Trimble SSE	2	modem (PEP)	rfile	19200	197622	1167	169

**Table C.1: ARI timing tests (Continued)**

receiver	computer	physical connection	download software	baud setting	file size (bytes)	time (sec)	cps
Trimble SSE	2	modem (PEP) no spoofing	rfile	57600	197622	1031	192
Trimble SSE	2	modem v.32bis	rfile	57600	197622	411	481
Trimble SSE	2	modem v.32bis	rfile	57600	197622	419	472
Trimble SSE	2	modem v.32	rfile	9600	474528	1254	378
Trimble SSI	2	modem v.32bis	rfile	57600	955504	1346	710
Trimble SSI	2	modem v.32bis	rfile	57600	955504	1361	702
Trimble SSI	2	modem v.32bis	rfile -f	57600	955504	crashed	crashed
Trimble SSI	2	modem v.32bis	rfile -f	57600	955504	crashed	crashed
Trimble SSI	2	modem v.32bis	getfile	57600	955504	1424	671
Trimble SSI	2	modem v.32bis compression on	rfile	57600	955504	1562	612

**Table C.1: ARI timing tests (Continued)**

receiver	computer	physical connection	download software	baud setting	file size (bytes)	time (sec)	cps
Trimble SSI	2	modem v.32bis compression on	rfile	57600	955504	crashed	crashed
Trimble SSI	2	modem v.32 compression on	rfile -f	57600	955504	crashed	crashed
Trimble SSI	2	modem v.32 compression on	rfile -f	9600	955504	1028	929
Trimble SSI	2	modem v.32	rfile -f	9600	955504	1028	929
Trimble SSI	2	modem v.32	rfile	9600	955504	2065	463
Trimble SSI	2	modem v.32	getfile	9600	955504	2077	460
Trimble SSI	2	modem v.32	rfile -f	19200	955504	crashed	crashed
Trimble SSI	2	modem v.32bis	rfile -f	19200	955504	crashed	crashed
Rascal	2	modem (PEP)	pcplus-xmodem	19200	103296	99	1043
Rascal	2	modem (PEP)	pcplus-xmodem	19200	103296	106	974
TurboRogue	2	modem (PEP)	pcplus-xmodem	19200	116864	105	1113

**Table C.1: ARI timing tests (Continued)**

receiver	computer	physical connection	download software	baud setting	file size (bytes)	time (sec)	cps
TurboRogue	2	modem (PEP)	pcplus-xmodem	19200	204800	189	1084
Trimble SSE	3	modem v.32bis	rfile	57600	197622	487	406
Trimble SSE	3	modem v.32bis	rfile -f	57600	197622	0	crashed
Trimble SSE	3	modem v.32bis	getfile	57600	197622	405	488
Rascal	4	modem (PEP)	pcplus-xmodem	38400	125056	162	772
Rascal	4	modem (PEP)	pcplus-xmodem	19200	489984	600	817
Ashtech	3	radio modem	remote	115200	27640	350	79 - crashed
Ashtech	3	radio modem	remote	115200	33792	360	94 - crashed
Ashtech	3	radio modem	remote	115200	31744	354	90 - crashed
Ashtech	3	radio modem	remote	115200	34816	356	98 - crashed
Ashtech	3	radio modem	remote	38400	1913834	2626	729

**Table C.1: ARI timing tests (Continued)**

receiver	computer	physical connection	download software	baud setting	file size (bytes)	time (sec)	cps
Ashtech	3	radio modem	remote	38400	1926122	2637	730
Ashtech	3	radio modem	hose	115200	127089	165	770 - crashed
Ashtech	3	radio modem	hose	115200	231159	152	1521
Ashtech	3	radio modem	hose	115200	231159	147	1573
Ashtech	3	radio modem	hose	38400	231159	132	1751
Ashtech	3	radio modem	hose	38400	783373	765	1024 - crashed
Trimble SSE	3	radio modem	4000	57600	418797	182	2301
Trimble SSE	3	radio modem	rfile	57600	197622	340	581
Trimble SSE	3	radio modem	getfile	57600	197622	197	1003
Trimble SSE	3	radio modem	getfile	57600	197622	191	1035
Trimble SSI	3	radio modem	rfile	57600	955504	1242	769

**Table C.1: ARI timing tests (Continued)**

receiver	computer	physical connection	download software	baud setting	file size (bytes)	time (sec)	cps
Trimble SSI	3	radio modem	rfile	57600	39305	47	836
Trimble SSI	3	radio modem	getfile	57600	955504	517	1848
Trimble SSI	3	radio modem	getfile	57600	39305	27	1456
Trimble SSI	3	radio modem	4000	57600	2262513	717	3156
Rascal	3	radio modem	pcplus-xmodem	38400	103424	190	544
Rascal	3	radio modem	pcplus-xmodem	38400	103424	207	500
Rascal	3	radio modem	pcplus-xmodem	19200	103424	108	958
Rascal	3	radio modem	pcplus-xmodem	19200	103424	116	892
TurboRogue	3	radio modem	pcplus-xmodem	38400	193920	227	854
TurboRogue	3	radio modem	pcplus-xmodem	38400	193920	234	829
TurboRogue	3	radio modem	pcplus-xmodem	19200	761728	943	807

**Table C.1: ARI timing tests (Continued)**

receiver	computer	physical connection	download software	baud setting	file size (bytes)	time (sec)	cps
TurboRogue	3	radio modem	pcplus-xmodem	19200	193920	239	811
Trimble SSE	4	radio modem	rfile	57600	197622	495	399
Trimble SSE	4	radio modem	rfile	57600	197622	577	342
Trimble SSE	4	radio modem	rfile	57600	197622	703	281
Trimble SSE	4	radio modem	rfile	57600	197622	773	256
Trimble SSE	4	radio modem	getfile	57600	197622	219	902
Trimble SSE	4	radio modem	getfile	57600	197622	230	859
Trimble SSE	4	radio modem	getfile	57600	197622	222	890
Rascal	4	radio modem	pcplus-xmodem	19200	34432	51	675
Rascal	4	radio modem	pcplus-xmodem	19200	98432	143	688
Rascal	4	radio modem	pcplus-xmodem	19200	103424	168	615

**Table C.1: ARI timing tests (Continued)**

receiver	computer	physical connection	download software	baud setting	file size (bytes)	time (sec)	cps
TurboRogue	4	radio modem	pcplus-xmodem	19200	7424	10	742
TurboRogue	4	radio modem	pcplus-xmodem	19200	7424	10	742
TurboRogue	4	radio modem	pcplus-xmodem	19200	761728	777	980
TurboRogue	4	radio modem	pcplus-xmodem	19200	761728	765	996
TurboRogue	4	radio modem	pcplus-xmodem	19200	761728	796	957

Computers:

1: CompuAdd, 486DX, 4MB RAM, 8250 UART, Desktop

2: AST 486DX, 4MB RAM, 8250 UART, Laptop

3: AST386SL with 387 math coprocessor, 4MB RAM, 8250 UART, Laptop

4: AST386SL, 4MB RAM, 8250 UART, Laptop

5: NCR486DX, 4MB RAM, 8250 UART, Laptop

## Appendix D. Real-time GPS Vectors

The DX,DY and DZ vectors with respect to station LGHN (Longhorn) were provided on floppy by each manufacturer. These vectors were then converted to North, East and Up components for comparison. The results are presented in order of observation as described in the text. A=Ashtech, L=Leica, T=Trimble. The first line for each station is the Static survey vector. A summary of the average and standard deviations for all measurements at a site is given at the bottom of the table.

Static R440	-2174.4285	433.3713	-35.9693	0.0000	0.0000	0.0000
A	-2174.4431	433.3814	-35.9725	-0.0146	0.0101	-0.0032
A	-2174.4399	433.3657	-35.9655	-0.0114	-0.0056	0.0038
A	-2174.4399	433.3657	-35.9655	-0.0114	-0.0056	0.0038
A	-2174.4398	433.3818	-35.9779	-0.0113	0.0105	-0.0086
A	-2174.4392	433.3654	-35.9662	-0.0107	-0.0059	0.0031
A	-2174.4392	433.3728	-35.9756	-0.0107	0.0015	-0.0063
A	-2174.4353	433.3831	-35.9678	-0.0068	0.0118	0.0015
A	-2174.4344	433.3752	-35.9751	-0.0059	0.0039	-0.0058
A	-2174.4249	433.3725	-35.9553	0.0036	0.0012	0.0140
L	-2174.4635	433.3781	-35.9560	-0.0350	0.0068	0.0133
L	-2174.4629	433.3751	-35.9598	-0.0344	0.0038	0.0095
L	-2174.4578	433.3702	-35.9442	-0.0293	-0.0011	0.0251
L	-2174.4508	433.3748	-35.9509	-0.0223	0.0035	0.0184
L	-2174.4506	433.3692	-35.9527	-0.0221	-0.0021	0.0166
L	-2174.4501	433.3734	-35.9471	-0.0216	0.0021	0.0222
L	-2174.4484	433.3676	-35.9584	-0.0199	-0.0037	0.0109
L	-2174.4442	433.3757	-35.9510	-0.0157	0.0044	0.0183
L	-2174.4427	433.3723	-35.9512	-0.0142	0.0010	0.0181
T	-2174.4390	433.3788	-35.9369	-0.0105	0.0075	0.0324
T	-2174.4387	433.3663	-35.9715	-0.0102	-0.0050	-0.0022

T	-2174.4384	433.3845	-35.9439	-0.0099	0.0132	0.0254
T	-2174.4382	433.3672	-35.9768	-0.0097	-0.0041	-0.0075
T	-2174.4372	433.3780	-35.9391	-0.0087	0.0067	0.0302
T	-2174.4346	433.3736	-35.9530	-0.0061	0.0023	0.0163
T	-2174.4331	433.3637	-35.9347	-0.0046	-0.0076	0.0346
T	-2174.4314	433.3633	-35.9399	-0.0029	-0.0080	0.0294
T	-2174.4299	433.3633	-35.9291	-0.0014	-0.0080	0.0402
Static Y320	2203.5125	-561.9467	-19.7265	0.0000	0.0000	0.0000
A	2203.5055	-561.9512	-19.7302	-0.0070	-0.0045	-0.0037
A	2203.5074	-561.9507	-19.7262	-0.0051	-0.0040	0.0003
A	2203.5085	-561.9488	-19.7259	-0.0040	-0.0021	0.0006
A	2203.5132	-561.9512	-19.7238	0.0007	-0.0045	0.0027
A	2203.5138	-561.9522	-19.7229	0.0013	-0.0055	0.0036
A	2203.5161	-561.9529	-19.7194	0.0036	-0.0062	0.0071
A	2203.5221	-561.9484	-19.7173	0.0096	-0.0017	0.0092
A	2203.5246	-561.9492	-19.7095	0.0121	-0.0025	0.0170
A	2203.5250	-561.9488	-19.7269	0.0125	-0.0021	-0.0004
L	2203.5113	-561.9534	-19.7355	-0.0012	-0.0067	-0.0090
L	2203.5162	-561.9547	-19.7227	0.0037	-0.0080	0.0038
L	2203.5173	-561.9574	-19.7100	0.0048	-0.0107	0.0165
L	2203.5188	-561.9536	-19.7304	0.0063	-0.0069	-0.0039
L	2203.5214	-561.9543	-19.7118	0.0089	-0.0076	0.0147
L	2203.5240	-561.9497	-19.7071	0.0115	-0.0030	0.0194
L	2203.5243	-561.9491	-19.7044	0.0118	-0.0024	0.0221
L	2203.5292	-561.9474	-19.7117	0.0167	-0.0007	0.0148
L	2203.5295	-561.9569	-19.7121	0.0170	-0.0102	0.0144
T	2203.5050	-561.9559	-19.7032	-0.0075	-0.0092	0.0233
T	2203.5094	-561.9563	-19.7116	-0.0031	-0.0096	0.0149
T	2203.5134	-561.9535	-19.7147	0.0009	-0.0068	0.0118
T	2203.5138	-561.9481	-19.7230	0.0013	-0.0014	0.0035
T	2203.5141	-561.9483	-19.7187	0.0016	-0.0016	0.0078
T	2203.5141	-561.9470	-19.7326	0.0016	-0.0003	-0.0061

T	2203.5206	-561.9563	-19.7171	0.0081	-0.0096	0.0094
T	2203.5224	-561.9560	-19.7238	0.0099	-0.0093	0.0027
T	2203.5302	-561.9579	-19.7315	0.0177	-0.0112	-0.0050
Static B322	263.4227	-572.0142	-21.6082	0.0000	0.0000	0.0000
A	263.4275	-572.0138	-21.6124	0.0048	0.0004	-0.0042
A	263.4276	-572.0110	-21.6188	0.0049	0.0032	-0.0106
A	263.4278	-572.0135	-21.6205	0.0051	0.0007	-0.0123
A	263.4288	-572.0102	-21.6140	0.0061	0.0040	-0.0058
A	263.4320	-572.0141	-21.6099	0.0093	0.0001	-0.0017
A	263.4342	-572.0124	-21.6250	0.0115	0.0018	-0.0168
A	263.4347	-572.0121	-21.6178	0.0120	0.0021	-0.0096
A	263.4371	-572.0079	-21.6160	0.0144	0.0063	-0.0078
L	263.4219	-572.0082	-21.6151	-0.0008	0.0060	-0.0069
L	263.4235	-572.0127	-21.6108	0.0008	0.0015	-0.0026
L	263.4236	-572.0127	-21.6202	0.0009	0.0015	-0.0120
L	263.4239	-572.0142	-21.6221	0.0012	0.0000	-0.0139
L	263.4278	-572.0167	-21.6112	0.0051	-0.0025	-0.0030
L	263.4297	-572.0161	-21.6166	0.0070	-0.0019	-0.0084
L	263.4335	-572.0175	-21.6102	0.0108	-0.0033	-0.0020
L	263.4338	-572.0196	-21.6199	0.0111	-0.0054	-0.0117
L	263.4360	-572.0197	-21.6086	0.0133	-0.0055	-0.0004
T	263.4178	-572.0135	-21.6288	-0.0049	0.0007	-0.0206
T	263.4209	-572.0135	-21.6263	-0.0018	0.0007	-0.0181
T	263.4241	-572.0139	-21.6207	0.0014	0.0003	-0.0125
T	263.4261	-572.0163	-21.6154	0.0034	-0.0021	-0.0072
T	263.4283	-572.0122	-21.6276	0.0056	0.0020	-0.0194
T	263.4290	-572.0140	-21.6220	0.0063	0.0002	-0.0138
T	263.4291	-572.0139	-21.6314	0.0064	0.0003	-0.0232
T	263.4302	-572.0145	-21.6234	0.0075	-0.0003	-0.0152
T	263.4309	-572.0161	-21.6304	0.0082	-0.0019	-0.0222
T	263.4343	-572.0198	-21.6453	0.0116	-0.0056	-0.0371

STATIC K405	-1145.5789	-605.9969	-7.9747	0.0000	0.0000	0.0000
A	-1145.5836	-605.9938	-7.9733	-0.0047	0.0031	0.0014
A	-1145.5818	-605.9960	-7.9724	-0.0029	0.0009	0.0023
A	-1145.5782	-605.9951	-7.9751	0.0007	0.0018	-0.0004
A	-1145.5781	-605.9930	-7.9799	0.0008	0.0039	-0.0052
A	-1145.5778	-605.9925	-7.9771	0.0011	0.0044	-0.0024
A	-1145.5776	-606.0002	-7.9742	0.0013	-0.0033	0.0005
A	-1145.5772	-605.9920	-7.9794	0.0017	0.0049	-0.0047
A	-1145.5757	-606.0023	-7.9827	0.0032	-0.0054	-0.0080
A	-1145.5743	-606.0037	-7.9782	0.0046	-0.0068	-0.0035
L	-1145.5907	-605.9974	-7.9618	-0.0118	-0.0005	0.0129
L	-1145.5895	-605.9993	-7.9601	-0.0106	-0.0024	0.0146
L	-1145.5869	-605.9955	-7.9647	-0.0080	0.0014	0.0100
L	-1145.5833	-606.0025	-7.9551	-0.0044	-0.0056	0.0196
L	-1145.5831	-605.9981	-7.9538	-0.0042	-0.0012	0.0209
L	-1145.5831	-605.9921	-7.9600	-0.0042	0.0048	0.0147
L	-1145.5830	-605.9927	-7.9678	-0.0041	0.0042	0.0069
L	-1145.5814	-606.0053	-7.9620	-0.0025	-0.0084	0.0127
L	-1145.5799	-606.0047	-7.9528	-0.0010	-0.0078	0.0219
T	-1145.5901	-605.9931	-7.9656	-0.0112	0.0038	0.0091
T	-1145.5893	-605.9964	-7.9759	-0.0104	0.0005	-0.0012
T	-1145.5880	-605.9933	-7.9650	-0.0091	0.0036	0.0097
T	-1145.5856	-605.9965	-7.9632	-0.0067	0.0004	0.0115
T	-1145.5828	-605.9943	-7.9603	-0.0039	0.0026	0.0144
T	-1145.5799	-606.0007	-7.9637	-0.0010	-0.0038	0.0110
T	-1145.5767	-606.0027	-7.9753	0.0022	-0.0058	-0.0006
T	-1145.5765	-605.9988	-7.9616	0.0024	-0.0019	0.0131
T	-1145.5758	-606.0037	-7.9795	0.0031	-0.0068	-0.0048

		North	East	UP	SigN SigESigU
R440	A	-0.0088	0.0024	0.0003	0.00530.00720.0070
R440	L	-0.0238	0.0016	0.0169	0.00750.00340.0051
R440	T	-0.0071	-0.0003	0.0221	0.00350.00800.0167
Y320	A	0.0026	-0.0037	0.0040	0.00740.00160.0062
Y320	L	0.0088	-0.0062	0.0103	0.00610.00350.0108
Y320	T	0.0034	-0.0066	0.0069	0.00750.00430.0094
B322	A	0.0075	0.0027	-0.0084	0.00470.00230.0045
B322	L	0.0050	-0.0017	-0.0083	0.00600.00270.0068
B322	T	0.0054	-0.0007	-0.0187	0.00390.00220.0085
K405	A	0.0006	0.0004	-0.0022	0.00290.00440.0034
K405	L	-0.0056	-0.0017	0.0149	0.00370.00480.0051
K405	T	-0.0038	-0.0008	0.0069	0.00580.00400.0071

**Appendix E. Vendor Responses**